AD NUMBER
AD277455
NEW LIMITATION CHANGE
TO   Approved for public release, distribution unlimited
FROM   Distribution authorized to U.S. Gov't. agencies and their contractors; Administrative/Operational Use; Jan 1962. Other requests shall be referred to the Aeronautical Systems Division, Wright-Patterson AFB, OH 45433.
AUTHORITY
SYS ENG GROUP [SEG] Ltr, 12 Jul 1965

ASD-TDR-62-73

AD0277455

EFFECTS OF ULTRAHIGH PRESSURES ON THE FORMATION AND PROPERTIES OF ORGANIC, SEMIORGANIC, AND INORGANIC MATERIALS

TECHNICAL DOCUMENTARY REPORT NO. ASD-TDR-62-73
January 1962

Directorate of Materials and Processes
Aeronautical Systems Division
Air Force Systems Command
Wright-Patterson Air Force Base, Ohio

Project No. 7340, Task No. 73404

45

YEARS
OF
MATERIALS
PROGRESS

SAPPHIRE ANNIVERSARY

20040225316

NOTICES

FOREWORD

This work was prepared by Battelle Memorial Institute under AF Contract No. AF 33(616)-7471. This contract was initiated under Project No. 7340, "Nonmetallic and Composite Materials", Task No. 73404, "Effects of Ultrahigh Pressures on the Formation and Properties of Organic, Semiorganic, and Inorganic Materials". This work was administered under the direction of the Directorate of Materials and Processes, Deputy for Technology, Aeronautical Systems Division, with Dr. Harold Rosenberg and Mr. Albert J. Sicree, Jr., acting as project engineers.

This report covers work performed during the period July 1, 1960 through December 31, 1961.

This work was conducted by E. J. Bradbury, H. H. Krause, C. B. Sclar, L. C. Carrison, H. E. Bigony, C. R. Gray, R. C. Himes, C. M. Schwartz, and R. I. Leininger.

ABSTRACT

Studies on the effect of ultrahigh pressures (up to 90,000 atmospheres on the "new" post-1960 absolute pressure scale) were carried out on organic polymers and semiorganic and inorganic materials in a Belt-type internally heated high-pressure apparatus.

With organic polymers, results indicate that the effect of compression is influenced by compression, compression rate, holding period, and polymer used. The most influential parameters appear to be the polymer and the holding period. Results do not show any generalized pattern and suggest that each polymer may well have its individual response to compression.

Among the semiorganic compounds studied, dimethyldicyanosilane apparently polymerized at 60,000 atmospheres through conversion of the nitrile groups to $> C=N-$. Other semiorganics, alumino-siloxanes, ethyldicyanophosphine, arseno-siloxane, phosphonitrilic chloride trimer and diphenylphosphinoborine showed little effect of pressure or decomposed.

With inorganic materials above 700 C contamination with alumina and silica from the pyrophyllite gasketing material was found. The problem was resolved by dehydrating the pyrophyllite. The contamination studies led to the synthesis of two and possibly four new compounds by reaction of hydrothermally carried alumina and silica with calcium oxide.

Ultrahigh pressure-high temperature studies of two heteropolynuclear acids (silico-tungstic and phosphotungstic) and two heteropolynuclear salts (ammonium-arseno-vanado tungstate and ammonium-phospho-vanado tungstate) revealed what appear to be pressure-dependent modifications over a broad pressure-temperature range to 75,000 atmospheres and 1300 C. The results of preliminary experiments on a group of sulfides, including Sb_2S_3 and As_2S_3, and on apatite $[Ca_5(PO_4)_3(OH,F)]$ were negative.

PUBLICATION REVIEW

This technical documentary report has been reviewed and is approved.

FOR THE COMMANDER

William E. Gibbs

WILLIAM E. GIBBS
Acting Chief, Polymer Branch
Nonmetallic Materials Laboratory
Directorate, Materials & Processes

TABLE OF CONTENTS

TABLE OF CONTENTS
(Continued)

PAGE

TABLE OF CONTENTS
(Continued)

LIST OF TABLES

LIST OF FIGURES

LIST OF FIGURES
(Continued)

PAGE

I. INTRODUCTION

The United States Air Force has a constantly increasing need for materials of improved properties to withstand ever more rigorous conditions. As manned and unmanned aircraft vehicles reach greater and greater speeds and higher and higher altitudes, thermal and radiation resistance become essential. Because of their light weight, thermal and electrical nonconductivity and higher strength-to-weight ratio, polymers are a class of materials necessary to aircraft of all types. These materials, however, are sometimes the limiting factors in design because of their relative sensitivity to heat and radiation.

Recognizing this limitation, the U. S. Air Force has pursued many avenues toward the improvement of polymers and the development of new materials. Polymers based on chelates, highly resonating compounds, semiorganic and inorganic materials are some of the approaches studied by the Air Force and its contractors.

Relatively recently (in the past few years) equipment and techniques for ultrahigh pressure* have been developed to the point where it is available for use as a method to modify or synthesize polymers.

Bridgman pioneered studies in the 1930's on very high pressures and interest continued but at a relatively low level until the last decade. At that time internally heated high-pressure devices, such as the Belt, were developed making the attainment of ultrahigh pressures at elevated temperatures feasible. Shortly thereafter came the development of a process (which quickly became commercial) for the production of diamonds from graphite and later the production of the heretofore unknown Borazon.

With this precedence, the question arose as to the possibility of improved polymers through such ultrahigh pressures.

As the background relating to the effects of ultrahigh pressure was quite limited, this program was directed primarily toward screening the effects upon three classes of polymers, organic, semiorganic, and inorganic. Past efforts in the field of ultrahigh pressures are reviewed in a separate report. As can be seen, emphasis has been on the determination of phase changes in metals and inorganic compounds with less effort on determining irreversible effects wrought by the extreme pressures.

There are a number of instances wherein chemical reactions did occur because of the high pressures. Examples of these included, in the case of inorganics, decompositions of metal salts and oxides, reduction of oxides to free metal and irreversible changes in glasses which might be the result of chemical changes.

In the case of organic materials, the most significant findings are that some normally unreactive compounds such as tetra-substituted ethylenes can be polymerized at high pressures and that some polymers are gelled under these conditions. Further, aromatic nitriles can be trimerized to triazines and compounds such as brom thymol blue

---

*Ultrahigh pressure is here meant to be equal to or greater than 30,000 atm (new 1960 scale).

Manuscript released by the authors December 31, 1961, for publication as an ASD Technical Documentary Report.

are insolubilized, perhaps through polymerization. Other compounds such as cellulose, Neoprene, benzamide, and benzaldoxine were also found to be irreversibly changed by the drastic conditions.

With this background of unusual reactions, the possibility exists that further reactions will be effected by these extreme pressure conditions especially when carried out at elevated temperatures.

In the case of organic polymers, two general types of changes can be expected — physical in which some property such as crystallinity is enhanced and chemical in which new bonds are established. It is the latter case which offers the most promise. It is expected that bonds which do not normally participate in polymerization reactions will be activated by the pressures exerted. These bonds include double and triple bonds, carbonyl linkages, aromatic carbon-carbon double bonds, nitrile, and the like. Evidence has been found of reaction of nitrile triple bonds under extreme pressure. It is known that rates and molecular weight increase as the pressures are increased in polymerizations but the phenomena have been studied only to much lower pressures than the target of this work. Possibilities here lie not only in the production of higher-molecular-weight materials but also in products of higher density through more complete crystallization. Unconventional routes to polymers through normally inactive groups are also of interest as is possible grafting to preformed polymers.

This program was designed to determine whether the extreme pressures would cause any of these changes in starting materials of the three classes of interest. Detection of these changes was to be made by measurement of physical or chemical properties by any one or a combination of suitable methods.

The modus operandi chosen for this study was, in essence, simple. Samples of compounds, monomer or polymer, are pressurized at chosen temperature, recovered, and studied for changes effected by the pressure. To carry this out, however, some development effort was necessary to handle and contain these varied materials under these drastic conditions. This phase of the project and the results obtained with each of the three types of materials are described in the following sections.

The high-pressure device used in all the studies on this project was the G. E. Belt based on the original design of H. T. Hall. Essentially, the Belt device consists of a pair of truncated tungsten carbide pistons which are forced by a hydraulic ram into a tungsten carbide die. Both the die and the pistons are surrounded by a series of concentric steel binding rings to afford massive support, and the device may be internally heated and instrumented. Hydraulic ram force was supplied by either a 1,000-ton Hall multiple-piston ram, a 100-ton Blackhawk jack, or a 150-ton Watson-Stillman press.

Although the Belt apparatus generally performed satisfactorily up to about 75,000 atm, an unacceptable incidence of ring and/or die failure occurred at higher pressures as the mechanical limits of the system were approached. Accordingly, a more massive set of binding rings with a higher ratio of steel to carbide was designed after an engineering analysis.

It should be noted that the pressure scale used in this research is the new (mid-1960) scale which is now generally accepted by workers in this field. A full discussion of the change in pressure scales is given in the body of the report. Seventy thousand atmospheres on the new scale corresponds to 100,000 atm on the scale used at the beginning of this study.

II. SUMMARY

Organic Polymers

Compression studies were conducted on a number of polymers including different generic materials and several types of the same generic material. Studies have included polyethylenes, several polyamides, polystyrene, polymethylmethacrylate, polyacrylonitrile, and ethyl cellulose under compressions up to 90,000 atm. The majority of compressions were conducted at ambient temperature, although several heated runs were made during the preliminary phase of the study. Results to date indicate that the effect of compression on organic polymers is influenced by:

(1) The compression attained
(2) The compression rate
(3) The holding period
(4) The polymer used.

The most influential parameters within the target range of compression appear to be the polymer and the holding period. Results to date do not show any generalized pattern of behavior for polymers. Rather the limited data suggest that each material may well have its individual response to compression. Since compression-induced changes generally were quite small, exceedingly sensitive methods for evaluation were required. Attempts to use highly refined infrared measurements for detecting structural changes were unsuccessful. Ultimately, the use of density gradient columns for evaluation of compression-induced effects proved very satisfactory. These can be designed with any degree of sensitivity desired. Columns used throughout these studies were constructed to detect changes as small as one unit in the fourth decimal place. Compression-induced changes were screened through net density differences in the sample before and after compression. Both positive and negative net changes were observed for several polymers depending upon compression conditions employed.

Supporting techniques were developed during the course of the study on organic polymers for extrusion, sample fabrication, encapsulation, and heating and instrumentation under superpressure conditions, and equipment modifications were made to give increased compression and improved service life.

Semiorganic Polymers

A number of semiorganic monomers and low polymers were prepared in this program and were subjected to pressures from 60,000 to 75,000 atm at various temperatures and in some cases, for varying periods of time.

It was hypothesized that a structure such as $(CH_3)_2Si(CN)_2$ might be polymerized by extreme pressure through conversion of the nitrile groups to $> C=N-$ groups. This result appears to have been achieved by pressurization at 60,000 atm at 100 C. Experiments are continuing in an effort to establish the range of conditions under which this reaction will take place.

Four low polymers of the alumino-siloxane series (Al-O-Si bonding) were prepared with either acetylacetone or isopropoxide bonded to the aluminum and with methyl, ethyl, or phenyl groups on the silicon. The effect of high pressure on these polymeric Al-O-Si materials at 300 C is to stabilize the aluminum-oxygen-carbon bonding whi h exists at the acetylacetone or isopropoxide linkages. The rupture of silicon-carbon bonds at this temperature appears to be inhibited by pressure, but this effect is not large.

Ethyldicyanophosphine underwent extensive decomposition at 50 C under 60,000-atm pressure, and may require significantly higher pressure at lower temperature to bring about a polymerization reaction, if such is possible.

An arseno-siloxane with a bicyclic structure having As-O-Si bonding was also prepared, using trivalent arsenic. The compound with phenyl groups on the silicon is thermally stable to 500 C, and pressurization at 60,000 atm appears to promote its decomposition, rather than to induce polymerization through opening of the rings.

A linear arseno-siloxane based on pentavalent arsenic proved to be quite unstable, with decomposition beginning at 100 C under pressure and leading to pyrolysis rather than polymerization at 200 C.

Phosphonitrilic chloride trimer was found to polymerize so readily on heating that the effect of pressure was negligible. A linear polymer of the phosphonitrilic chloride series was made somewhat more tractable, and probably of shorter chain length, by pressurization at 60,000 atm and 200 C.

Diphenylphosphinoborine trimer underwent little change before pyrolysis at 400 C, and high pressure did not appear to accomplish any effect that heating did not achieve. An as-yet unidentified residue obtained during preparation of the trimer became more stable as a result of pressurization at 60,000 atm and 400 C.

The most promising materials found in this study will be subjected to pressures up to 100,000 atm to examine further the effects of pressure. The program will be expanded to include additional semiorganic materials such as aluminoxanes, stannoxanes, ferrocene derivatives, and coordination compounds.

Inorganic Polymers

The Belt ultrahigh-pressure high-temperature apparatus was used in an exploratory program on the effect of ultrahigh pressure and concomitant temperature on polymerization of inorganic compounds. A description of the Belt apparatus and auxiliary equipment is given, and the evolution of the absolute pressure scale is reviewed. The Belt apparatus was calibrated on the "new" post-mid-1960 absolute pressure scale by means of the following fixed pressure points (electrical resistance transitions): Bi I-II at 25,000 atm, Tl II-III at 37,000 atm, Ba II-III at 58,000 atm, and Bi V-VI at 87,000 atm. The Belt apparatus is essentially a linear device, in terms of pressure on sample versus press load, to at least 90,000 atm.

The electrical-resistance transitions were run in silver chloride, a quasi-ideal pressure-transmitting medium, but, in actual practice, samples are pressurized in a platinum heater tube which is in direct contact with the pyrophyllite gasketing material.

4

From the results of a series of experiments, it is possible to assess the relative influence of the pyrophyllite gasketing, the platinum heater tube and the sample itself on the ram force required for the Bi I-II transition. The pyrophyllite is by far the most important of the three components, although there is a small but measurable effect due, respectively, to the platinum heater tube and the powder sample. The combined effect of the three components is not additive, and the ram force required for the Bi I-II transition is about 20 per cent higher for an actual experiment than for a silver chloride calibration run.

The equilibrium line for the well-known experimentally established calcite-aragonite transition was extended from about 13,000 atm and 600 C to about 35,000 atm and 1400 C. The Belt-determined portion of the equilibrium line was displaced along the pressure axis as based on the Bi I-II transition determined in silver chloride. If the pressure data are corrected using the actual ram force required for the Bi I-II transition without silver chloride, the corrected data are in reasonably close accord with the results of previous investigators who worked at lower temperatures and pressures with other pressure devices.

The pyrophyllite gasketing material (Grade A Lava) is composed predominantly of the mineral pyrophyllite ($Al_2O_3 \cdot 4SiO_2 \cdot H_2O$), but it contains subordinate amounts of diaspore ($Al_2O_3 \cdot H_2O$) and halloysite ($Al_2O_3 \cdot SiO_2 \cdot 2H_2O$). It is shown that alumina and silica carried in vapor solution in supercritical steam at high pressures and at temperatures between 700 and 1300 C will enter the platinum sample capsule through one or both of its ends which are mechanically cold sealed with platinum foil. The source of the contaminants is the pyrophyllite gasketing material which contains about 6 per cent of water. At least two and possibly four new compounds, which are probably pressure dependent, have been synthesized in the $CaO-Al_2O_3-SiO_2-H_2O$ system by reaction of hydrothermally carried silica and alumina with calcium oxide which was used as an indicator of contamination. The contamination problem may be resolved by prefiring at 925 C the machined pyrophyllite jacket which encloses the platinum heater tube. This is below the mullitization point of this pyrophyllite so that the fired material has the structure and mechanical properties of pyrophyllite but contains only about 0.3 per cent of water. The mobility of the alumina and silica is thus restricted and high-pressure products are free of contamination.

The results of ultrahigh-pressure high-temperature studies of two heteropolynuclear acids (silicotungstic and phosphotungstic acid) and two heteropolynuclear salts (ammonium-arseno-vanada tungstate and ammonium-phospho-vanado tungstate) are presented. All these materials appear to have pressure-dependent modifications over a broad pressure-temperature range to 75,000 atm at 1300 C. Preliminary high-pressure experimental work was done anhydrously on a group of sulfides, including Sb_2S_3 and As_2S_3, but no changes were detected. As the initial effort in a projected program on the effect of pressure on phosphates of divergent structures, high-pressure experiments have been started on the apatite [$Ca_5(PO_4)_3 (OH,F)$] structure; the first results on crystalline apatite under anhydrous conditions were negative. Notes on the recrystallization of zircon ($ZrSiO_4$) under high pressure and temperature and on the transformation of GeO_2 (quartz form) to GeO_2 (rutile form) under pressure are included.

III. EXPERIMENTAL SECTION – ORGANIC POLYMERS

Introduction

Although the prime target of this study is the determination of the effect of super-pressure conditions on preformed polymers and on materials formed by polymerization under superpressure conditions, subordinate effort on development of techniques and the study of critical parameters appeared advisable. No attempt will be made in this Annual Report to include all data and a complete résumé of every subordinate development reported during the course of this work. Rather, the results to date will be incorporated into a review of the highlights of the several areas of effort pertaining to the organic polymers with references to sources of more detailed information. Initially investigations of the effect of superpressure compression on various materials were predicted on a bismuth transition presumably occurring at 125,000 atm. Subsequent developments have shown this relationship to be considerably in error such that presently reported compressions above 70,000 atm are higher, relatively speaking, than the 100,000 atm initially specified for this work. Modification and improvements effected during the course of this work have permitted compression excursions around 140,000 atm based upon the initially accepted resistance-compression scale. It is hoped that additional contemplated modifications will permit a useful service life above 100,000 atm on the corrected calibration scale. Thus, if a working compression of 105,000 atm can be attained, this will represent 150,000 atm based upon compression concepts at the time this program was initiated.

Experimental Results

Polymer Compression

Compression studies conducted during the course of this program have been divided into two categories for convenience in discussion. First, those conducted in an intermediate range to investigate the effects of different parameters, and, second, compressions conducted within target range. Characterization in all instances was based upon net density change of the polymer.

Parameter Investigation at Intermediate Compression. Effect of Assembly Components on Compression. Although considerable general background on superpressure techniques and the necessary equipment was available, preliminary studies were devoted to appraising the adaptation of the application to polymer research. Included, therefore, in early work was a study of the effect of component materials of assembly on transition and compression internal pressure. First evidence of the importance of this factor was noticed early. Runs were made with presumably duplicate assemblies in which the sample space was filled with different materials. Since questions had arisen concerning whether significant pressure gradients might exist either in the pyrophyllite sample holder or in polymer samples of significant size, transition monitors were used at several locations in the runs. Results of the transition behavior at similar locations for pyrophyllite, polyethylene, and silver chloride are summarized in Table 1. Results of single runs suggest that a slight pressure gradient does exist in the sample holder.

Generally, transition was observed at the lowest ram force in the center of the slug and required the highest load at the edge. The lone exception to this was in the run with the silver chloride-filled pyrophyllite sleeve. Here the transition in the center occurred at a ram force higher than that of either of the other two locations. The relative values, however, of the two outer positions were consistent with the early observation.

TABLE 1. COMPARISON OF COMPRESSION[a] CHARACTERISTICS FOR PYROPHYLLITE, POLYETHYLENE, AND SILVER CHLORIDE

Identification	Sample Holder	Location of Monitor	Observed Ram Force at Bismuth II-III Transition, tons	Estimated Maximum Internal Pressure Attainable in 100-Ton Press at Location, kilobars
17571-34	Pyrophyllite	Center of sample holder	54.0	45.0
		Edge of sample holder	58.8	41.3
17571-35	Polyethylene	Center of sample holder	51.5	47.1
		Half radius from edge	51.8	46.9
		Edge	52.0	46.7
17571-36	Silver chloride[b]	Center of sample holder	42.5	57.2
	Pyrophyllite	Half radius from edge	41.5	58.6
		Edge of sample holder	42.3	57.5

(a) Compressions run under presumably identical conditions except for material of sample holder (0.35-in. OD x 0.450-in. cylinder).

(b) Silver chloride cylinder (0.25-in. OD x 0.450 in.) melt-loaded in drilled pyrophyllite sample holder.

Probably the most significant information from this series of runs is shown in Figure 1. Results indicate that some gradation in internal pressure is possible in the polymer samples but that this may be less than in pyrophyllite alone and generally appears to be inconsequential. More important is the observation of the significant differences in the pressures achieved when different materials are used in otherwise identical assemblies. These results suggest that the compressibility, flow characteristics, and likely the amount of sample can greatly affect the pressure achieved in a given assembly. Thus, it appears highly advisable to determine the pressure directly in the experimental unit rather than in a highly sensitive, virtually incompressible unit. If the silver chloride standardization value of the polyethylene run were accepted without the experimental determination of transition in the presence of polymer, the estimated compression would be about 25 per cent high.

Possibly these were not duplicate assemblies and hence an erroneous conclusion was being drawn. A run was made, therefore, in which three monitors were inserted equidistant in a pyrophyllite sample holder. One was installed directly in a fine hole in the pyrophyllite. Another was inserted in a small-diameter polyethylene cylinder in the pyrophyllite, and the last monitor was similarly mounted in a silver chloride cylinder. Pertinent resistivity-ram force data on this run are presented in Figure 2. Examination shows that the sharpest transition was obtained at the lowest loading in the presence of silver chloride. The monitor in the polyethylene shows an intermediate behavior, and the monitor mounted directly in the pyrophyllite required the highest pressure and gave the least sensitive determination. Results of this run are summarized in Table 2.
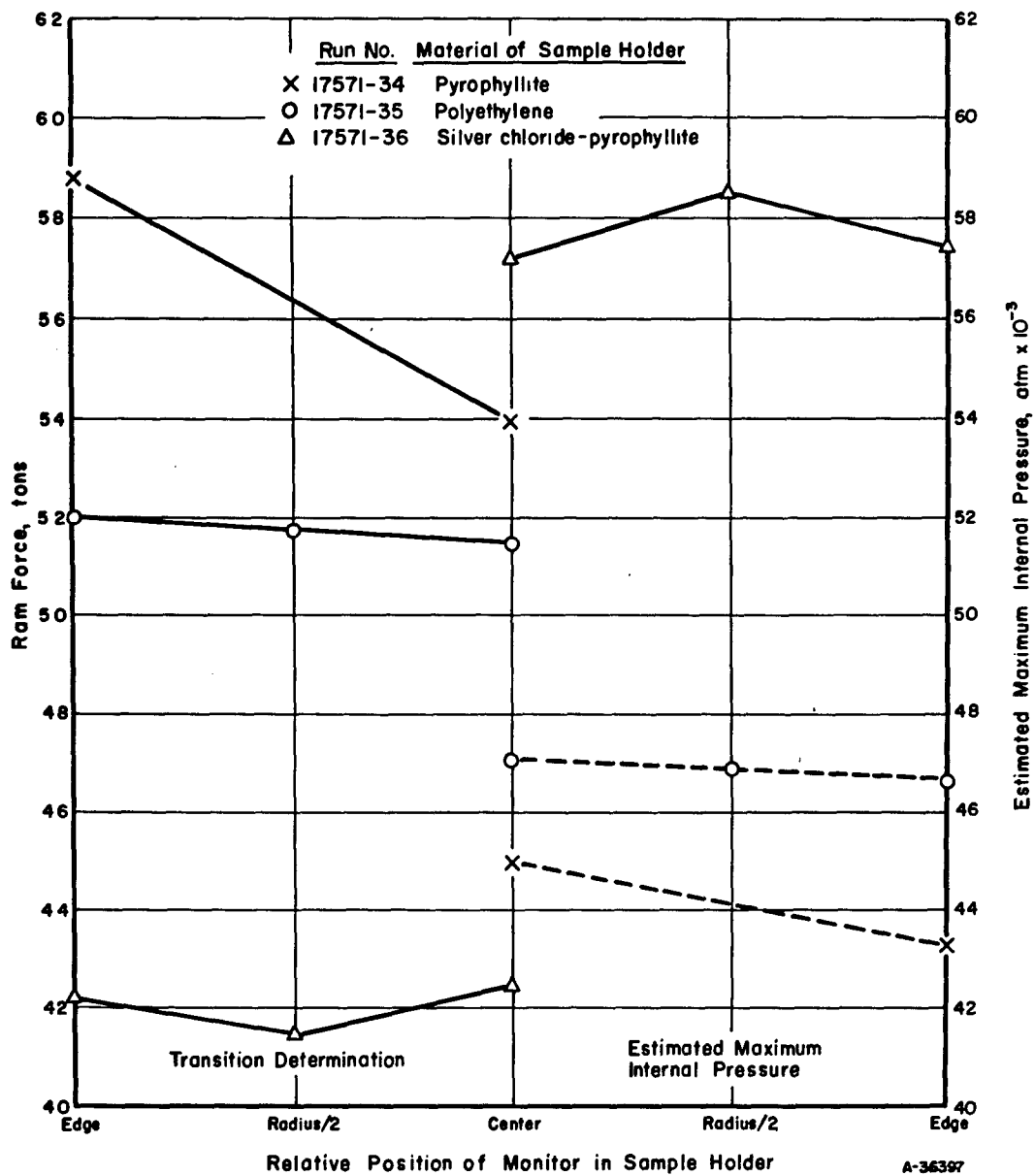
FIGURE 1. EFFECT OF COMPONENT MATERIALS IN SUPERPRESSURE
ASSEMBLY ON TRANSITION AND MAXIMUM INTERNAL
PRESSURES ATTAINABLE IN 100-TON PRESS
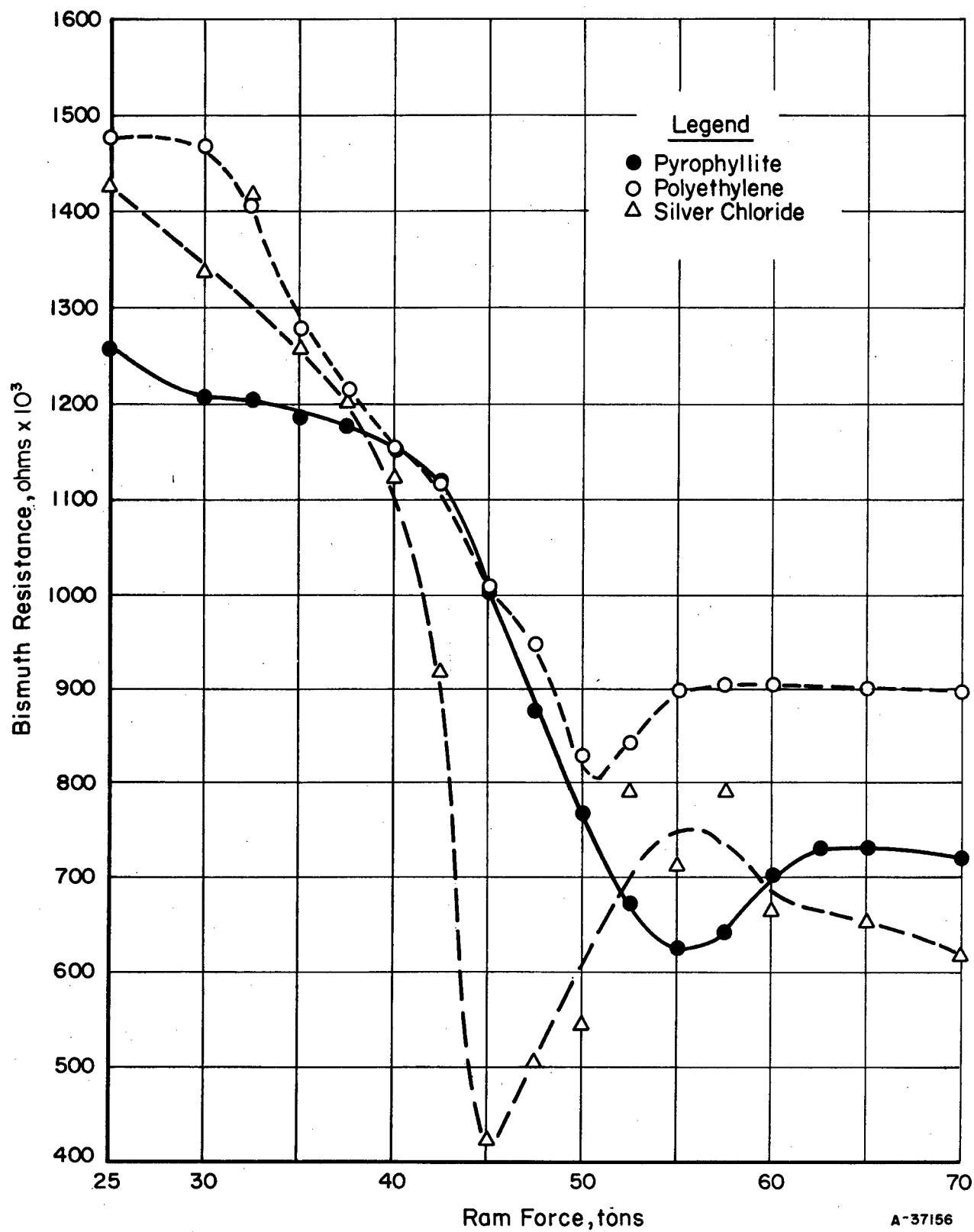
FIGURE 2. EFFECT OF CONTAINING MEDIUM ON BISMUTH TRANSITION

TABLE 2. EFFECT OF CONTAINING MEDIUM ON BISMUTH TRANSITION

Containing Medium	Ram Force at Bismuth I-II Transition, tons	Remarks
Pyrophyllite (a)	49.0	Monitor in hole equidistant from b and c
Polyethylene (b)	48.0	Monitor in polyethylene cylinder equidistant from a and c
Silver chloride (c)	43.3	Monitor in silver chloride cylinder equidistant from a and b

Subsequent work and calibration data presented for various polymers have further confirmed the significance of this factor. Inspection of Figure 3, which summarizes data obtained with two different dies shows, in general, fairly satisfactory correlation. A small consistent difference in operating characteristics was shown for the two dies, regardless of the material used for monitor imbedment. Conversely, the imbedment material still appears to be the critical factor in the compression-press load relationship and, in the region studied, appears to be linear.

However, exceptions to this generalization do appear in this figure. The first anomaly is the lack of correlation of the barium transition which occurred at 99 tons, but which, predicated on the previous calibration behavior, would be expected at 80 tons. This discrepancy may be due in part to die failure during the run. This, however, does not account for the failure of the Bi I-II, Bi II-III, and Tl II-III transitions to lie on a straight line, thus implying that some value may be in error.

Effect of Compression on Density. Currently the density-gradient apparatus appears to be the most satisfactory method for rapidly determining the extent of change in the polymers used in this study. The units are easy to make and can be designed to read with extreme sensitivity if desirable. At present, the columns are designed to give resolution to one in the fourth decimal place. Density gradient columns were used to provide a comparison of the density of molding materials with extruded material. There generally was a slight increase, possibly due to some loss of volatile components, but more likely due to slower cooling rates after molding, permitting a higher degree of crystallization than is found in the molding pellets. This effect was rather pronounced in the case of the high-density polyethylene. Initially, the density was determined to be 0.9581 g/cc, but after molding the density was 0.9647 g/cc.

The effect of compression on polymers appeared to vary with the material, maximum pressure, rate and time of loading and temperature. These factors were not comprehensively studied during the intermediate compression program, nor have these preliminary results been verified by confirmatory runs.
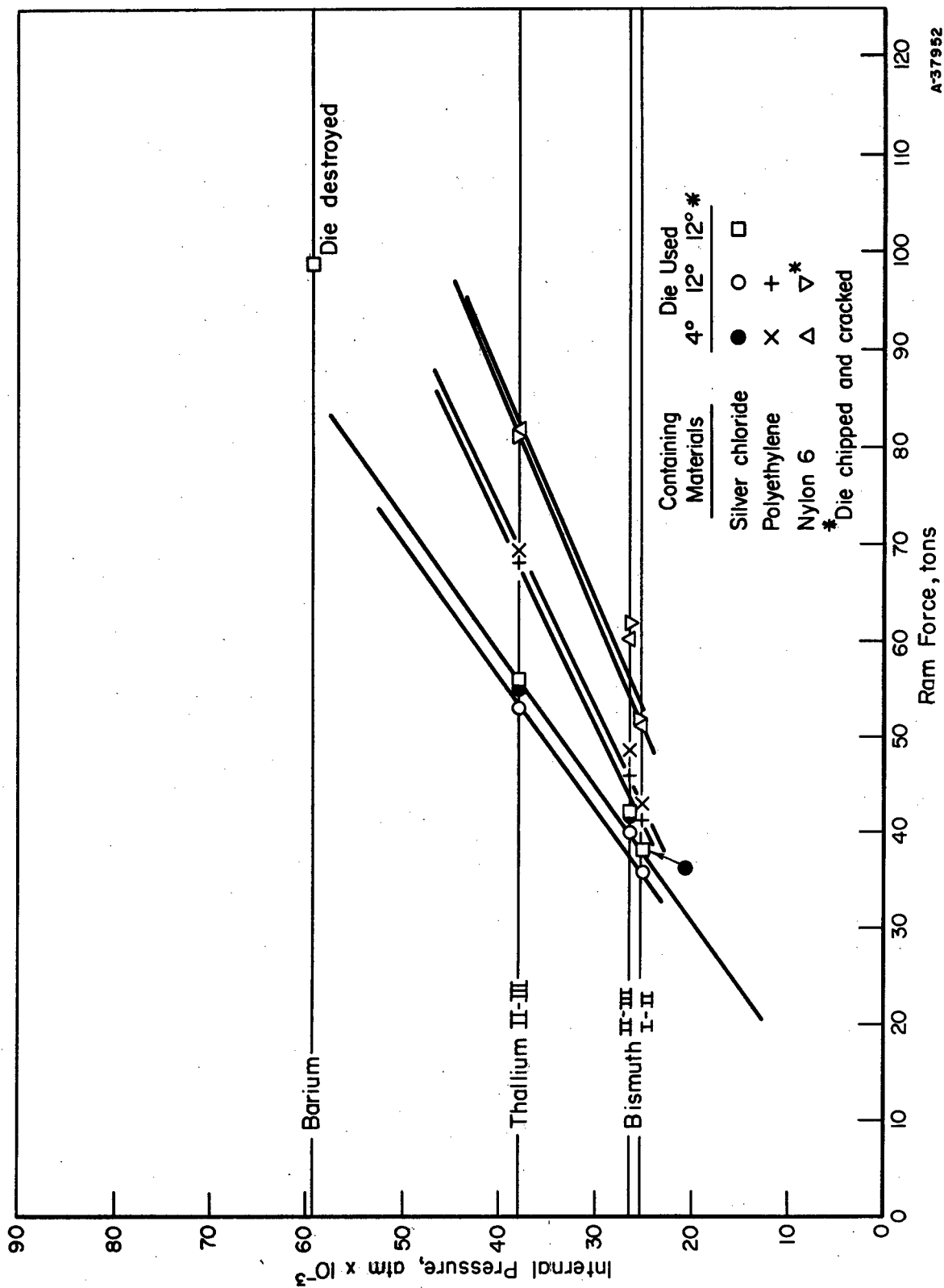
FIGURE 3. EFFECT OF DIE DESIGN AND ASSEMBLY COMPONENTS ON INTERNAL PRESSURE

11

Reductions in density were observed for most of the short-period runs at moderate compressions. This was true for runs with low- and high-density polyethylene, and polypropylene. However, several runs were made in which reductions either were not observed or the density was increased by the compression conditions used. These runs were made either by slow compression, prolonged holding under pressure, or by heating under pressure. This behavior was observed for low-density polyethylene which was used for the greater part of the study directed toward an extension of techniques. It appears reasonable to expect somewhat similar behavior with the high-density polyethylene and possibly polypropylene.

Compressions with polystyrene and polymethylmethacrylate, on the other hand, showed increasing densities roughly correlatable with estimated compression pressures. Results appear to be in general agreement with work reported by several investigators[1,2]*. Larsen and Drickamer applied a shearing force to polymers under 50,000 atm. Short-time loads were used in which degradation was observed for polyethylene, polymethylmethacrylate, and others. Polymers containing unsaturation (olefinic or aromatic), such as polyisoprene or polystyrene, were crosslinked by this treatment. The mechanism postulated was free-radical formation by bond rupture. In systems containing unsaturation, the free radicals apparently reacted readily to form crosslinked materials. Similar studies by Professor Roy were reported to give degradation with polyethylene and polyacrylonitrile, but to have no effect on polystyrene.

In this work, density reductions, suggestive of degradation, occurred with moderate superpressures, up to 35,000 to 40,000 atm under fairly rapid loading and short holding periods. This conceivably could produce sufficient stress to cause bond rupture similar to that reported by Larsen and Roy. However, slower loading, longer compression periods, higher temperatures or pressures have in several cases shown a reversal of this trend.

It is suspected that the effect of the currently used hydrostatic compression would be considerably less drastic than the effect of high-pressure shearing of a polymer. Correlations of over-all experimental results to date with Larsen-Drickamer's results appear to confirm this. Since their studies indicate the degradation reaction, as determined by infrared methods, is virtually complete within a minute compared to the very small changes noted in the present work.

During preparation of equipment capable of attaining pressures of about 100,000 atm, the effect of several compression parameters on density was studied for polyethylene and two types of polyamides. It was hoped that critical parameters could be further defined during this period to minimize the runs required to obtain a fairly valid appraisal of the maximum effect of 100,000-atm compression. The results suggest that both loading rate and maximum compression modify the effect on a given polymer. However, in the range of parameters studied in the intermediate compression range, the most critical parameter still seems to be the polymer used.

Effect of Loading Rate on Polymer Density and Compression. Studies to evaluate the effect of this factor were conducted on polyethylene, and two types of polyamides.

Results of this study are shown in Figures 4 and 5. In general, results for polyethylene (Petrothene) and polyhexamethylenediamine sebacic acid (Nylon 610) show fairly

*References are listed on pages 99 through 102.

12
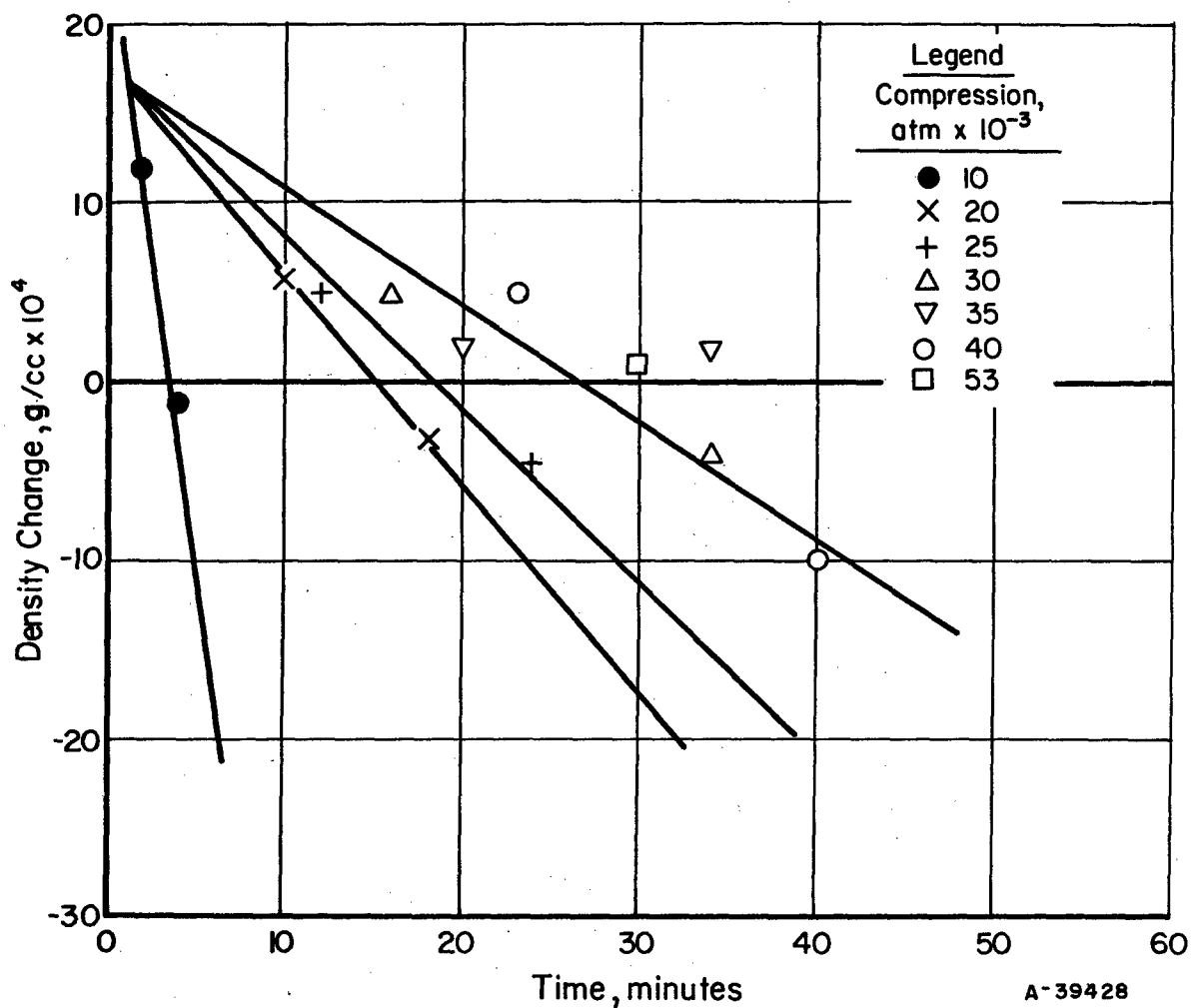
FIGURE 4. EFFECT OF TIME TO REACH MAXIMUM LOAD ON
POLYETHYLENE DENSITY
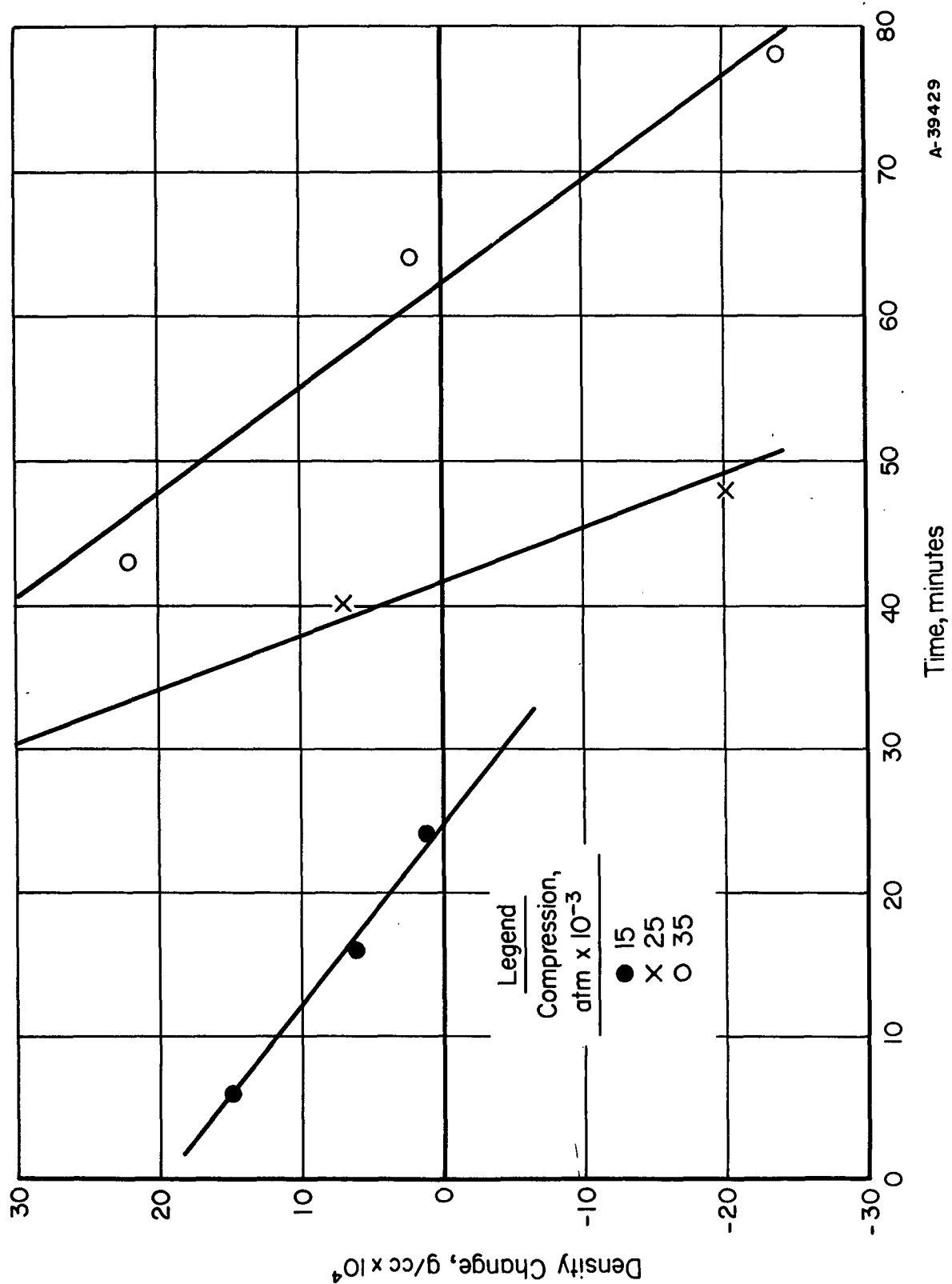
FIGURE 5. EFFECT OF TIME TO REACH MAXIMUM LOAD ON NYLON 610 DENSITY

A-39429

14

well-defined patterns at least in the lower compression ranges. The polyethylene showed some irregularities above 35,000 atm, but results qualitatively agree with the projected trend. Generally, results to date with Petrothene and Nylon 610 indicate that slow compression of a sample tends to produce increased density reduction. However, the tendency for the polyethylene patterns to converge might imply that density increases would be effected at sufficiently high compressions. The pattern is more random for the polyamide, and projection, at present, less meaningful. Where Petrothene and Nylon 610 appear to show higher relative densities as compression pressures are raised at constant time, the reverse is shown for polycaprolactam (Nylon 6). The more rapid loading rate appears to produce greater reductions in density. The data for studies with this polymer do not show the well-defined patterns of Petrothene and Nylon 610, but graphical interpretation of the data tends to support the observation.

Concurrently with the evaluation of the effect of loading rate on density, a brief study was made of the effect of loading rate on internal compressions. This work, conducted on Nylon 610, compared the behavior of this system through the lower bismuth transition at three different loading rates. Results of this work, Figure 6, indicate that, at least for this system, slower loading rates are more efficient. About 20 per cent more loading was required to produce the bismuth I-II transition at a loading rate of 3.3 tons/min than at a loading rate of 1.1 tons/min.

Correlation of Polymer-Compression Studies. Although data from an adequate number of runs to determine the interrelationship of internal compression, loading rate, and density change with unquestionable validity for the polymers studied were not available, an attempt was made to correlate these effects to determine possible trends. Sufficient data were obtained for polyethylene (Petrothene) and polyhexamethylenediamine sebacic acid (Nylon 610) to show slight similarity in pattern. Polycaprolactam (Nylon 6) appeared to behave differently. Preliminary work with these materials was conducted with a short holding time (2 minutes) at maximum compression.

In the case of Petrothene, Figure 7, the effect of compression rate appears to diminish as compression pressures are raised. Rapid loading, however, appears to give the greatest increase in density. While data suggest the convergence of polymer densities under higher compressions to minimize the effect of compression rate, the projection suggests that only limited density increases may be obtained. A somewhat similar situation exists for Nylon 610. Fewer data, however, were available for correlation with this system and results are inconclusive at present.

Data available for Nylon 6 on the effect of time to reach maximum load were interpolated to provide a pattern for projecting Figure 8. This also indicates a tendency for the rate effect to diminish as the compression pressure is raised. This projection, however, indicates a marked tendency for a reduction of polymer density with increasing compression.

Projected correlation of data for Petrothene and Nylon 610 suggested that under present target compression, around 100,000 atm, present compression rates, and short holding times, very little net density change would be predicted. Data for Nylon 6, however, suggested that similar superpressure treatment might effect significant density reductions.

Present conclusions based upon data available to date are: (1) that compression rate, compression used, temperature, and undoubtedly holding time, effect the net
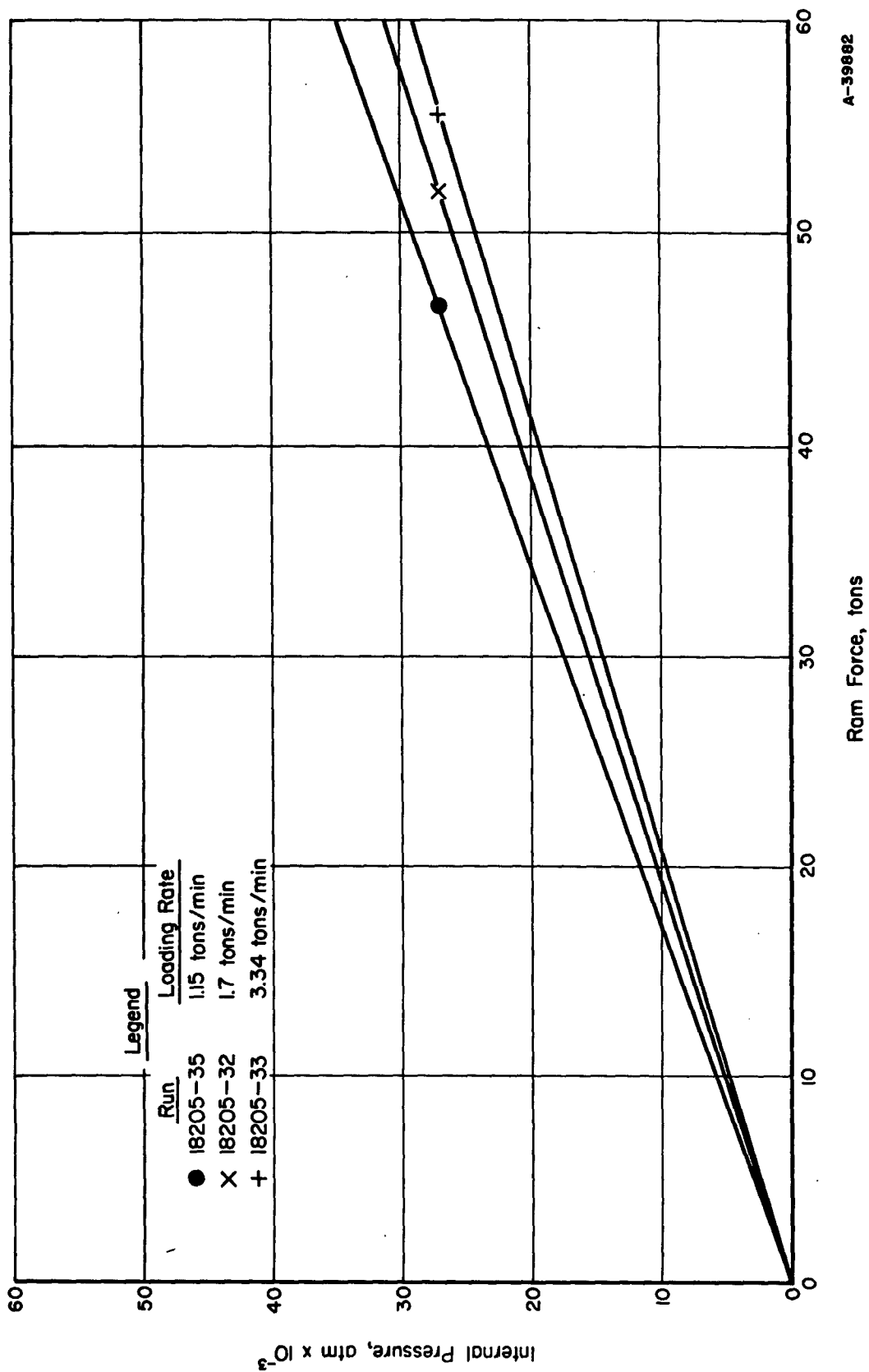
FIGURE 6. EFFECT OF LOADING RATE ON INTERNAL COMPRESSION IN NYLON 610

A-39882
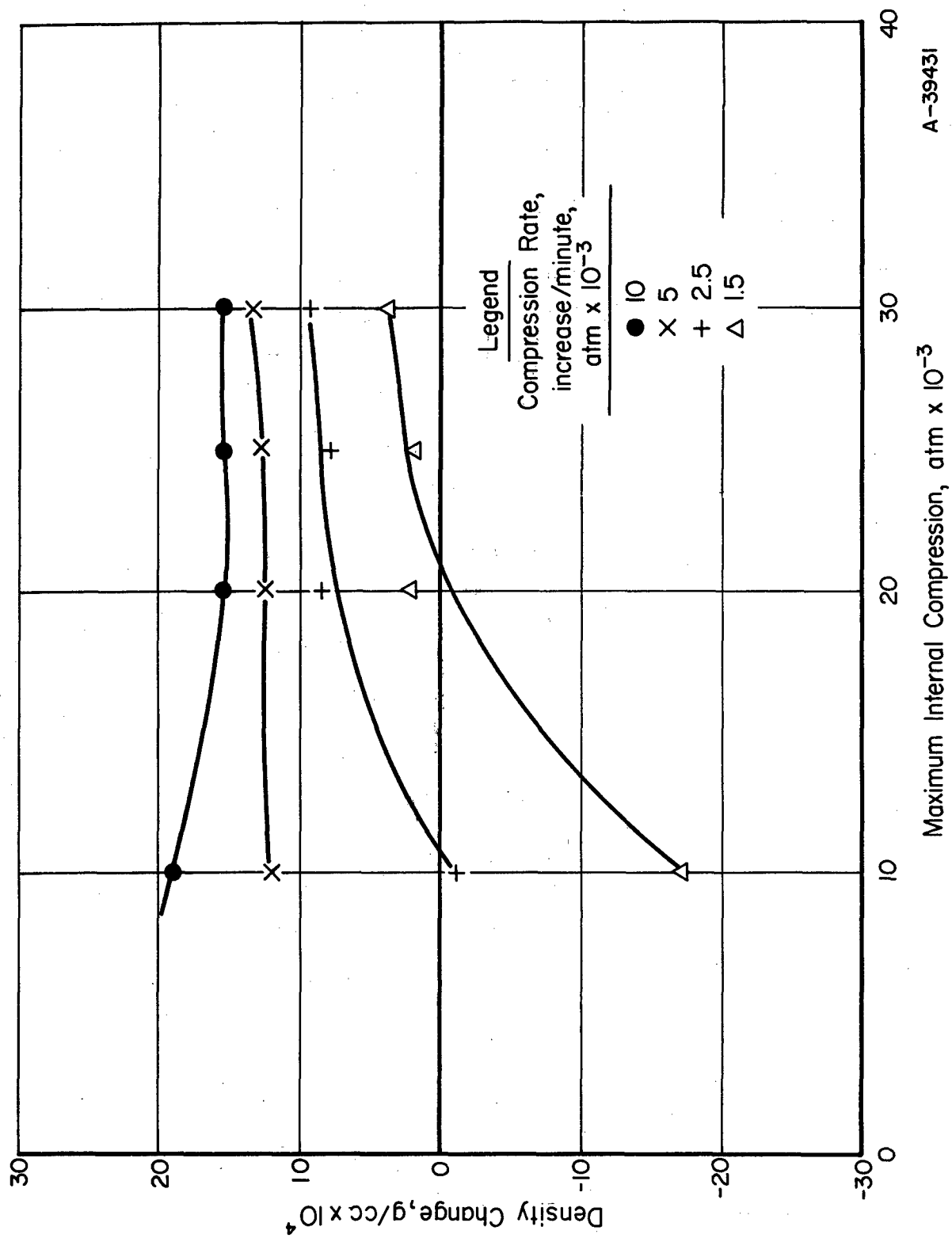
FIGURE 7.   PROJECTED EFFECT OF INTERNAL COMPRESSION AND COMPRESSION
RATE ON DENSITY OF POLYETHYLENE

A-39431
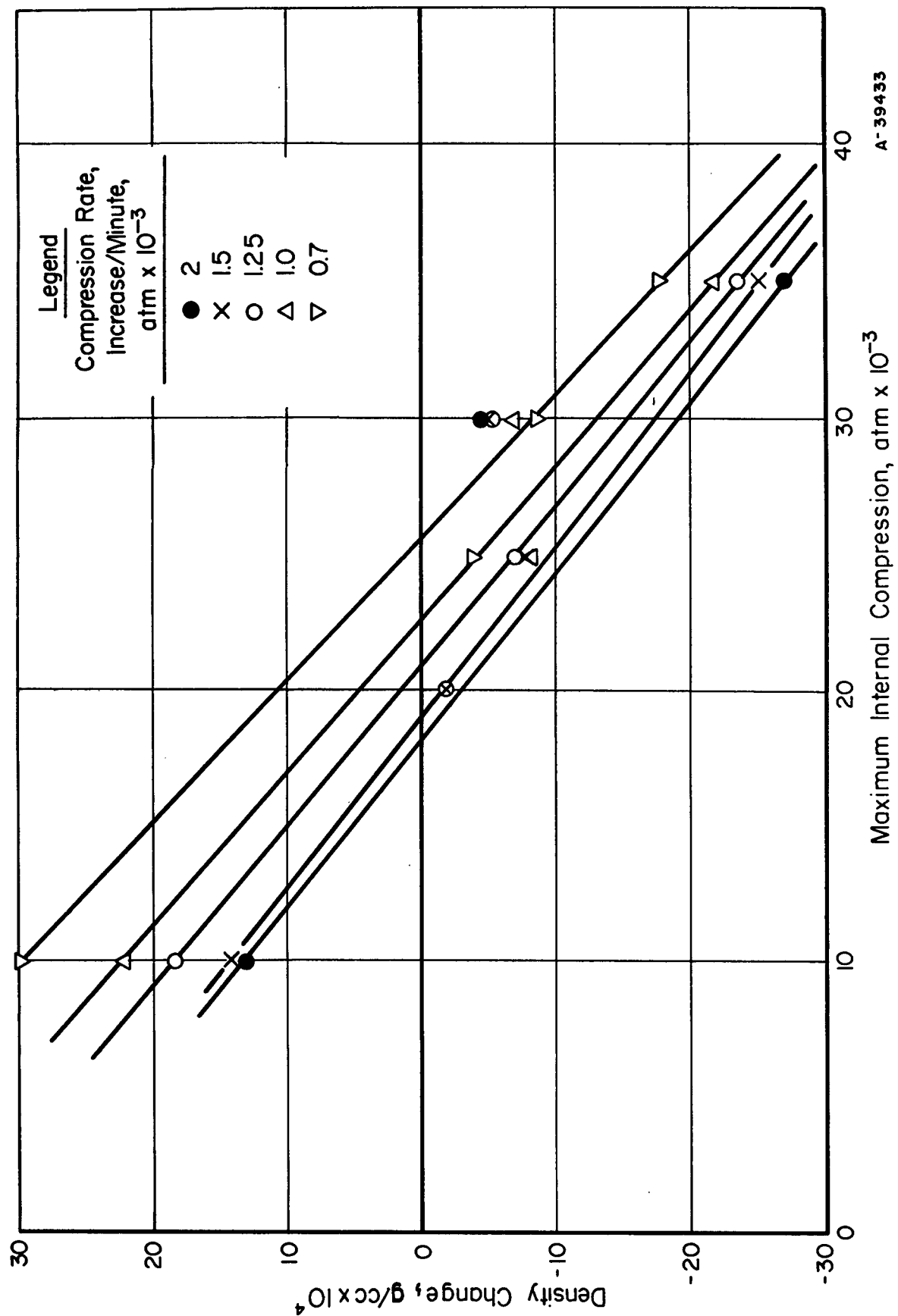
FIGURE 8. PROJECTED EFFECT OF INTERNAL COMPRESSION AND COMPRESSION RATE ON POLYMER DENSITY FOR NYLON 6

A-39433

18

density change, (2) that different polymers may have a characteristic response to a given set of compression conditions.

Polymer Compression in Target Range. Upon completion of the improved, modified die for use in this program, work progressed into the target range as discussed in the "Introduction" of this section. Although considered relative to bismuth transitions, work at 70,000 atm on the corrected transition scale is above the target range, current indications are that excursions can be made into compressions around and possibly above 100,000 atm on the corrected pressure scale and effort will be directed toward this further raising of compressions. As effort progressed into this higher compression range, much of the work on compression parameters was discontinued in favor of broadening the range of polymer coverage. Several runs, however, were made to provide correlation with the previous parameter studies and a brief study made of the effect of compression holding time.

Effect of Compression Holding Time and Correlation With Intermediate Compression Data. After completion of the modified pancake capable of operating in the target range, work was conducted with polyethylene to verify the projected trend and runs of longer duration made to determine the effect of compression holding time. The predicted effect of negligible density change for a 2-min holding period was confirmed at 90,000 atm with an observed net density change of (-0.0001 g/cc), Figure 9. However, prolonged holding periods (30 and 60 min) at comparable compressions produced significant density increases (0.0010 to 0.0026 g/cc). Similarly density increases were observed for ethyl cellulose and polystyrene. Prolonged holding of polycaprolactam (Nylon 6), Figure 10, did produce net density increases greater than that predicted from the preliminary correlation, but increasing compressions continued to show reductions in density which are consistent with the established behavior at lower compressions. Similar prolonged compressions of polyformaldehyde (Delrin) will require evaluation in a salt column since the compressed material appears sensitive to the solvent column.

Effect on Polymer Properties. This factor has not been studied in detail. Density evaluations have been used for the most part to determine whether pressure-induced changes have been effected. Early studies with high-density polyethylene and polypropylene revealed that electron-microscopy techniques could be used to show differences in fine structure of control and compressed polymers. This, however, has not been employed in the more recent runs at the higher pressures. Some evidence has been obtained to indicate changes in the solubility characteristics of compressed polymers. Polyformaldehyde appears unaffected by the solvent density gradient columns before compression. Solvent absorption of the compressed polymer, however, appears so rapid that meaningful density data cannot be obtained with the solvent columns.

Effect of Generic Types on Polymer Compression. The fact that early work indicated varying behavior for different polymers under compression makes this correlation of extreme interest. The program was set up to study a broad spectrum of carbon backbone polymers modified either in the main chain or on a side chain. Materials scheduled in the study included several types of polyethylenes, and polyamides, polypropylene, polystyrene, polyacrylonitrile, polymethylmethacrylate, and ethyl cellulose. Results of work to date suggest differing behavior for individual polymers. Data presently are
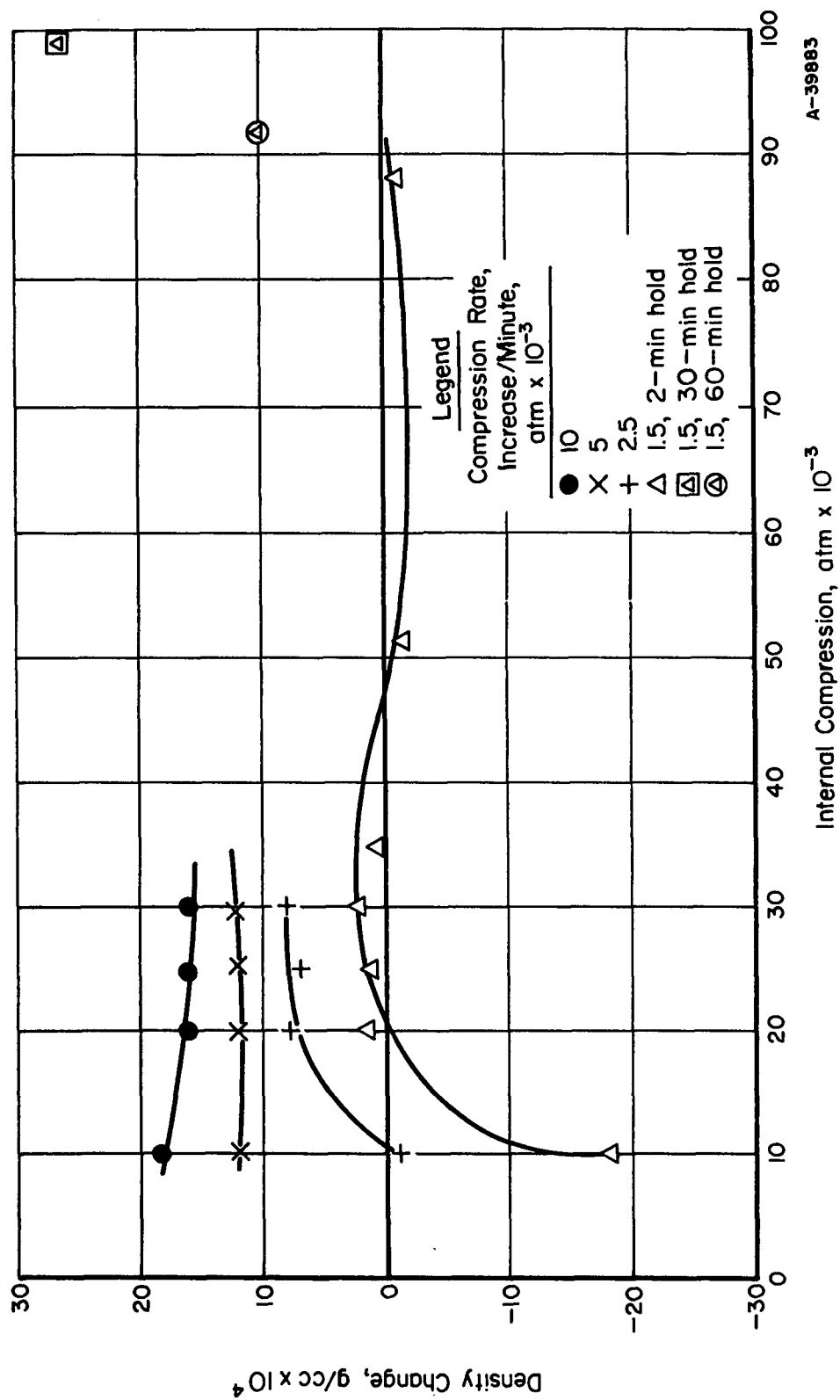
FIGURE 9. EFFECT OF COMPRESSION HOLDING TIME ON POLYMER DENSITY-POLYETHYLENE

A-39883

20
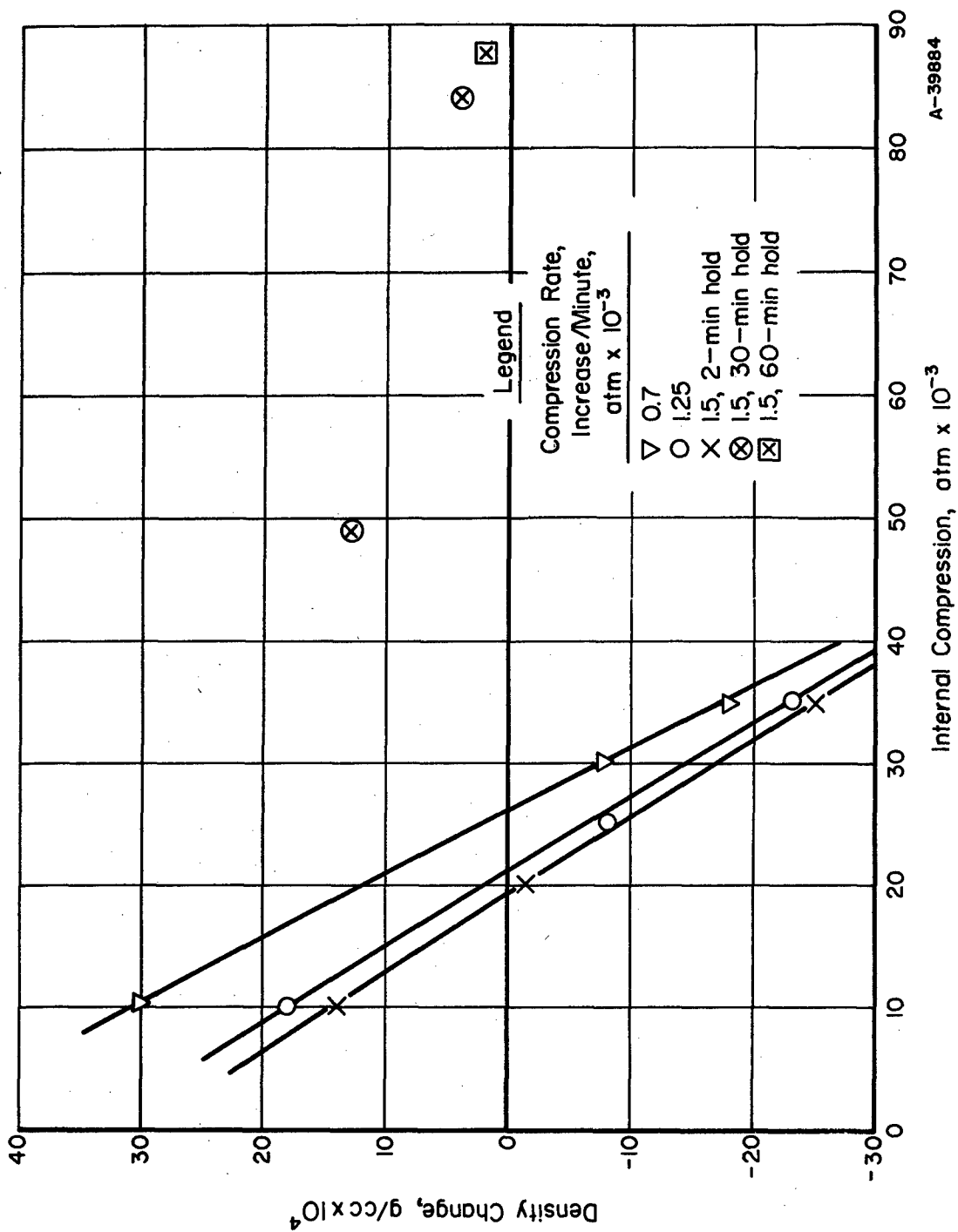
FIGURE 10. EFFECT OF COMPRESSION HOLDING TIME ON POLYMER DENSITY — NYLON 6

A-39884

21

incomplete for all materials under target conditions, but polymer behavior under compression appears, to date, to be more influenced by the generic structure than by the types within a given generic structure.

Development of Equipment and Techniques

Instrumentation. Although equipment and background were readily available on techniques involved in superpressure work, it was necessary to verify the applicability of these techniques to the organic-polymer program because of the high compressibility of these materials. Minor modifications have been introduced throughout the course of the program.

Pressure. Initially it was advisable to verify the behavior of pressure monitors in an organic-polymer sample. Considerable smearing was shown with such systems and methods were investigated to improve the efficiency and to maintain as large a polymer sample as practicable for ultimate characterization. This involved working with component parameters to upgrade efficiency and with monitor systems to optimize sensitivity and sharpness of transition.

Efforts to develop a method by which pressure data could be obtained routinely for experimental runs led into a study of several parameters before a promising system was developed.

Initial transition determinations were conducted with a 2-mil platinum wire pour-coated with molten bismuth.* This was substituted for the center thermocouple and run through the pyrophyllite end plugs to make contact with the anvils. Resistivity measurements recorded as a function of pressure indicated the transition by a sharp change in resistance. The small size and low tensile strength of the platinum core made this pressure monitor highly susceptible to breakage during assembly. Further, pouring molten bismuth down a vertical wire gave very nonuniform coatings. Much better uniformity was obtained by the melt-chill technique subsequently developed. In this method, the bottom of a metal crucible was drilled with a fine hole slightly larger than the wire. The wire was inserted in the hole and a shallow layer of bismuth warmed to fusion. Rapidly drawing the wire through the orifice caused a thin coating of bismuth to solidify on the wire. This technique allowed the thickness of coating to be varied by the rate of draw, the melt temperature, and the number of passes of the wire through the melt.

The extreme fragility of the coated platinum wire prompted a search for a more serviceable system. Since the very fine platinum wire was used to minimize the conductance of the core material, substitutes were sought in resistance wires which would possess better tensile properties and would permit a larger wire to be used without significant change in core conductivity. Initially, the effect of coating thickness was ignored until the chill-coating technique, which permitted controlled application, was developed. Comparison of transition determinations with platinum and different-sized Chromel wire, Figure 11, indicated that bismuth-coated Chromel transition wires could be substituted for bismuth-coated platinum for monitoring pressure. Further, results suggested that proper specification of dimensions would give a monitoring device of improved sensitivity.

---

*Technique based on work for AEC Contract No. W-7405-eng-92 by W. B. Wilson, Battelle Memorial Institute.
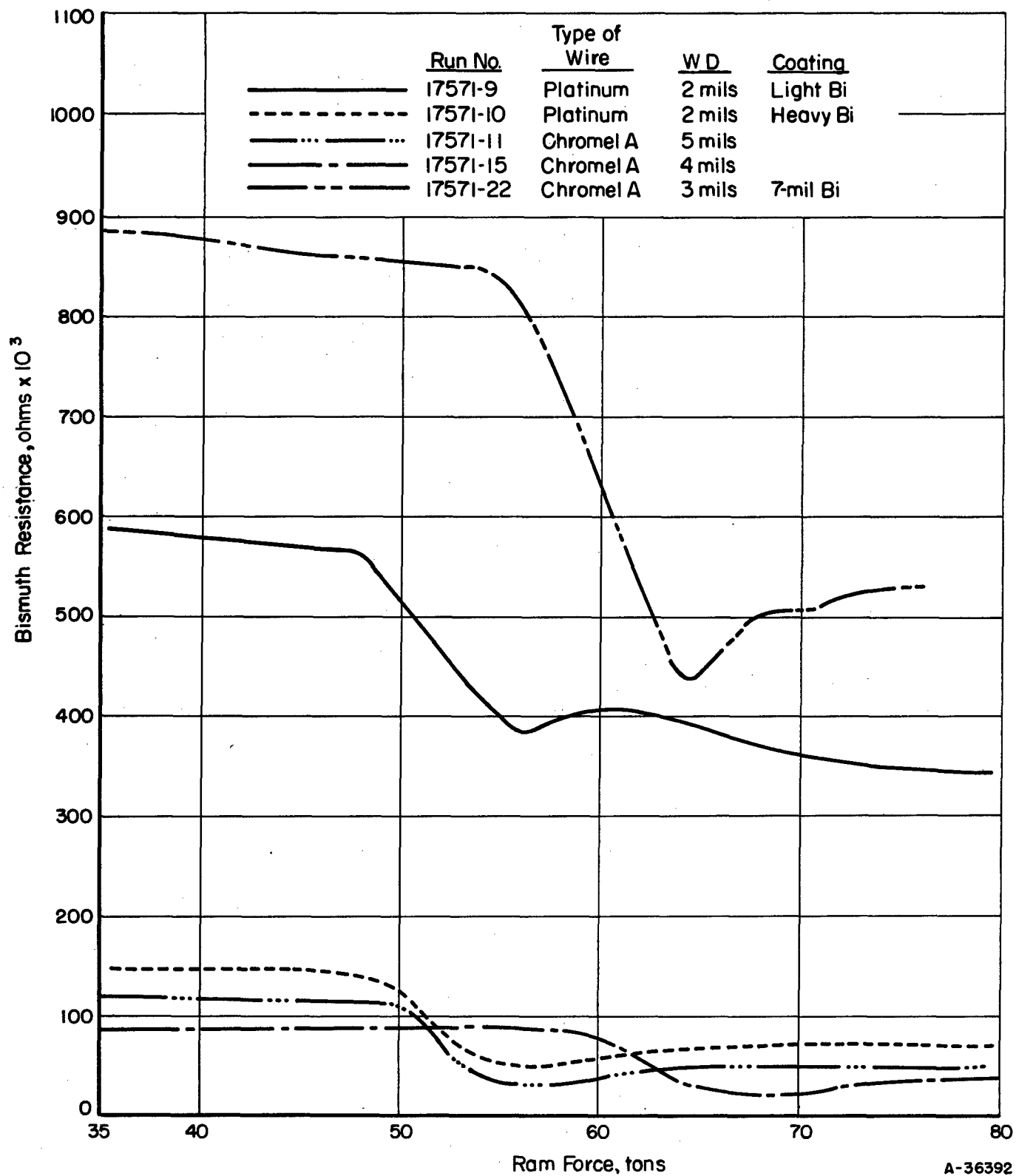
FIGURE 11. EFFECT OF CORE WIRE AND WIRE SIZE ON BISMUTH
TRANSITION DETERMINATIONS

23

Two implications of the effect of the bismuth-to-wire ratio were investigated further and results are presented in Figure 12. The data indicate that a high order of sensitivity is obtained with bismuth-to-wire ratios around 3. Some advantage may exist in the use of core wires finer than 3 mils, but the advantage would seem to be in the amount of space occupied in the specimen. There is no indication that sensitivity would be improved, and the use of smaller gage core wires would give a significantly weaker unit.

The pressure-induced Bi I-II and II-III transitions have been extremely useful as reference values in this compression study. However, in view of the observed differences in behavior between the fairly ideal silver chloride system and the polymers studied it seemed worthwhile to monitor the compressive behavior of representative polymers at several points within the present operating limits of the apparatus. This could provide useful information in attempting to overcome the tendency of the equipment to fail under the more rigorous loadings.

An attempt was made to use several bismuth-lead alloys, reported by Bridgman[3] to show pressure-induced resistivity changes, as monitors. Three alloys were tried. The first containing a fraction of an atomic per cent of lead in bismuth produced the pronounced increase in resistivity change at the Bi I-II and II-III transition without appearing to change the compression requirements. This confirmed the behavior reported by Bridgman. It was hoped, therefore, to use two other Bi-Pb alloys, 15Bi-85Pb and 10Bi-90Pb (atomic per cent), as monitors for 49,000 and 75,000 atm. Attempts, however, to find a resistance change for the 15Bi-85Pb alloy were unsuccessful even with continuous monitoring. Operation in the range of the 10Bi-90Pb alloy resulted in die damage and was discontinued.

Runs using thallium as a monitor for compressions of about 40,000 atm were successful in that a fairly satisfactory resistance change was detected. An attempt was made to use a 98.5Tl-1.5Bi (atomic per cent) alloy reported by Bridgman[3] to show a significant resistance inflection at about 50 kilobars. Several runs were made to try to obtain meaningful data. Considerable fluctuation in signal was recorded in the range where a resistance break was expected, but no definitive data were obtained.

A single run was made using a barium monitor in silver chloride for die-calibration purposes. As previously shown, the anticipated inflection in resistivity was obtained. The press-load requirement, however, was greater than expected from previous calibration data. The deviation could be due to die distortion prior to the destruction occurring at the end of the run.

Concurrently with compression studies, a run was made to determine the effect of monitor hole size on press-load requirements. A standard polyethylene assembly was used with three bismuth wire monitors placed equidistant through the length of the cylinders. Results are shown in Table 3. It was noted that consistently higher loadings were required for the larger holes. The magnitude of the difference, however, was such that it is probably within experimental limitations of the work. Monitor installations invariably have been made in holes drilled as small as possible to accommodate the monitor used.

24
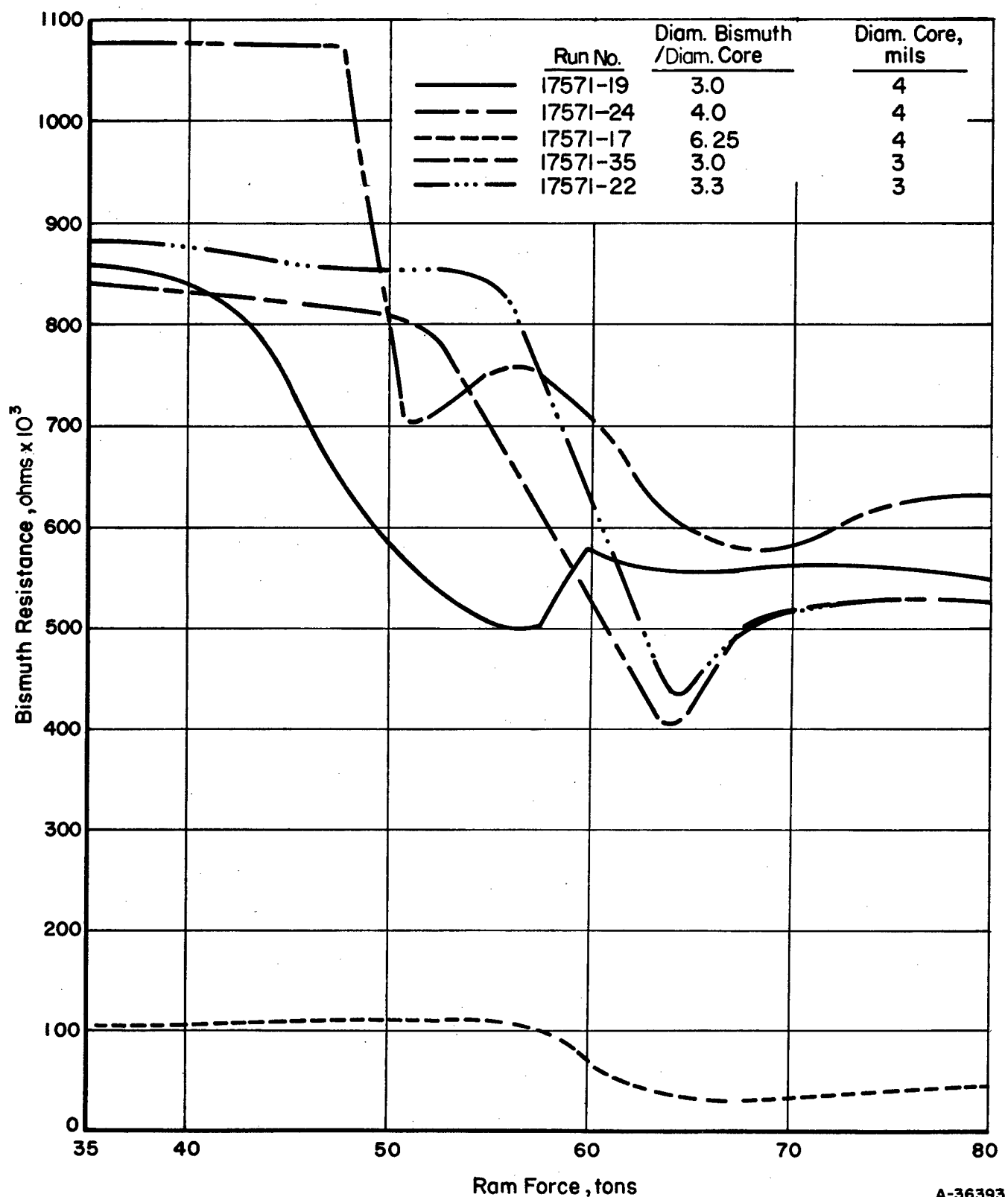
FIGURE 12. EFFECT OF RATIO OF BISMUTH TO CORE DIAMETERS ON
TRANSITION DETERMINATION

25

TABLE 3. EFFECT OF MONITOR HOLE SIZE ON LOADING TO PRODUCE TRANSITION

Monitor Hole Size, mils	Ram Force to Produce Bi I-II Transition, tons
14	47. 1
20	47. 45
25	48. 25

Note: Assembly – polyethylene sample contained within concentric pyro-
phyllite and silver chloride sleeves. Monitors placed equidistant
from each other and from the center of the polymer slug.

It was observed that standardization runs in the 100-ton press with silver chloride inserts consistently gave maximum compressions around 60,000 to 65,000 atm. Runs with different polymeric material were invariably lower, ranging from 37,000 to 44,000 atm in the preliminary runs. The observed variation could be real, that is, due to the unavoidable difference in compressibility and flow characteristics, or it could be due to lower press efficiency resulting from voids introduced during assembly. A series of runs were made to determine whether improvement in press efficiency could be effected by increasing the pyrophyllite loading of the cavity. While some improvement in estimated maximum compression was attained, the value was still about 30 per cent short of the standardization value obtained with silver chloride inserts. The appearance of the polymer slugs after compression in this series suggested the possibility of localization of pressure under the center of the anvils where transition determinations normally were made. It appeared worthwhile to determine whether a significant pressure gradient did exist in the compression zone before attempting to further increase internal pressure by cavity loading. However, since variations in transition pressures were observed in presumably duplicate runs, it was advisable to determine the transition behavior for a single run at different locations, rather than for a series of runs at various locations.

Initial attempts to simultaneously measure several transition characteristics consisted of running variously placed transition wires out through grooves in the Belt gasket. The bismuth-coated 3-mil Chromel wires were joined to 25-mil copper wire immediately outside the gasket to reduce the effect of external resistance. Satisfactory continuity was maintained over the pressure range attained, but resistivity measurements were erratic and did not provide the desired resolution. It was apparent that to be meaningful the order of resolution for all transition determinations would have to approach data such as are obtained through the anvil circuit where smooth curves with characteristic transition breaks are obtained. Considerable improvement in sensitivity was obtained with two pressure-sensitive wires when contact for one was made through the metal cones. * In this run, the bismuth coating was stripped from the core wire except for the length running through the sample holder. Although the sensitivity of this assembly showed considerable improvement, the resolution for both the anvil-circuit and the cone-contact monitors was inferior to many anvil-circuit measurements. A subsequent run in which the bismuth coating was left intact over the entire length of core wire produced the desired sensitivity and resolution (Figure 13). In addition, it was shown that a modification

---

*Method used on Air Force Office of Scientific Research Contract No. AF 49 (638-441) by A. P. Young, Battelle Memorial Institute.
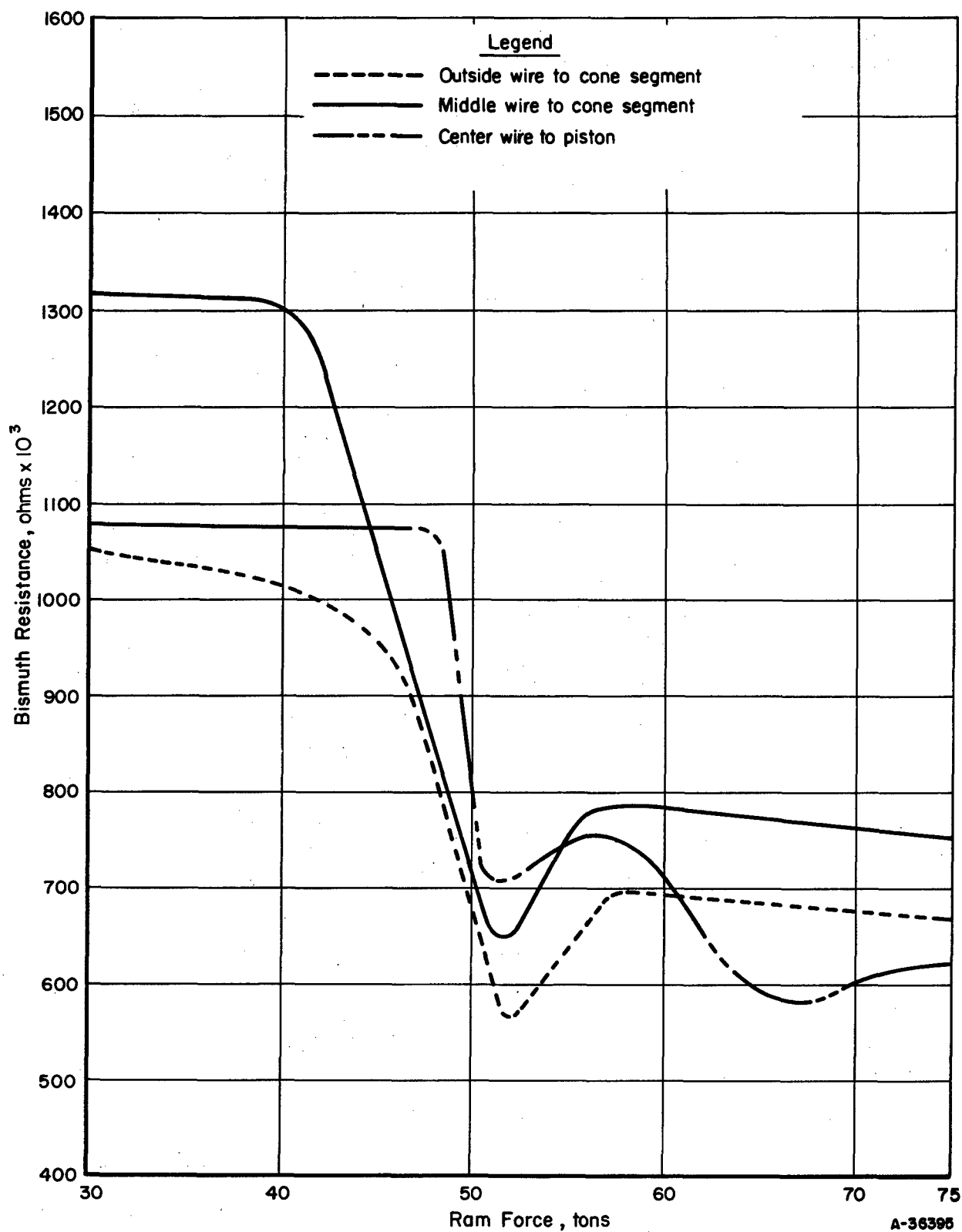
FIGURE 13. MULTIPOINT BISMUTH TRANSITION DETERMINATION IN A
POLYETHYLENE CORE

Bismuth coating full length of core.

27

of the cone-contact method could be used for increasing the amount of instrumentation by increasing the number of electrical contacts in the superpressure assembly. The operability of the technique shown in Figure 14 has not been verified for compressions exceeding 59,000 atm, but, in principle, it would seem suitable for higher service.

The compression pattern and flow properties of materials used in the superpressure assemblies raised the question of whether significant pressure gradients might exist either in the pyrophyllite sample holder or in polymer samples of significant sizes. Information relative to this point was obtained on the presence and magnitude of pressure gradients from the multipoint instrumentation runs. A comparison is made in Table 1 of the transition behavior at similar locations for pyrophyllite, polyethylene, and silver chloride. Results of single runs with multipoint monitors suggest that a slight pressure gradient does exist in the sample holder. Generally, however, transition was observed at the lowest ram force in the center of the slug and required the highest load at the edge. The effect of assembly components is also discussed from the standpoint of calibrations in the section on "Effect of Assembly Components on Compression".

Relatively early in this program it was shown that compression values could be markedly affected by different assembly components. The introduction of several dies into the experimental program required a review of the operating behavior of the different units. Since monitors imbedded in silver chloride give the best determinations of the internal pressure-ram load relationship, calibration runs were conducted using silver chloride imbedment with both bismuth and thallium monitors. Calibration data with the modified die, while new and after cracking and chipping in service, are compared (Figures 15 and 16) with an unchipped 4-deg (old design) die. Results indicate that the modified (12-deg) die is slightly more efficient than the 4-deg die while both are new. After slight service chipping and cracking, the calibration relationship of the 12-deg die nearly coincides with that of the 4-deg die.

Temperature. Concurrent with initial compression studies techniques were developed for monitoring temperatures. Instrumentation initially was for monitoring temperature changes at the center of the polymer slug and at the face of the metal sheath. The purpose was threefold:

(1) To establish whether significant temperature increase was produced by compression

(2) To develop a method for measuring the polymerization temperature of monomers

(3) To develop a method for measuring temperature of heated runs.

No significant temperature rise or difference was noted in the runs instrumented in this manner. However, pressure normally was applied slowly during a run to permit plastic flow of the gasket material. Consequently, heat of compression might easily have been dissipated. Several ways of arranging 36-gage Chromel-Alumel thermocouples were investigated. The most successful arrangement appeared to be that shown in Figure 17. The oxidized thermocouple wires were precoated with Krylon and placed in grooves cut in the pyrophyllite with a jewelers' saw. Powdered pyrophyllite was then packed over the wires to provide protection against shorting on the cones.

28

Inner pyrophyllite
gasket

Flattened copper lead wire

Split steel cone

Pyrophyllite end plug

Outer pyrophyllite gasket

Test-sample holder

Bismuth-coated Chromel wires
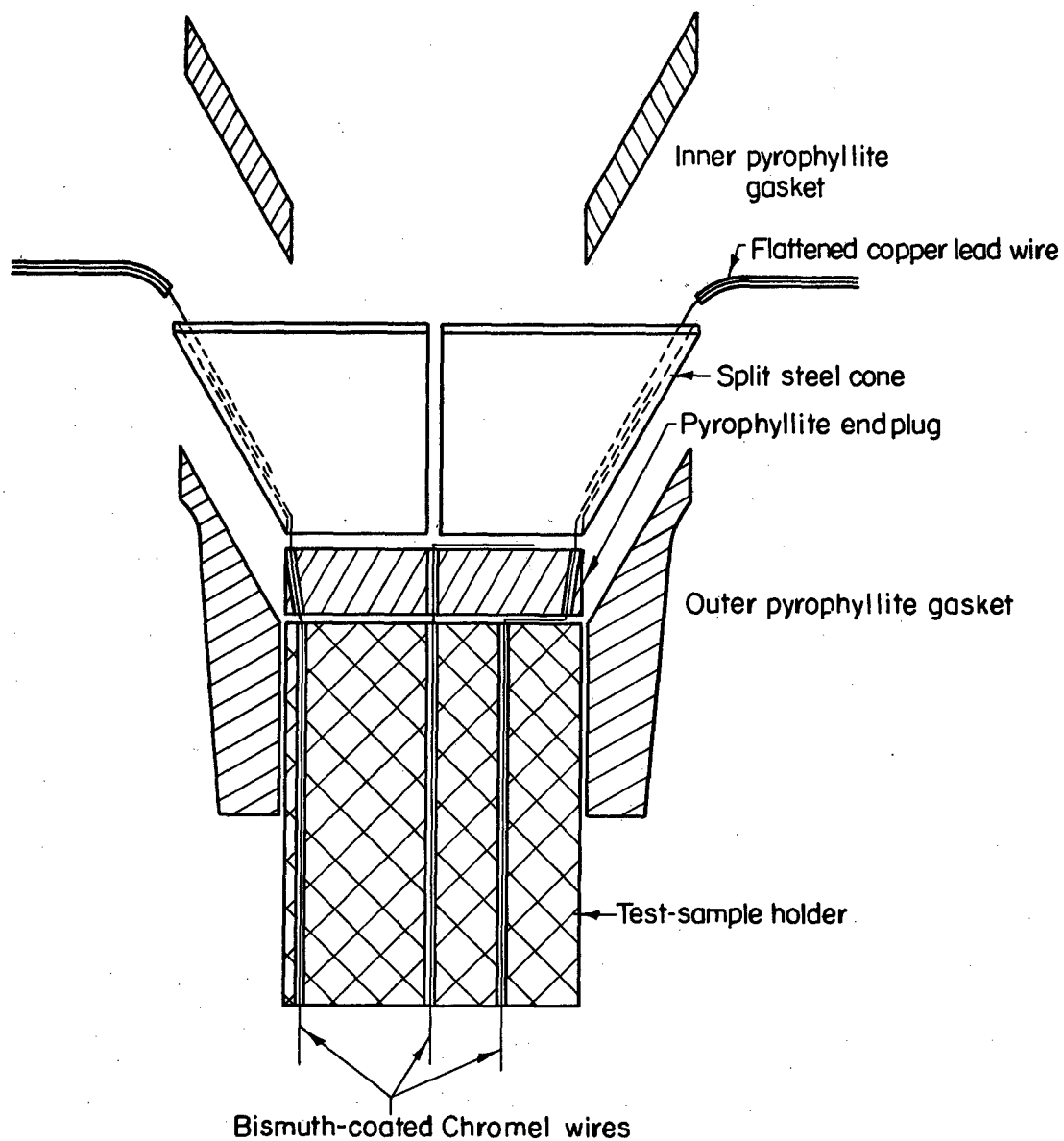
A-36394

FIGURE 14. METHOD USED FOR MULTIPOINT INSTRUMENTATION
UNDER SUPERPRESSURE OPERATION
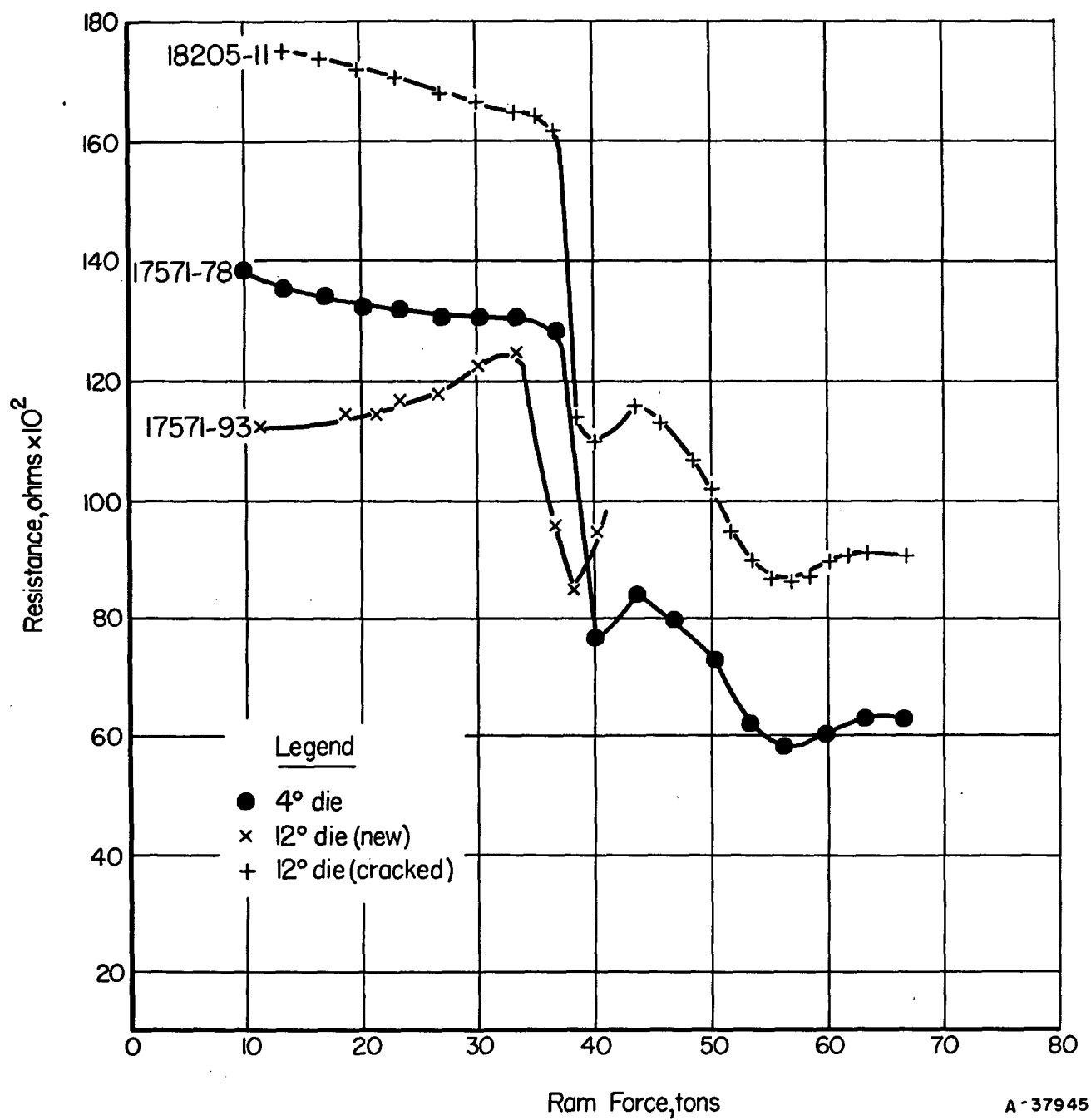
FIGURE 15.   EFFECT OF DIE VARIABLES ON BISMUTH I-II TRANSITION
IN SILVER CHLORIDE
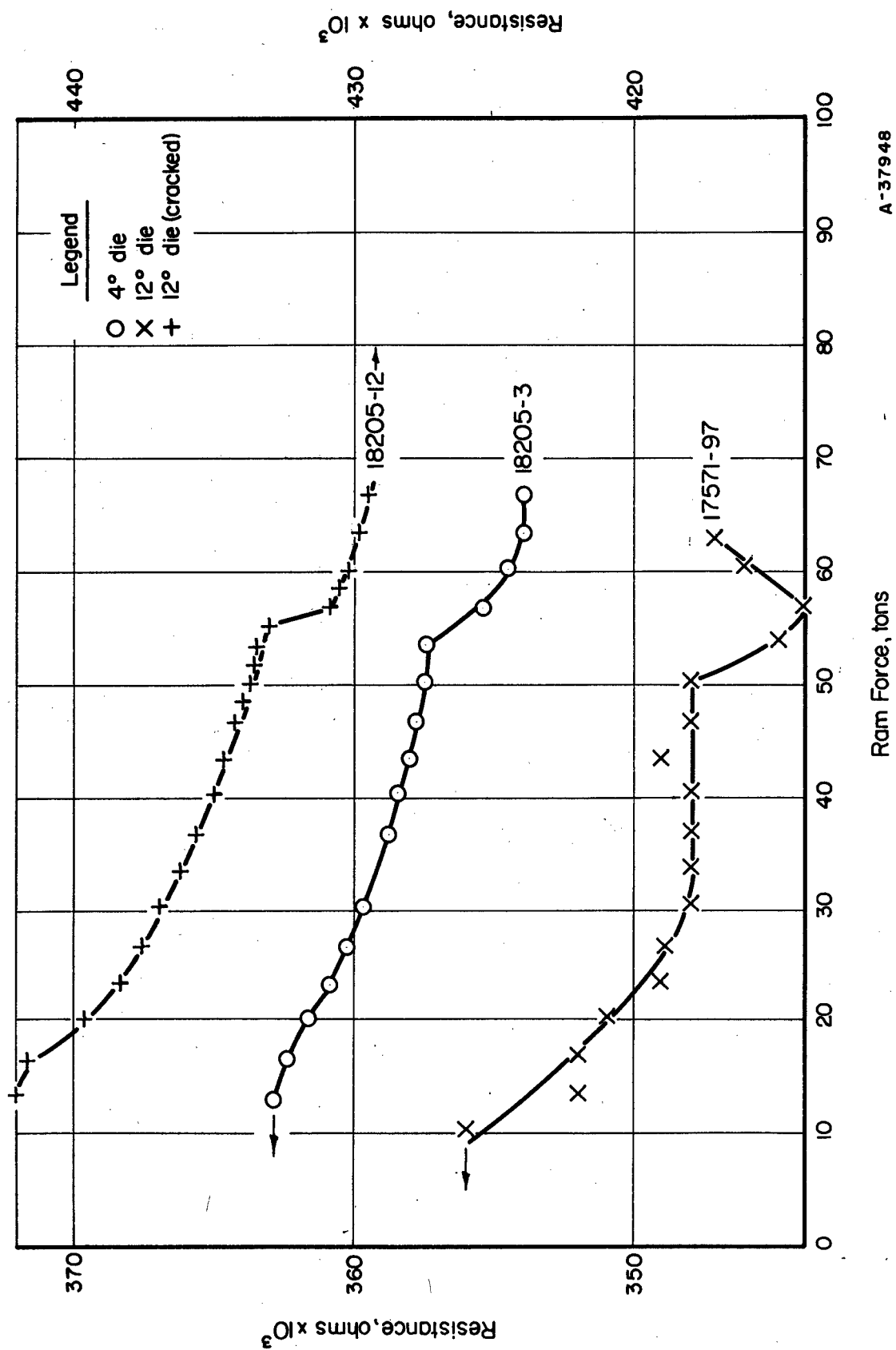
FIGURE 16. EFFECT OF DIE VARIABLES ON THALLIUM II-III TRANSITION IN SILVER CHLORIDE

A-37948
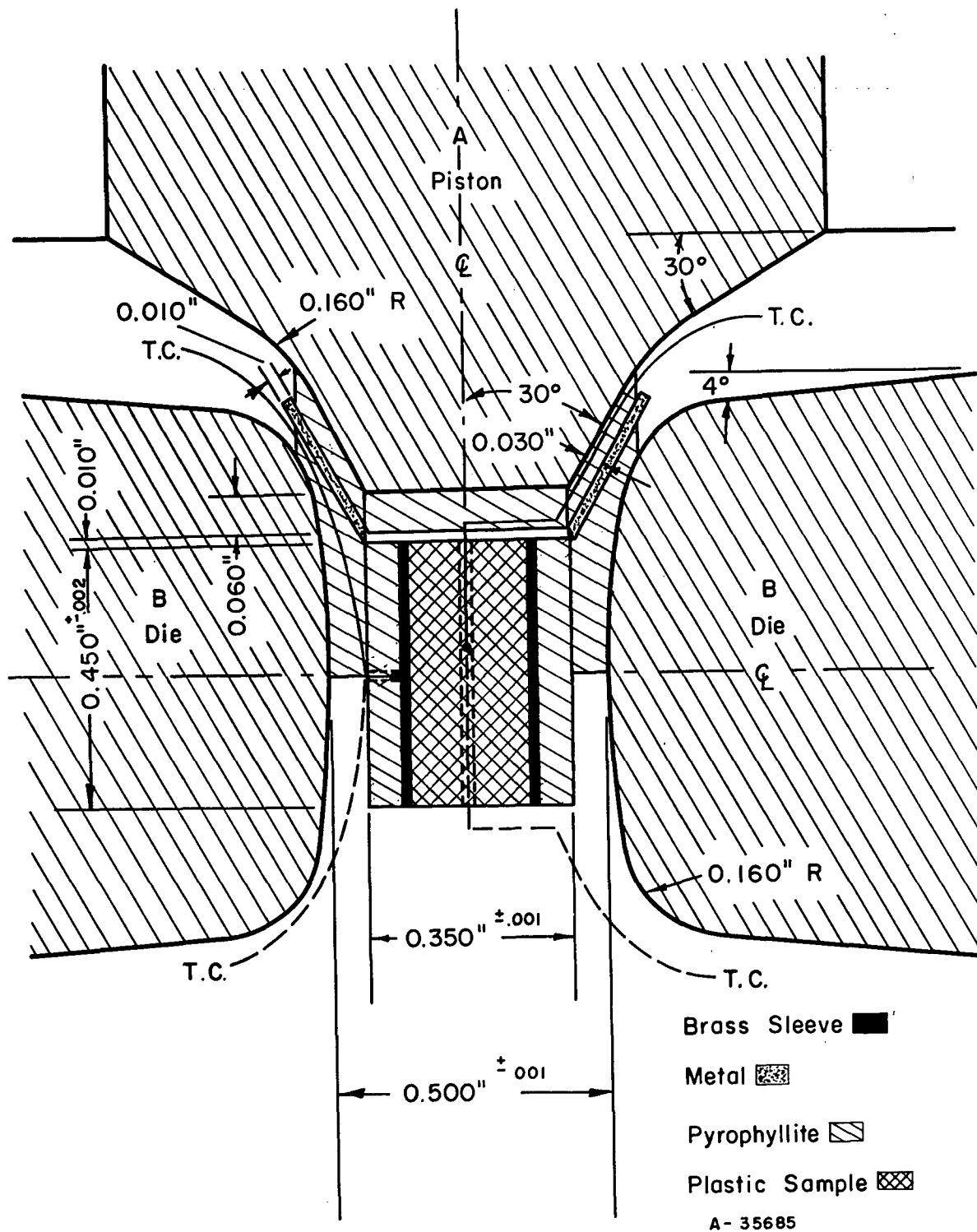
FIGURE 17. ULTRAHIGH-PRESSURE GASKET AND SAMPLE ASSEMBLY
SHOWING THERMOCOUPLE PLACEMENT

32

Heating. Techniques also were developed during the initial phases of work to allow for internal heating should this be necessary or advisable either during the polymer or monomer studies.

Initial attempts to use a silver chloride pressure-transmitting sleeve between the heater and the specimen were unsatisfactory. The inorganic sleeve acted as an insulator and effectively reduced the heat transmitted. Much better transmission was obtained when the silver chloride sleeve was placed outside the heater assembly and several successful runs were made in which the sample was heated. As a result of these studies, it appears advisable to use 5-mil resistance wire which has better heating chracteristics and occupies less space than the 8-mil wire. Further, it seems to be desirable to install the heater as close to the sample as possible. Techniques developed during this study were used in runs pressurized to 40,000 to 50,000 atm with temperatures in the range 30 to 80 C.

Compression Assembly. Ultimately polymerizations will be conducted in monomers under superpressures, therefore, it appeared expedient to develop techniques with polymers which might be extrapolated to monomers. Thus it was proposed to run polymer samples in a metal sheath with surfaces and size comparable to that contemplated for the monomer work and concurrently to the compression program to develop instrumentation for use with the monomer system.

The techniques for making thin-wall tubes and sheathed polymer rods proved satisfactory for most polymers. Where shrinkage became excessive upon cooling, heavy-wall tubes were required and in practice pressure was required during cooling. Compression molding and machining was required for polyacrylonitrile. Initially, it was believed that internal operating pressures with polymer runs possibly were between 60,000 and 65,000 atm, which is normally obtained in calibration runs on the equipment. However, results of a polymer compression monitored with a pressure-sensitive wire indicated that the maximum pressures were considerably lower than first estimated. Major effort, after discovery of the low pressures was directed toward techniques for routine instrumentation of runs to determine valid pressure values and toward methods for increasing the efficiency of compression in the 100-ton apparatus. Since considerable difficulty was encountered in obtaining bismuth transitions at press loadings as low as those obtained for calibration runs with the internal geometry used in the inorganic and semiorganic polymer work, several modifications of assembly configurations and materials were tried to improve the press efficiency in the organic-polymer program. It was confirmed that the use of an incompressible filler such as a massive metal sleeve could be used to reduce system compressibility. However, since this introduced possible complications in heating and monitoring methods, a substitute was sought which would serve as well without being electrically conductive. The properties of silver chloride suggested promise, and subsequent runs tended to confirm its usefulness. Examination of data pertinent to this study suggested that the silver chloride sleeve may serve a twofold purpose in this application:

(1) As an incompressible filler

(2) As a fluidized pressure transmission medium.

Although some improvement was effected in press efficiency by the reported modification of assembly configurations and materials, results were not entirely satisfactory.

33

Duplicate assemblies frequently showed significant differences in the press loading required to produce transitions. Study of the assembly suggested that part of the difficulty may be due to slight misfits between the Belt gaskets and the Belt. A technique was developed for grinding this gasket to fit the Belt profile. Work using this technique did reduce the ram force required to produce a given internal pressure and improved the reproducibility of operation.

Results of work involving the use of a silver chloride sleeve as an incompressible filler and pressure-transmitting medium indicated that satisfactory reproducibility, sharpness of transition, and minimum press loading to effect the Bi I-II transtition were obtained with an assembly modified from that shown in Figure 17. The modified sample assembly (Figure 18) was shortened to 0.400 in. to minimize loss of silver chloride from the assembly. The sample-holder assembly consists of a silver chloride sleeve over a pyrophyllite heater sleeve around the polymer sample. The end-cap assemblies consisted of a pyrophyllite-filled steel ring 0.35 in. in OD and 0.100 in. high, and a pyrophyllite disk 0.35 in. in diameter, and 0.30 in. thick to give a nominal over-all assembly height of 0.660 in. The run made with a silver chloride slug substituted for the polymer correlates satisfactorily with values obtained by members of the Physics of Solids group. Runs in which brass disks were used next to the piston gave evidence of a slight amount of cold flow of the brass toward the seal, suggesting that the internal pressure might be developing more rapidly than effective sealing. Flowout, however, was not observed with the steel ring, and it is believed that these rings may expand as the pistons apply loading to the pyrophyllite filler to give improved sealing.

The majority of the polymer-compression studies were conducted with the modified assembly shown in Figure 18. This performed quite satisfactorily until attempts were made to use lead-encapsulated samples in the assembly. Difficulties encountered and modifications evolved are reported in the section following.

Encapsulation. Techniques and equipment were developed for fabricating cans out of lead foil for encapsulation studies of polymer-monomer systems and ultimately monomer systems. Initially an attempt was made to fabricate a can to fit within the sample space of the assembly discussed in the previous section. An attempt to compress a unit containing a lead-sheathed polyethylene sample resulted in a major blowout at low loading. Comparison of the standard sample assembly (Figure 18) and the first sheathed sample assembly showed that the incorporation of the lead encapsulation raised the incompressible material in the sample chamber from 28.5 per cent to 32.6 per cent. Additional runs in which the incompressible material was reduced to 28.5 by reduction of the height of the sample and sample assembly were satisfactory. Preliminary results with monitored runs indicated that the modification, Figure 19, would retain similar calibration characteristics for a given polymer as the assembly used in the polymer-compression studies. Further work is in progress to verify the operability with polymer-monomer systems before proceeding to monomers alone.

Current Status of the Program

Polymer Compression. Compression techniques, instrumentation and critical parameters of this phase of study have been resolved and a number of polymers compressed in the target range. The most influential parameter appears to be the holding
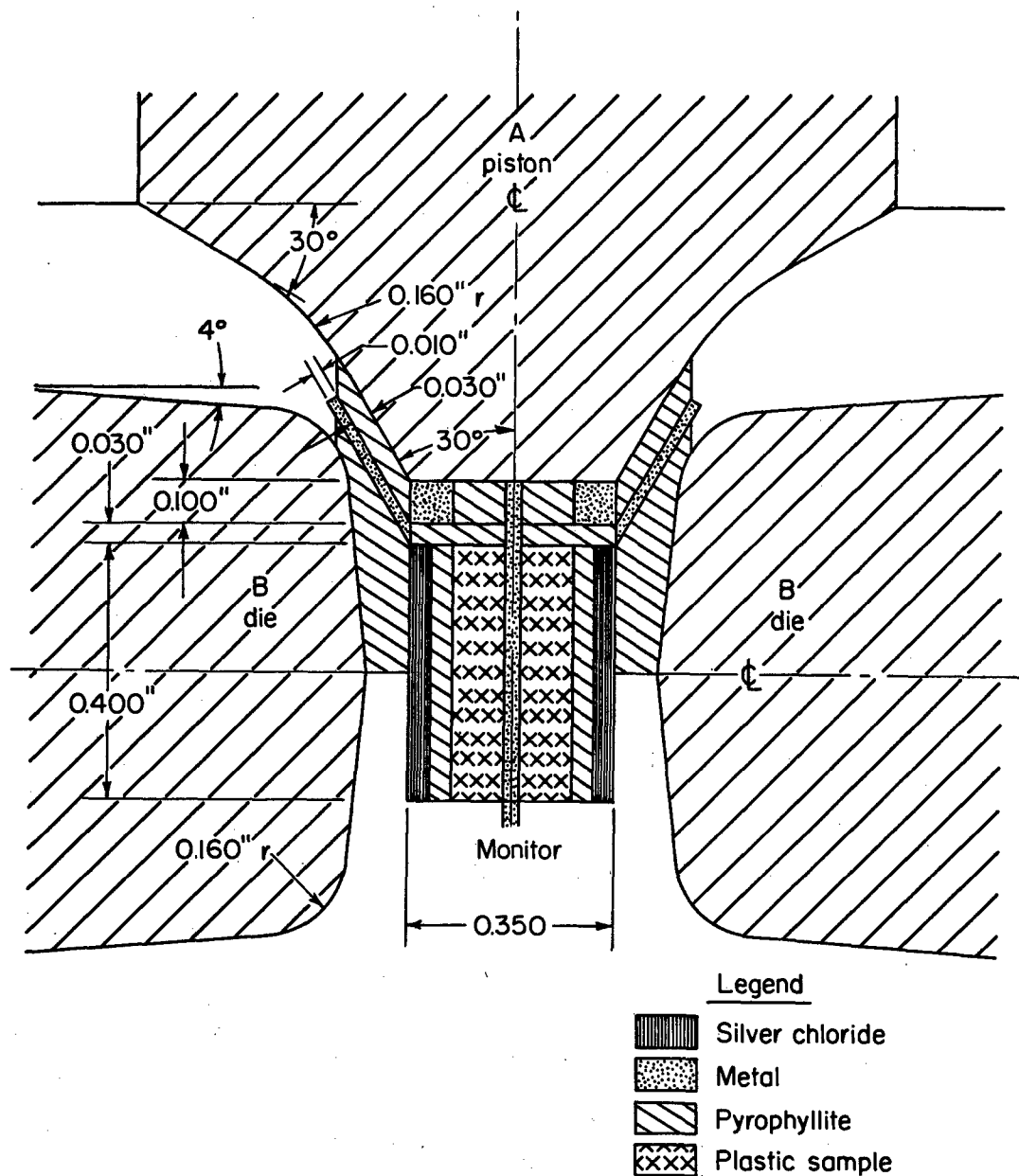
FIGURE 18. ULTRAHIGH-PRESSURE ASSEMBLY USED IN
POLYMER COMPRESSION STUDIES
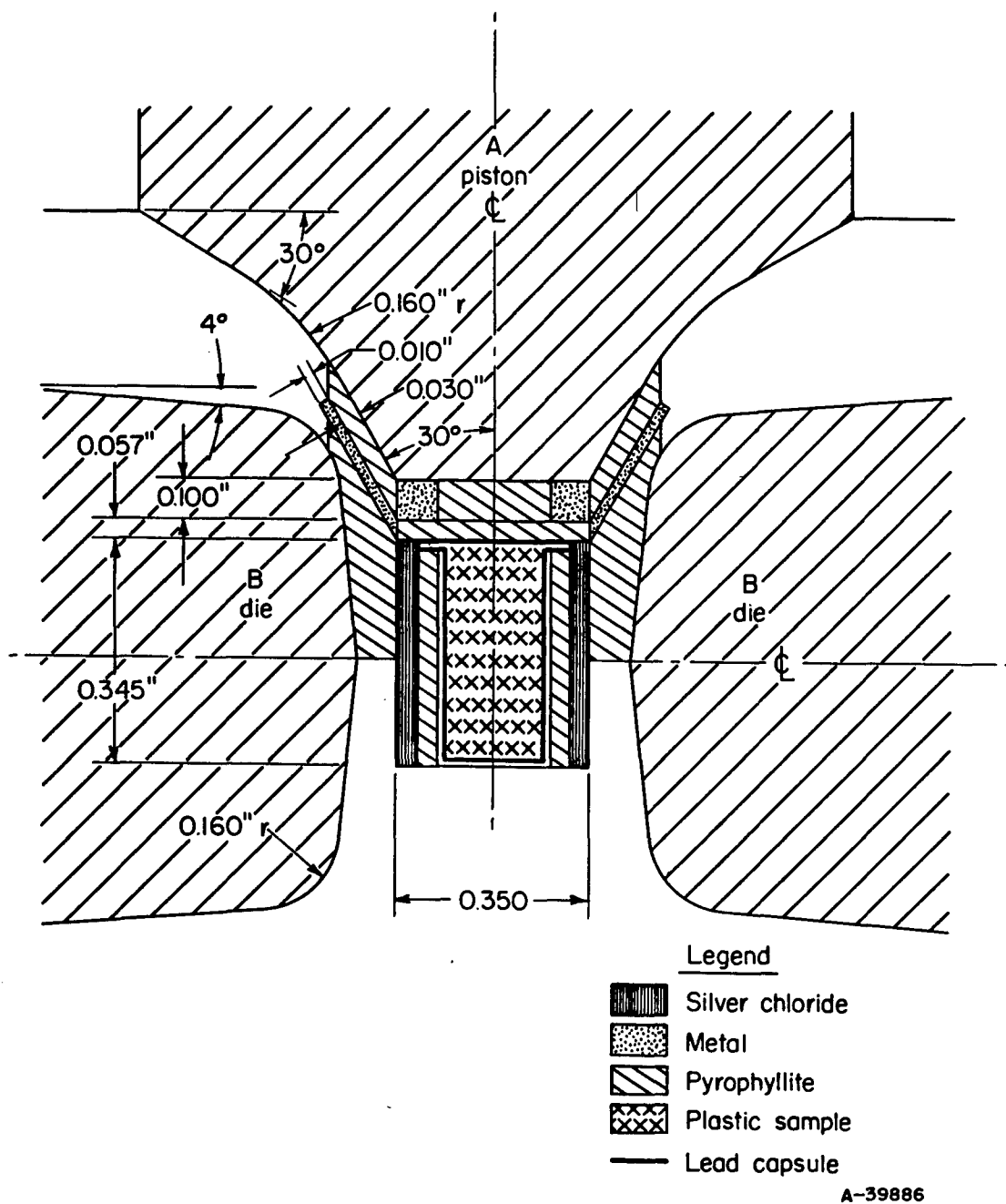
FIGURE 19. ULTRAHIGH-PRESSURE ASSEMBLY USED IN
ENCAPSULATION STUDIES

36

time. Data pertinent to this observation are summarized in Table 4. Results indicate that increased holding time is effective in increasing polymer density under compression. Prolonged runs, however, have not been made to determine whether equilibrium densities of compressed polymers ultimately reach the same value regardless of compression. Runs are contemplated under target conditions to explore this effect and with the remainder of the polymer series to further clarify the generic effect on polymer compression.

TABLE 4. EFFECT OF EXTREME COMPRESSION ON
THE DENSITY OF ORGANIC POLYMERS

Run	Material	Maximum Press Load, tons	Estimated Maximum Compression, atm x 10^3	Holding Time, min	Density Change, g/cc
64	Petrothene	140	90	2	-0.0001
65	Petrothene	150	92	30	+0.0010
66	Petrothene	150	98	60	+0.0020
68	Nylon 6	50	30	Blow-out	-0.0007
67	Nylon 6	80	49	30	+0.0013
68	Nylon 6	145	83	30	+0.0004
69	Nylon 6	150	86	60	+0.0002
71	Ethocel	125	72	30	+0.0040
70	Ethocel	150	84	60	+0.0045

Polymer-Monomer Compression. Techniques and fixtures have been developed to permit fabrication of lead cans to reasonably close tolerances. Satisfactory test runs have been made with polymers encased in the units. Compression characteristics of assemblies containing these encapsulations have appeared to correlate acceptably with standard compression runs.

Runs have not been made with assemblies containing encapsulated liquid although successful sealing with liquid in the capsule has been accomplished. Samples and assemblies have been prepared for a polystyrene-styrene transition study to resolve operational behavior both in the compression and in the characterization. The monomer has not been sealed in the system pending scheduling the compression. It is hoped that varying ratios of polymer-monomer can be used to establish the behavior of assemblies containing the liquid systems. It is believed also that the small amounts of residual catalyst in the polymer may give an indication of the behavior of the catalyzed monomer system under compression.

IV. EXPERIMENTAL SECTION – SEMIORGANIC POLYMERS

Introduction

In recent years semiorganic polymers have been prepared in which elements providing thermally stable primary chains have been utilized. The elements for such chains have been selected from various alternating combinations of aluminum, boron, silicon, tin, and titanium with less electropositive elements such as oxygen, sulfur, nitrogen, phosphorus, and arsenic. Preparation of polymers having this type of primary chain with alkyl or aryl sidechains has been accomplished by conventional reactions of organometallic compounds. Although polymers of moderately high molecular weight have been obtained, there is still room for improvement in either thermal stability, resistance to hydrolysis, or moldability. Consequently, it is of value to investigate the possibility of using extreme pressure to bring about new polymerization reactions or modifications in known polymers that would result in improved properties.

On the basis of achieving polymerization through reactive unsaturated groups, which at the same time offer potential thermal stability, the compound $(CH_3)_2Si(CN)_2$ was selected. It was felt that under high pressure and at elevated temperature a polymer incorporating $C\!=\!N$ linkages or a triazine structure could be obtained. Similarly, $C_2H_5P(CN)_2$ was included because phosphorus offers potential for additional bonding beyond that occurring with silicon.

Low polymers of the type

$$
\begin{bmatrix}
& R' & \\
& | & \\
-Al-O-Si-O- & \\
| & | & \\
O & R' & \\
R & &
\end{bmatrix}_X
$$
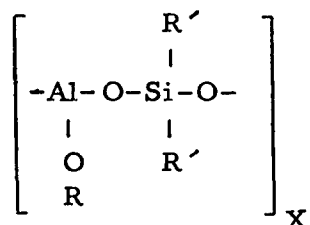
offer the possibility of increasing their molecular weight by crosslinking of side chains. In this series polymeric materials were prepared having either acetylacetone or isopropoxide attached to the aluminum, and methyl, ethyl, or phenyl on the silicon. With the same objective in view, a bicyclic compound incorporating arsenic (III)-oxygen-silicon linkages and a low polymer having arsenic (V)-oxygen-silicon bonding were included.

Phosphonitrilic chloride trimer $(PNCl_2)_3$ is known to polymerize to a rubberlike material on heating. It was decided to investigate the effect of extreme pressure on this reaction, to see if a new polymeric product could be obtained. Linear polymers of low molecular weight were included in this study also.

In a similar vein, a phosphinoborine trimer, $[(C_6H_5)_2PBH_2]_3$, was selected for examination because of the possibility of ring opening to form polymeric materials with varied amounts of crosslinking.

Experimental Results

Preparation of Materials

The preparations were designed to obtain approximately 20 g of each material. Although this amount is several times what may ultimately be consumed, it permits the use of containers of reasonable size and permits handling of materials on a macro scale.

Dimethyldicyanosilane Preparation.

Dimethyldicyanosilane was prepared by the following sequence of reactions:

$$(CH_3)_2SiCl_2 + 2\ C_6H_5MgBr \rightarrow (CH_3)_2Si(C_6H_5)_2 + MgCl_2 + MgBr_2$$

$$(CH_3)_2Si(C_6H_5)_2 + 2\ Br_2 \rightarrow (CH_3)_2SiBr_2 + 2\ C_6H_5Br$$

$$(CH_3)_2SiBr_2 + 2\ AgCN \rightarrow (CH_3)_2Si(CN)_2 + 2\ AgBr.$$
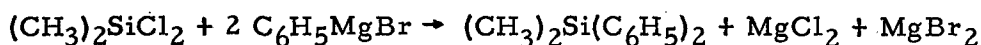
The method in general was that described by McBride and Beachell[4], although the procedures were modified where it seemed advantageous. The intermediates were separated but were not highly purified before reacting them further.

Dimethyldiphenylsilane.

Dimethyldichlorosilane (134 g, 1.04 moles) was added dropwise, with stirring, to 2.1 moles of phenylmagnesium bromide in ether solution. The reaction was carried out in a 1-liter three-neck flask fitted with a reflux condenser. A drying tube attached to the condenser excluded atmospheric moisture. After the addition was completed, the mixture was refluxed gently for 2 hr. Water was then added dropwise to destroy any unreacted phenylmagnesium bromide.

The contents of the reaction vessel were filtered through a Buchner funnel, and the residue was washed several times with ether. The ether was then distilled from the mixture at atmospheric pressure in a system protected from moisture. The distillation was continued until a temperature of 71 C was attained. The solution remaining was then distilled at a pressure of 46 mm in a stream of dry nitrogen. Distillate of 172.3 g boiling between 172 and 180 C was collected. This represents a yield of 78 per cent if the product is pure dimethyldiphenylsilane. The boiling point previously reported[4] is 176 to 178 C (45 mm). Although the distillate was not pure, no attempt was made to purify it further because it was an intermediate in the over-all preparation.

Dimethyldibromosilane.

The 172 g of distillate, which represented about 0.8 mole of dimethyldiphenylsilane, was transferred to a 500-ml three-neck flask. This was fitted with a stirrer and a reflux condenser to which a drying tube was attached. The flask was cooled with an ice bath. Approximately 1.6 moles of bromine (261 g) were added dropwise to the dimethyldiphenylsilane over a 6 to 7-hour period, after which the mixture was refluxed for 63 hr at 50 to 60 C. The unreacted bromine was then consumed by dropwise addition of pentene. The resulting solution was colored light orange. This solution was distilled from the reaction vessel through a Vigreaux column and collected in a flask protected by a drying tube. During the changing of receivers a stream of dry nitrogen purged the system. The distillate obtained between 95 and 127 C was collected in a three-neck

flask and retained for the final reaction. This fraction weighed 111.0 g and represented a yield of 63 per cent, based on dimethyldibromosilane. The boiling point of this material is reported to be 110 to 112 C[4], but a wider cut was taken to insure sufficient volume of liquid for the final step.

Dimethyldicyanosilane. The final reaction was carried out in a 500-ml three-neck flask which was fitted with a stirrer and reflux condenser. The product was then distilled through an air condenser into a receiver protected with a drying tube.

Silver cyanide (148 g, 1.1 moles) was added stepwise with stirring over a period of 1.25 hours to the 111.0 g (0.5 mole) of the dimethyldibromosilane which had been dissolved in benzene. During the reaction, heat was evolved, and the white solid became a canary yellow. The mixture was refluxed 2.75 hr with stirring after adding the silver cyanide. The benzene was then distilled directly from the flask and the flask purged overnight with dry nitrogen. Water-clear, needlelike crystals of dimethyldicyanosilane were noted in and above the solid cake when the mixture had cooled.

The dimethyldicyanosilane was distilled from the mixture at 165 to 171 C (749.5 mm). The product was a waxy crystalline solid melting at 81 to 83 C. The yield in the last step was 35.2 per cent, and the over-all yield, computed from the amount of dimethyldichlorosilane taken originally, was 17.1 per cent.

Diisopropoxy-Aluminum Acetylacetonate. Freshly distilled acetylacetone (1.1 moles) was added dropwise with stirring to a slurry of 1.1 moles of aluminum isopropoxide in 200 ml of hexane contained in a 500-ml three-neck flask which was fitted with a reflux condenser. The addition of the acetylacetone was so regulated that the heat of reaction produced a gentle refluxing. Upon completing the addition of the acetylacetone, the mixture was stirred until it had cooled to room temperature.

The slurry was then transferred to a vacuum distillation flask and the hexane distilled off at atmospheric pressure. The residue consisted of a white cloudy liquid and a white, finely divided solid. The mixture was vacuum distilled at a pressure of 5 mm in a stream of dry nitrogen. As the distilling temperature of 150 to 153 C was attained, the liquid turned light yellow. Foaming also occurred early in the distillation. This carried over impurities, making it necessary to redistill the product.

The second distillation was carried out as the first distillation but at a pressure of 1 mm. Also, the still head was wrapped with a heating tape to maintain a more uniform temperature in this region.

The diisopropoxy-aluminum acetylacetonate was a light-yellow, viscous liquid which distilled readily at 142 to 143 C (1 mm). The product weighed 187.4 g, which represents a yield of 68.9 per cent. Upon standing, white crystals formed slowly.

The boiling point of diisopropoxy-aluminum acetylacetonate has been reported to be 135 to 138 C at 0.2 mm.[5]

Dimethyldiacetoxysilane. One-half mole (64.5 g) of dimethyldichlorosilane dissolved in 100 ml of dry ether was added with stirring to a slurry of 2 moles of powdered

40

anhydrous sodium acetate in 400 ml of dry ether. The slurry was contained in a 1-liter three-neck flask which was fitted with a reflux condenser. A drying tube filled with Drierite was attached to the condenser to exclude atmospheric moisture. The dimethyldichlorosilane-ether solution was added rapidly enough to insure gentle refluxing from the heat of reaction. The mixture was stirred for 2 hr, and the slurry was then transferred under a dry-nitrogen atmosphere to a filter column fitted with a fritted glass filter (medium porosity). Filtration was carried out under a slight pressure of dry nitrogen. The residue was washed twice with dry ether. The ether extract and washings were then transferred to a vacuum-distillation flask which was fitted with a Vigreaux column, and the ether was distilled off at atmospheric pressure. The water-white liquid which remained was then distilled at a pressure of 2 mm and a temperature of 39 to 40 C in a stream of dry nitrogen. The water-clear distillate weighed 72.7 g. This represents a yield of 82.6 per cent.

Diethyldiacetoxysilane. Diethyldichlorosilane (84.2 g, 0.536 mole) was dissolved in 100 ml of low-boiling petroleum ether and added dropwise, with stirring, to a slurry of anhydrous sodium acetate (164 g, 2 moles) in 400 ml of the petroleum ether. The reaction was conducted in a three-neck flask provided with a reflux condenser which was protected from atmospheric moisture by a drying tube. The diethyldichlorosilane was added slowly enough to prevent boiling of the reaction mixture as a result of the of reaction. The mixture was then refluxed for 2 hr, with stirring, after which it was transferred under dry-nitrogen pressure to a filter column containing a fritted glass disk. Filtration was carried out under a slight pressure of dry nitrogen, and the residue was washed with petroleum ether. The solvent was then stripped off from the combined filtrate and washings by distillation at atmospheric pressure. The diethyldiacetoxysilane was then distilled through a Vigreaux column in a stream of dry nitrogen at a pressure of 3 mm. The boiling point of the product was 65 to 67 C (3 mm), and the yield was 61 per cent. A previous report of this compound in the literature[6] gave a boiling point of 70 to 72 C at 4 mm.

Diphenyldiacetoxysilane. This compound was prepared in the same manner as the diethyl derivative, using diphenyldichlorosilane (189.7 g, 0.75 mole) and anhydrous sodium acetate (246.1 g, 1.5 moles). The diphenyldiacetoxysilane had a boiling point of 143 to 146 C (1 mm). A yield of 78.4 per cent was obtained. The product remained as a liquid for several days, after which it crystallized to a solid having a melting point of 34 to 37 C.

Aluminum-Oxygen-Silicon Polymers. Polymers of the type

$$
\begin{bmatrix}
 & & R' \\
 & & | \\
-O-Al-O-Si- \\
 & | & | \\
 & O & R' \\
 & R &
\end{bmatrix}_n
$$
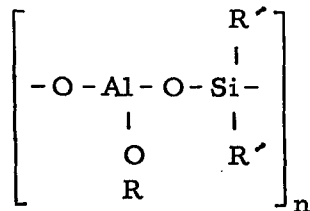
were prepared by splitting out isopropyl acetate from aluminum isopropoxide and acetoxysilane derivatives. A generalized equation can be written thus:

$$\begin{array}{ccc} CH_3 & CH_3 & R' \\ | & | & | \\ n\ HC-O-Al-O-CH & +\ n\ CH_3COO-Si-OOCCH_3 & \rightarrow \\ | \quad | \quad | & | \\ CH_3 \quad O \quad CH_3 & R' \\ \quad\ \ R \end{array}$$

$$\begin{array}{cc} CH_3 & \qquad\qquad R' \\ | & \qquad\qquad | \\ (2n\text{-}1)\ HC-OOCCH_3\ + & \left[\ -O-Al-O-Si-\ \right] \\ | & \qquad\qquad |\qquad\ | \\ CH_3 & \qquad\qquad O\qquad R' \\ & \qquad\qquad R \qquad\qquad\ _n \end{array}$$
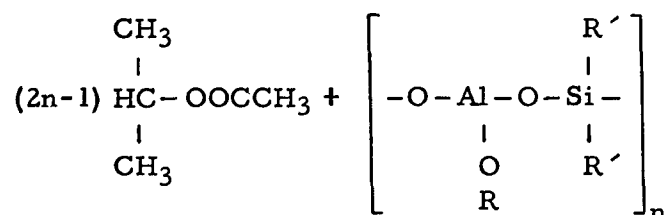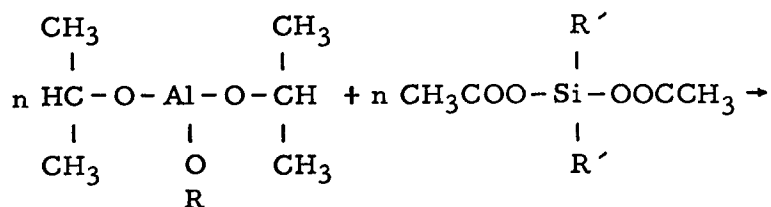
The "OR" groups attached to the aluminum have been isopropoxide and acetylacetone, the latter undoubtedly bonded to the aluminum by a coordinate bond in addition to the covalent link indicated. The R' groups attached to the silicon have been methyl, ethyl, and phenyl. The following combinations were prepared:

OR	R'
Isopropoxide	Ethyl
Isopropoxide	Phenyl
Acetylacetone	Methyl
Acetylacetone	Ethyl

Dimethylsiloxy-Aluminum-Acetylacetonate Polymer. The polymeric materials were prepared by methods developed by Gibbs and associates.[7] Diisopropoxy-aluminum acetylacetonate (41.9 g, 0.172 mole) was slurried in 45 ml of anhydrous hexane. The mixture was maintained at a gentle reflux while a solution of dimethyldiacetoxysilane (30.2 g, 0.172 mole) in anhydrous hexane was added dropwise. Refluxing was continued for 1/2 hr after addition was completed. During the reaction, the acetylacetonate disappeared slowly and a white crystalline material was formed. The hexane was distilled off at 68 C, and the isopropyl acetate formed in the reaction was removed likewise at 84 C. The product was a brittle solid, light amber in color. No melting point could be observed, as the material softened at 175 C and decomposed between 220 and 240 C.

Diethylsiloxy-Aluminum-Acetylacetonate Polymer. This material was obtained by the same procedure as outlined above for the polymer in which methyl groups were attached to the silicon. In this case, 35.9 g, (0.147 mole) of diisopropoxyaluminum acetylacetonate were reacted with 30.0 g (0.147 mole) of diethyldiacetoxysilane. It was found advantageous to distill out the isopropyl acetate at reduced pressure to avoid decomposition of the product. A white crystalline product was obtained which melted over a temperature range of 150 to 200 C. Above 200 C the liquid became amber in color, and decomposition with charring occurred at about 270 C.

Diethylsiloxy-Aluminum-Isopropoxide Polymer. Diethyldiacetoxysilane (21.4 g, 0.1 mole) was added dropwise to aluminum isopropoxide (20.3 g, 0.1 mole) while the

temperature of the latter was maintained at about 75 C by means of an oil bath. When the addition was complete, the bath temperature was raised to 100 C and held there for 6 hr. The isopropyl acetate formed was distilled from the mixture in a stream of dry nitrogen at 34 to 38 C (80 to 150 mm). The remaining polymeric product was waxy and somewhat sticky, so it was dissolved in benzene, a small amount of insoluble impurity separated by filtration, and then the polymer was recrystallized.

This polymer softened at 200 C, and began to darken on the surface at 275 C. Active decomposition began at 300 C.

Diphenylsiloxy-Aluminum-Isopropoxide Polymer. This material was prepared in the same manner as the diethyl derivative, through the interaction of diphenyldiacetoxysilane (30.0 g, 0.1 mole) and aluminum isopropoxide (20.4 g, 0.1 mole). When this product was heated, it seemed to sinter at 170 C, and then did not undergo any further change as the temperature was raised to 270 C.

Ethyldicyanophosphine. This compound was prepared by the following sequence of reactions:

$$2PBr_3 + (C_2H_5)_4Pb \rightarrow 2C_2H_5PBr_2 + (C_2H_5)_2PbBr_2$$

$$C_2H_5PBr_2 + 2AgCN \rightarrow C_2H_5P(CN)_2 + 2AgBr.$$
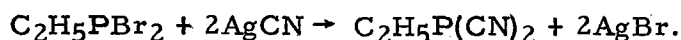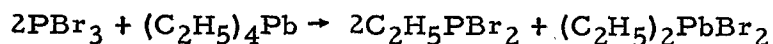
Ethyldibromophosphine. The method used for this preparation was essentially that employed by Sacco.[8] Tetraethyl lead (21 g, 0.065 mole) was added dropwise, with stirring, to phosphorus tribromide (38 g, 0.14 mole) contained in a three-neck flask. The tetraethyl lead was added from a dropping funnel fitted with a sidearm through which a stream of dry nitrogen was passed. The nitrogen was led out through a trap containing concentrated sulfuric acid. The reaction flask was heated intermittently by means of a steam bath to maintain a temperature of 100 C in the reaction mixture during the addition of the tetraethyl lead. When addition was complete, heating on the steam bath was continued for 3 hr. The ethyldibromophosphine was distilled out of the reaction mixture at reduced pressure. This product was a water-white liquid which distilled over the range 43 to 59 C at 12 mm. The yield was 57.8 per cent.

Conversion to Cyanophosphine. The ethyldibromophosphine (16.5 g, 0.075 mole) was dissolved in benzene and reacted with a slurry of silver cyanide in benzene (25 g, 0.18 mole). During the reaction heat was evolved and the white solid became yellow. The mixture was refluxed for 3 hr after the reagents had been mixed. The benzene was then distilled from the flask and the flask was purged with dry nitrogen. The ethyldicyanophosphine was distilled from the mixture at 87 to 93 C (10 to 20 mm). After standing overnight the liquid product crystallized, forming a solid that had a melting point of 35 C. In an attempt to determine a boiling point for the material, decomposition began at 157 C.

The ethyldicyanophosphine was purified by vacuum sublimation (1 mm Hg) at room temperature. The melting point of the material was increased from 35 to 36.5 C by this treatment. The analysis of the compound is close to the theoretical weight percentages:

	C	H	N
Calculated	42.8	4.5	25.0
Found	42.3	5.0	23.8

The compound is very easily hydrolyzed by atmospheric moisture and thus presents difficulties in handling. Partial hydrolysis could account for the difference from theoretical values. The molecular weight, as determined by freezing-point depression of benzene, was 112.7 as compared to 112.1, the calculated formula weight.

Product of Cohydrolysis of $AsCl_3$ and $(C_6H_5)_2SiCl_2$.

For the cohydrolytic reaction, water (3.2 g) and ammonia solution (15 ml of 30 per cent NH_3) were added slowly to a solution of arsenic trichloride (11.4 g, 0.063 mole) and diphenyldichlorosilane (16.4 g, 0.065 mole) in 300 ml of benzene. The mixture was stirred during the addition, and then was shaken vigorously for 20 min. The benzene-insoluble material was separated by filtration. The filtrate was evaporated under vacuum at room temperature to yield a white crystalline solid. This product melted over a wide temperature range (123 to 154 C) and attempts to purify it by recrystallization from benzene did not yield a higher melting material. Consequently, the preparation was repeated with a longer agitation time in a mechanical shaker and a product which melted sharply at 185 C was obtained. In the meantime a portion of the filtrate from the first preparation crystallized on standing, to yield the same material.

According to Chamberland and MacDiarmid[9] this reaction produces a material melting at 195 C which has a molecular weight corresponding to the formulation
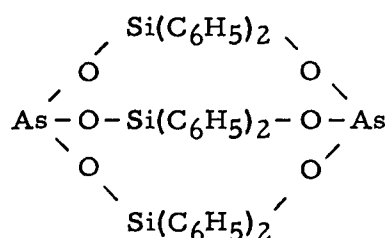
The infrared spectrum of the product obtained in the current study was the same as that obtained by Chamberland and MacDiarmid for their material.

Reaction Product of KH_2AsO_4 and $(C_6H_5)_2SiCl_2$.

A polymeric material reputed to have alternating Si-O-As linkages was prepared according to the method employed by Chamberland and MacDiarmid. A mixture of potassium dihydrogen arsenate (24.8 g, 0.138 mole, 50 per cent excess) and diphenyldichlorosilane (11.6 g, 0.0458 mole) dissolved in 200 ml of ether was stirred for 98 hr at room temperature.

The reaction proceeds as shown in the following equation

$$4X\ KH_2AsO_4 + 2X\ (C_6H_5)_2SiCl_2 \rightarrow \underset{\substack{| \\ H}}{\overset{\substack{O \\ || \\ HO-As \\ | \\ O}}{}} \left[\underset{\substack{| \\ C_6H_5 \\ | \\ H}}{\overset{\substack{C_6H_5 \quad O \\ | \qquad || \\ -O-Si-O-As \\ | \qquad |}}{}} -O-H \right]_{2X}$$

$$+\ (2X-1)\ H_3AsO_4 + 4X\ KCl$$
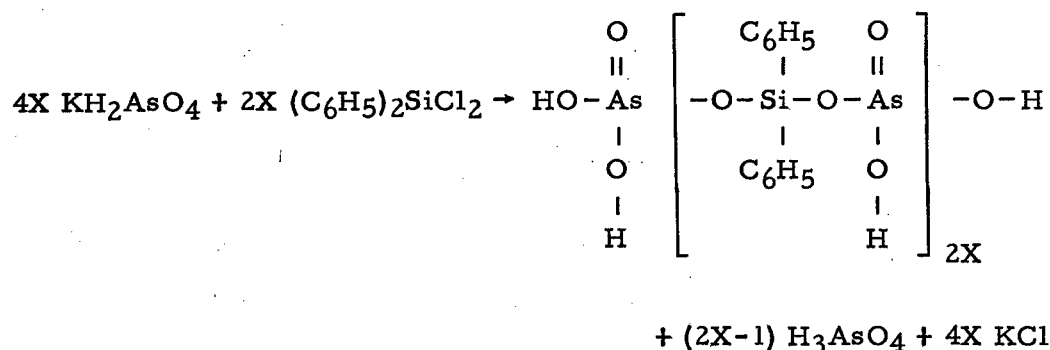
The H_3AsO_4 and KCl were removed by filtration and discarded. The ether was then slowly evaporated from the filtrate by passing dry nitrogen through the solution until the volume had been reduced approximately half. A small amount of insoluble white solid was separated during this process and appeared to be the $[(C_6H_5)_2SiO]_3$ reported by Chamberland and MacDiarmid[9] as a by-product of their synthesis. As additional ether evaporated, a white greasy solid separated. This material had a softening range of 105 to 160 C as compared to 153 to 180 C reported by the above investigators, and had the same infrared spectrum as their polymer.

Phosphonitrilic Chlorides. A commercial mixture of phosphonitrilic chlorides and some of the pure trimer were obtained from the Hooker Chemical Corporation. The molecular weight of the $(PNCl_2)_3$ obtained from the Hooker Chemical Company was determined by freezing-point depression in camphor. The experimentally determined value was 351 as compared to a calculated value of 348. It is concluded that the sample is essentially free of tetramer or higher polymers.

The linear polymers of phosphonitrilic chloride were extracted from the commercial mixture of cyclic and linear polymers. Glacial acetic acid was used to dissolve the trimer and tetramer out of the mixture leaving the linear polymers behind. The extraction was carried out at room temperature with small quantities of glacial acetic acid, and it was considered to be complete when the acid extract showed no color. After each extraction the acid solution was decanted and separated by filtration. The insoluble linear polymers were finally washed several times with small quantities of ethanol to remove traces of the acetic acid. The product was then dried by pumping off the ethanol at room temperature.

Diphenylphosphinoborine Trimer. Diphenylphosphinoborine trimer was prepared by the reduction of $(C_6H_5)_2PCl$ with $NaBH_4$. The reaction proceeds in two steps:

$$(C_6H_5)_2PCl + NaBH_4 \rightarrow (C_6H_5)_2PHBH_3 + NaCl$$

$$3(C_6H_5)_2PHBH_3 \rightarrow [(C_6H_5)_2PBH_2]_3 + 3H_2$$
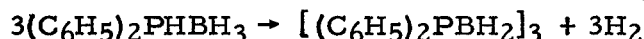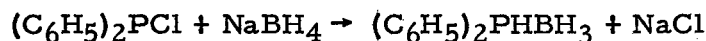
In the initial step, $(C_6H_5)_2PCl$ (30 g, 0.14 mole) was dissolved in 50 ml of diethylene-glycol dimethyl ether and added slowly to a solution of $NaBH_4$ (14 g, 0.37 mole) in the same solvent, under a dry-nitrogen atmosphere. Some hydrogen was evolved during the addition of the $(C_6H_5)_2PCl$. When no more gas was evolved, the precipitated NaCl was separated by filtration. The remaining solution was allowed to stand overnight and a waxy, white solid precipitated. This solid was also filtered off, and the solvent was then

45

distilled from the mixture under vacuum. The heating was continued and about 1.5 ml of unreacted $(C_6H_5)_2PCl$ was recovered. The solid which remained was heated until gas evolution stopped, and was then washed with acetone and water. The yield of diphenyl-phosphinoborine trimer (mp 157 to 160 C) was 5.6 g which is 21 per cent of theoretical.

The solid which separated during the preparation of the diphenylphosphinoborine trimer may be of some interest. This material melts at 188 to 192 C and remains liquid to 360 C where it volatilizes slowly. Molecular-weight determinations have been inconclusive, while analysis of the material shows a lower carbon and hydrogen content than that of the trimer.

Apparatus and Techniques

For all of the pressurization experiments, the sample was enclosed in a platinum capsule 1/2 in. long and 1/16 in. in diameter. To form the capsule, a length of platinum tubing was held in a steel die while the bottom was sealed by tamping platinum foil into the base. The sample was then tamped into the capsule, and the top seal of platinum foil applied similarly. When the sample was to be heated beyond its melting point, the end seals were strengthened by sandwiching wadded foil between disks of platinum. For experiments at elevated temperatures, the platinum capsule served as a resistance heater.

For materials which are sensitive to atmospheric moisture, it was found necessary to load the capsules under a blanket of dry nitrogen or argon. Lamp-grade nitrogen proved to be suitable for this purpose, but for prolonged use of the "dry atmosphere box" the greater density of argon made it preferable. After pressure experiments with these sensitive materials, the capsules were opened in the dry atmosphere, and the contents were then transferred to a desiccator.

Pressurization Experiments

The semiorganic materials were subjected to compressive forces which produced 60,000 to 75,000 atm when silver chloride was used as a calibration medium. The experiments at 60,000 atm were performed on either the 100- or the 150-ton press, while those at 75,000 atm were done on the 1000-ton press.

Dimethyldicyanosilane. This compound is very sensitive to moisture and changes from a white crystalline solid to a colorless oil in 1 to 2 min when exposed to the atmosphere. Consequently, it was loaded into the platinum capsule under dry argon.

When this material is pressurized (at 60,000 atm), reaction as indicated by changes in its infrared spectrum does not occur until the temperature is raised to 100 C. Heating the compound in a sealed Pyrex tube at 100 C for 3 hr leaves it unchanged, but combined pressure and heat cause the dimethyldicyanosilane to change to a brownish-black product, which is not moisture sensitive and is no longer soluble in common organic solvents. The infrared spectrum of the product indicates the formation of some $C=N$ bonds, although not all of the $C\equiv N$ character has disappeared. Analysis for C, H, and N shows a loss of all three components which is equivalent to the loss of 3 HCN from 4 molecules of $(CH_3)Si(CN)_2$. However, the result is complicated by the appearance of

absorption bands in the spectrum, which may come from water introduced from the pyrophyllite gasket material. Further investigation with baked-out pyrophyllite will be made. Increasing the pressure to 75,000 atm at 100 C increases the amount of C≡N that appears.

Figure 20 shows the conditions of temperature and pressure under which reaction has been observed. It is expected that subsequent experiments will define a boundary between the regions of reactivity and inactivity. Efforts will also be made to resolve the nature of the C≡N bonding. It could be the result of either partial condensation to a triazine structure, or linking of adjacent molecules in a linear structure.

Aluminum-Oxygen-Silicon Polymers. The pressure experiments on the four polymeric materials having Al-O-Si bonds were all performed at 60,000 atm. The temperature ranged from 100 to 400 C and the time of pressurization varied from 2 to 8 hr.

Dimethylsiloxy-Aluminum-Acetylacetonate Polymer. The combined heat and pressure had no permanent effect on this material at 100 or 200 C. At 300 C no change was observed after 2 hr at pressure. However, when the time was extended to 8 hr, some of the silicon-carbon bonds were broken, as indicated by the infrared spectrum, with consequent reduction in carbon and hydrogen content. A comparison experiment, run at 300 C and atmospheric pressure, resulted in breaking of the acetylacetonate ring in addition to silicon-carbon bonds and showed greater loss of carbon and hydrogen. At 400 C pyrolysis occurred.

Diethylsiloxy-Aluminum-Acetylacetonate Polymer. This material was unchanged under pressure at 100 C and at 200 C in 3-hr experiments. The silicon-carbon bonds were affected at 300 C and, as the time of exposure at this temperature was increased to 8 hr, differences between the pressurized and unpressurized samples were observed. The acetylacetonate ring was broken in the case of the unpressurized sample, but the over-all loss of carbon and hydrogen was less than that for the pressurized sample. This material also underwent pyrolysis at 400 C.

Diethylsiloxy-Aluminum-Isopropoxide Polymer. This material was unaffected by the combined heat and pressure at 100 and 200 C. At 300 C, the breaking of the silicon-carbon bonds occurred more rapidly than it did for the polymers in which the acetylacetonate was bonded to the aluminum. The unpressurized sample showed greater effect on the group bonded to aluminum than on that bonded to silicon. Pyrolysis occurred at 400 C in this case also.

Diphenylsiloxy-Aluminum-Isopropoxide Polymer. No change occurred in this material when pressurized at 100 or 200 C, but when the temperature was raised to 300 C, pyrolysis took place rapidly.

Ethyldicyanophosphine. This compound is extremely sensitive to atmospheric moisture and had to be loaded into the pressure capsules under the blanket of dry argon. Extensive decomposition of this compound began at 50 C under 60,000-atm pressure.
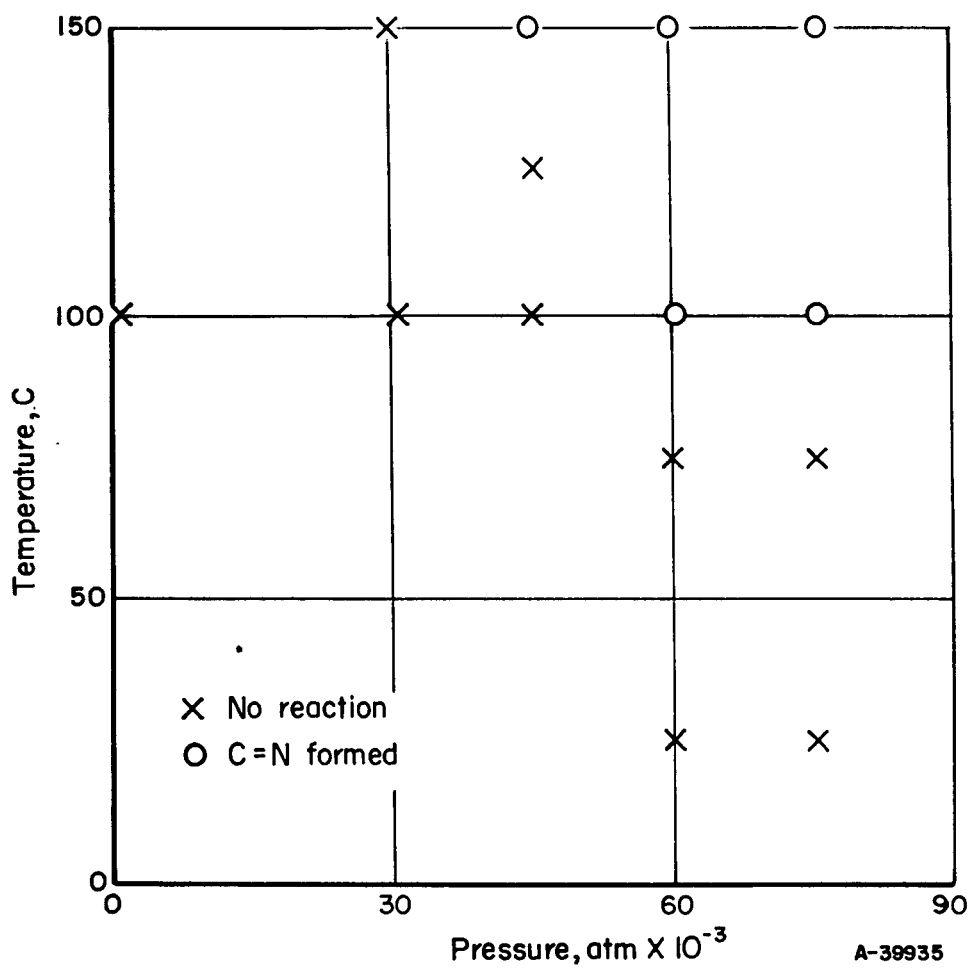
FIGURE 20. EFFECT OF PRESSURE AND TEMPERATURE
ON C=N FORMATION IN $(CH_3)_2Si(CN)_2$

Pressurization at room temperature resulted in the disappearance of $C \equiv N$ bonding, as indicated by infrared spectra. However, allowing the compound to stand uncovered in air at ambient temperature brought about these same structural changes. In future experiments, it may be possible to separate the effects of moisture and oxygen from those of pressure on this compound, to establish whether or not there is any real effect of pressure.

Tris (Diphenylsiloxy) Diarsenic (III). This cyclic material having As-O-Si bonding, As$[OSi(C_6H_5)_2O]_3$As, was unaffected by pressures of 60,000 atm at temperatures as high as 400 C for periods of several hours. When pressurization was conducted at 500 C for 3 hr, definite structural changes occurred. As indicated by the infrared spectra, these appear to be breaking of the silicon-carbon bonds. Unpressurized samples held at 500 C for a 3-hr period did not degrade quite as extensively. This case was the first encountered in this study in which high pressure appears to have increased the rate of decomposition of a material.

Diphenylsiloxy-Arsenoxane Polymer. The linear polymer of the As-O-Si series, which has been formulated as $AsO(OH)_2[OSi(C_6H_5)_2OAsO(OH)]_n$OH started decomposing when subjected to 60,000 atm at 100 C for 3 hr. Pyrolysis occurred readily when the material was pressurized at 200 C.

Phosphonitrilic Chlorides. The phosphonitrilic chloride trimer, $(PNCl_2)_3$, was subjected to 60,000-atm pressure and a temperature of 240 C was maintained for 30 min. The sample changed in color from white to tan and the melting point was lowered from 113 to 114 C to 106 to 107 C. However, identical results were obtained by simply heating a sample of the trimer at 240 C for 30 min. The infrared spectra of the two samples were identical also. In another experiment the temperature was maintained at 300 C while the pressure was applied. A high polymer which could be heated to 500 C without melting was obtained. However, in this case also, the same result was obtained by application of heat alone. Thermal energy appears to be sufficient to break the bonds in the ring structure of the $PNCl_2$ trimer, and pressure does not contribute any permanent effect.

The linear polymer fraction of phosphonitrilic chloride, which had been extracted from a mixture of the cyclic and linear polymers, was subjected to 60,000 atm also. After 3 hr at 200 C the thermal stability of the material was altered. The starting material did not melt, but slowly charred as the temperature was raised to 300 C. However, the pressurized product melted in the range 270 to 300 C. This result points to the formation of lower-molecular-weight polymers than the starting material, but no suitable solvent for molecular-weight determination could be found. Infrared analyses were inconclusive also, as there was no significant absorption in the infrared region for either the treated or untreated specimens.

Phosphinoborine Polymers. Diphenylphosphinoborine trimer, $[(C_6H_5)_2PBH_2]_3$, was pressurized at 60,000 atm at temperatures up to 400 C, where pyrolysis occurred. Only slight structural changes were observed below the pyrolysis temperature, and these could be brought about by heat alone.

A solid which separated during the preparation of the diphenylphosphinoborine trimer appears to have some unusual properties, although it has not been characterized completely. This material melted at 188 to 192 C and remained liquid to 360 C, where it volatilized slowly. Analysis showed lower carbon and hydrogen content than the trimer, and molecular-weight determinations were inconclusive. Under pressure it did not pyrolyze until the temperature reached 500 C, although an unpressurized sample held at 400 C for 8 hr in a sealed Pyrex tube degraded extensively. Further study of this material seems to be warranted.

V. EXPERIMENTAL SECTION – INORGANIC POLYMERS

Ultrahigh-Pressure High-Temperature Apparatus: Design, Calibration, and Operation

The Belt Apparatus

The ultrahigh-pressure high-temperature device used in the experimental work on inorganic polymers is the G. E. Belt modified from the original design of H. T. Hall[10]. The Battelle Belt apparatus is shown schematically in Figure 21. It consists of a pair of opposed truncated conical pistons (A) of cemented tungsten carbide which are forced by a hydraulic press ram into a doughnut-shaped tungsten carbide die (B). The die and the pistons are each surrounded by a series of three hardness-graded concentric steel binding rings with tapered mating surfaces which are force fitted to provide precompression of the carbide inserts and, thus, massive support. The fourth and outermost ring in each set is a water-cooled jacket.

The sample, in the form of a powder, is packed into a 1/16-in.-diameter cylindrical heater tube of platinum 0.450 in. in height with a wall thickness of 5 mils. The ends of the platinum sample capsule are mechanically cold sealed with platinum foil 0.5 mil in thickness and the capsule is then inserted into a close-fitting cylindrical jacket of pyrophyllite* (OD = 0.350 in.) of the same height. The remaining space between die and pistons is filled by specially shaped conical pyrophyllite gaskets (Figure 22). As the die closes, the pressure seal is effected by extrusion of gasket material which also provides for considerable compression of the sample volume and for thermal and electrical insulation. The pressure build-up in the pyrophyllite also transmits mutually supporting forces to the pistons and die. The device is internally heated by passage of high current (at low voltage) through the platinum heating tube. Current for this purpose is supplied through the carbide pistons, and contact with the platinum heater tube is obtained by means of metal end plugs and platinum end disks (Figure 23). The temperature is measured by means of a thermocouple, the junction of which is spot welded to the side of the heater tube and the leads of which are brought out through the gasketing material between the piston and the die.

In the original design by Hall[10,11] the thermocouple leads were brought out along grooves in the outer wall of the outer conical gasket in the upper half of the gasket assembly (Figure 23a). Initial exploratory work with the Belt apparatus showed that the thermocouple leads in this arrangement were easily ruptured at internal pressures above

---

*Lava Grade A supplied by the American Lava Corporation, Chattanooga, Tennessee.
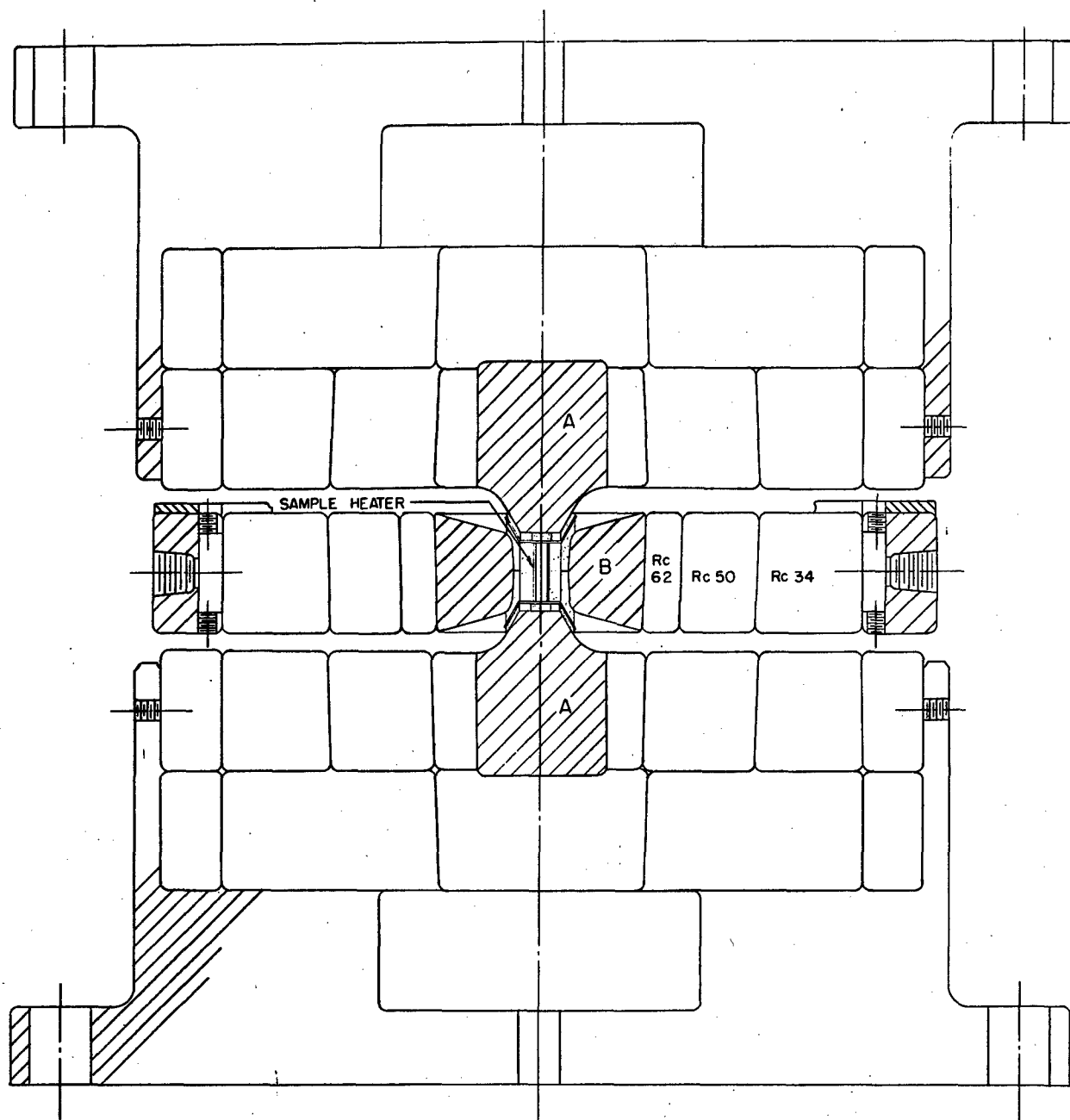
FIGURE 21.   BELT ULTRAHIGH-PRESSURE APPARATUS
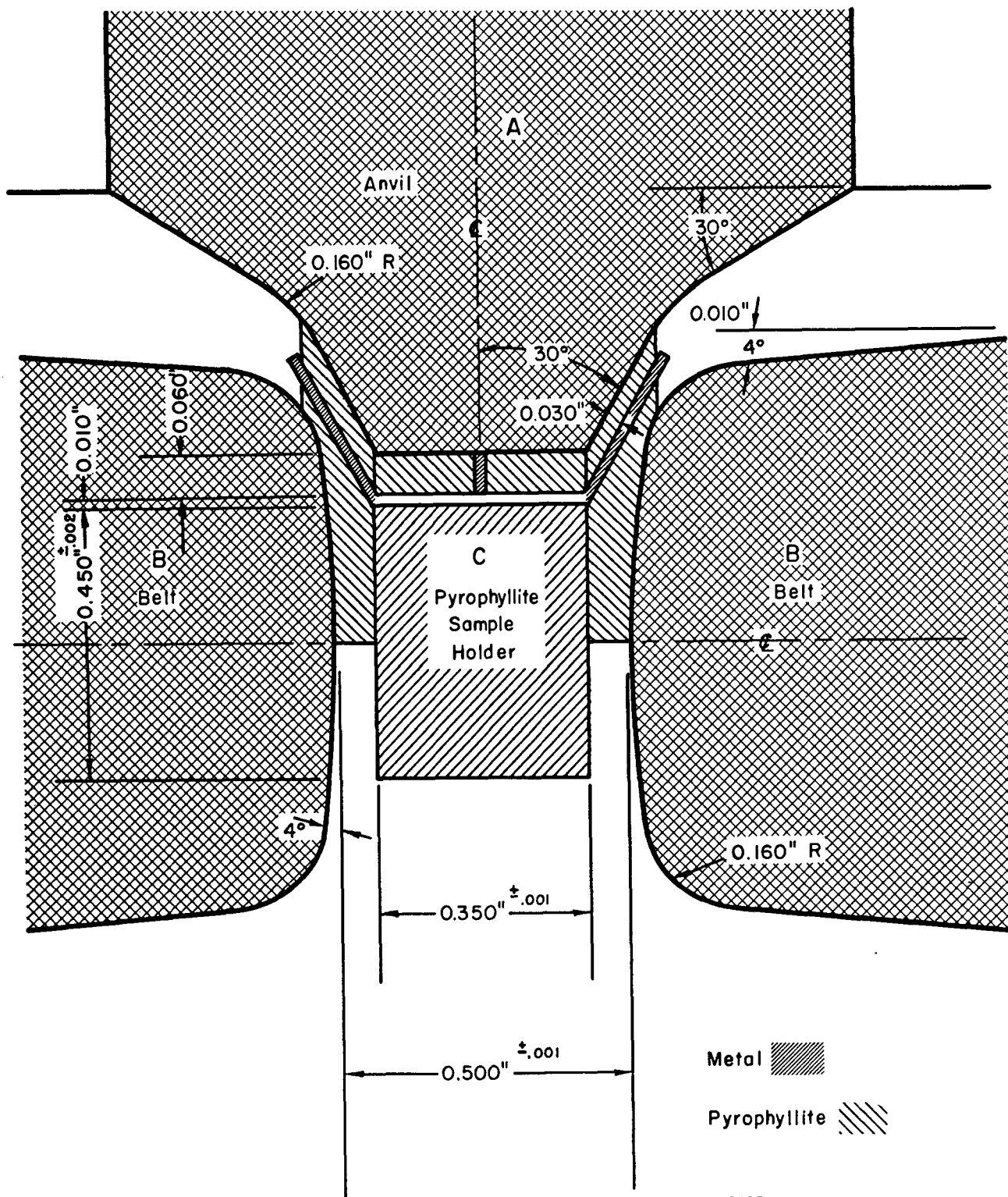
FIGURE 22. INTERNAL GEOMETRY OF BELT APPARATUS AND
UPPER HALF OF GASKET ASSEMBLY

52

30,000 atm. In addition, it was found that the conical inserts of 1112 steel placed between the outer and inner pyrophyllite gaskets frequently broke at pressures above 30,000 atm and that this was accompanied by disruption of the thermocouple leads. This problem has been resolved by (1) changing the configuration of the thermocouple wires, and (2) changing the type of steel used in the conical steel inserts and by heat treating. Each thermocouple lead is now brought out along the interface of one of the two steel cones and its corresponding outer pyrophyllite gasket so that, in the event of wire breakage, electrical continuity will be maintained through the steel cone* (Figure 23b). To accommodate this thermocouple arrangement, the end plugs of the sample holder and the inner conical pyrophyllite gasket have been modified to prevent shorting of the thermocouple circuit. Steel cones machined from cold-rolled 1020 stock and then heated between 750 and 800 C for 1 hr and cooled 50 C per hr remain intact at internal pressures up to 90,000 atm.

The tungsten carbide die used in the first part of this project had an aperture of 0.500 in. and a taper angle of 4 deg (Figure 22). Later in the project, a modified tungsten carbide die, based on more recent drawings obtained from H. Tracy Hall of Brigham Young University, was fabricated for use in the Belt apparatus. The modified die has an aperture of 0.415 in. and a taper angle of 12 deg. Calibration of the two dies by means of fixed pressure points showed that the 12-deg die was slightly more efficient at pressures greater than 20,000 atm, but that otherwise there was no significant difference between them. As a result, both 12- and 4-deg dies have been used interchangeably for experimental work during this project.

Hydraulic ram force for the Belt apparatus has been provided by a Blackhawk 100-ton press for studies to 60,000 atm and, for the latter third of the project period, by a Hall-type multiple-piston 1000-ton ram[11] which was constructed at Battelle for studies upwards of 100,000 atm although it can be used at much lower pressures. Inasmuch as a pressure of 100,000 atm is generated in the Battelle Belt apparatus at only about 170 tons, it is evident that an abundant reserve of ram force is available and the limiting factor in these ultrahigh-pressure studies is the inherent strength of the high-pressure device.

Absolute Pressure Scale and Calibration of the Belt Apparatus

The internal pressure in the Belt apparatus cannot be calculated from the ram force and the area of the truncated surface of the piston because of losses due to friction and to the force acting on the conical surfaces of the die. It is necessary, therefore, to calibrate the internal pressure against ram force by means of known pressure transitions. P. W. Bridgman has shown that elements such as bismuth, thallium, and barium undergo marked discontinuities in electrical resistance concomitant with pressure-induced phase transitions in the pressure range of 25,000 to 90,000 atm. These transitions constitute fixed pressure points on an absolute pressure scale. A summary review of the evolution of the absolute pressure scale and the establishment of the "new" (post-mid-1960) absolute pressure scale is presented below.

Bridgman[12,13] found that the Bi I-II transition as determined by discontinuity in electrical resistance in a piston-anvil device and by volume discontinuity measurements in a piston-cylinder device were in excellent agreement and located the transition at

---
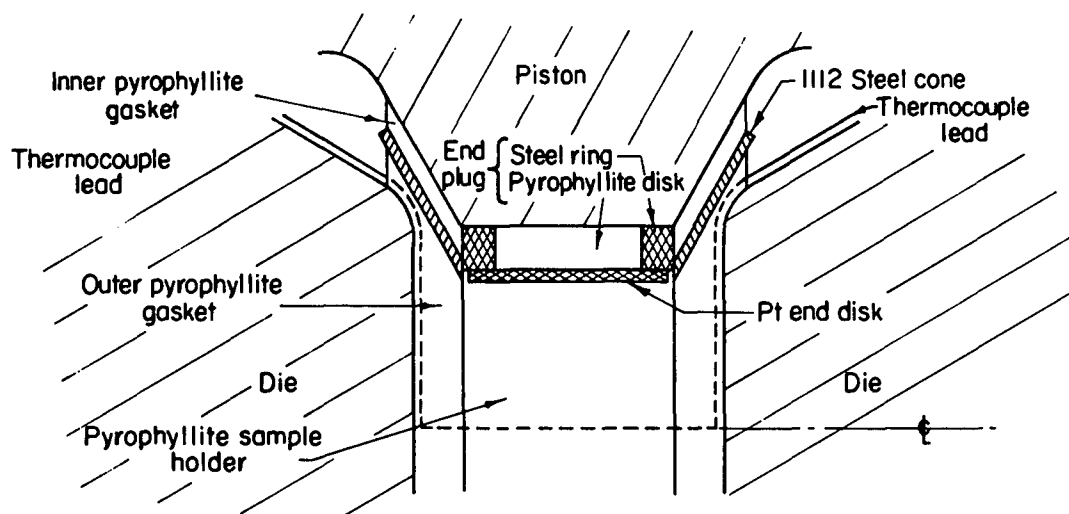
a. Original Design
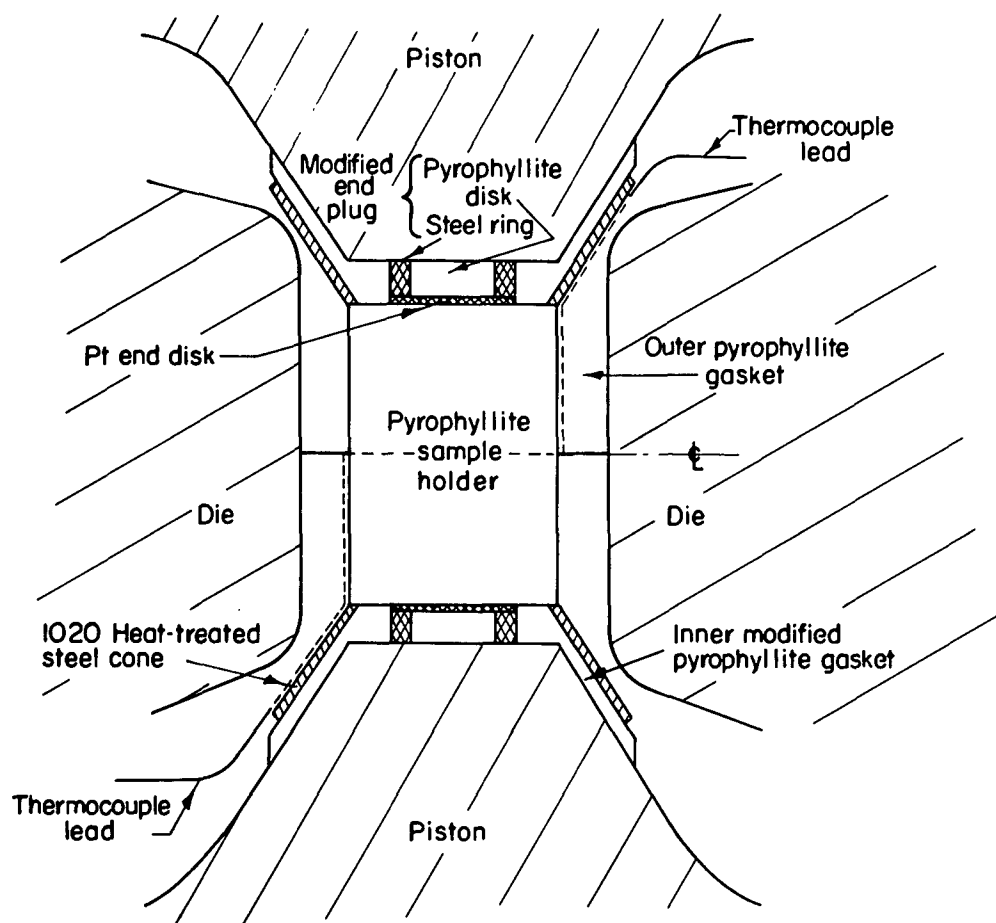
b. Current Design

A-36386

FIGURE 23. THERMOCOUPLE CONFIGURATION, GASKETS, AND END PLUGS FOR BELT ULTRAHIGH-PRESSURE APPARATUS

54

24,800 atm. Recently, Kennedy and La Mori[14] redetermined the Bi I-II transition by volume discontinuity measurements in a piston-cylinder device in which the piston could be rotated to relieve friction, and placed the transition at 25,100 ± 95 atm. Boyd and England[15] have also redetermined the Bi I-II transition by electrical discontinuity measurements in a piston-cylinder device and located it at 24,800 atm. For this experimental program, the Bi I-II transition is considered to be 25,000 atm.

Bridgman found that the Tl II-III transition by volume discontinuity in a piston-cylinder device occurred at 38,700 atm[16] whereas the same transition by electrical resistance discontinuity in a piston-anvil device was located at 43,500 atm. [12] Kennedy and La Mori[14] report 36,200 ± 110 atm for the Tl II-III transition on the basis of volume measurements in a piston-cylinder device whereas Boyd and England[15] located the Tl II-III transition at 36,600 ± 1300 atm on the basis of electrical discontinuity measurements in a piston-cylinder device. For the purposes of this study, the Tl II-III transition is taken as 37,000 atm.

Although Bridgman's volumetric and electrical transition points for the Bi I-II transition were in excellent agreement and the respective volume and electrical points for the Tl II-III transition were fairly close, the respective volume and electrical points for the Ba II-III transition were not. Bridgman obtained the volumetric barium transition in a piston-cylinder device at 58,100 atm[17] whereas the electrical barium transition measured in a piston-anvil device was located at 77,400 atm[12]. Recent volumetric measurements by Kennedy and La Mori[14] in a piston-cylinder device equipped with a lever arm for rotation of the piston to relieve friction have shown that Bridgman's volumetric discontinuity measurements for various metals, including bismuth, thallium, and barium, are very close to correct. They conclude that Bridgman's electrical transition point for barium at 77,400 atm is too high by about 25 per cent and that it is equivalent to the Bridgman volumetric transition point for barium at 58,100 atm. Kennedy and La Mori locate the Ba II-III transition at 58,400 ± 3,000 atm. This conclusion is supported by measurements of Balchan and Drickamer[18] made in an optical apparatus[19] which was calibrated by means of Bridgman's volume transitions for KCl, HgI$_2$, AgBr, and AgCl. Although it is not explicitly stated, measurement of the Ba II-III transition was presumably by electrical resistance and the transition was placed at between 57,300 and 59,300 atm. For the purposes of this report the Ba II-III transition is considered to be 58,000 atm.

Bridgman[17,20,21] showed by volume discontinuity measurements in a piston-cylinder device the occurrence of a transition in bismuth (Bi V-VI) at 90,000 kg/cm^2 (87,000 atm), and he later reported[12] that a consistent electrical resistant change associated with this volumetric transition was not obtained in his piston-anvil device. Subsequently, Bundy[22], using the Belt apparatus, reported the occurrence of an electrical-resistance transition in bismuth at 125,000 kg/cm^2 (121,000 atm) which he called Bi VI-VIII. This transition point was located on the pressure scale by linear extrapolation from two absolute-pressure calibration points originally determined by Bridgman, e.g., the Bi I-II electrical and volumetric transition at 25,000 atm and the Ba II-III electrical transition at 77,400 atm. As discussed in the preceding paragraph, however, the Bridgman volumetric transition for Ba II-III at about 58,000 atm appears to be the correct value for the Ba II-III transition. Kennedy and La Mori[14] have suggested that the Bi VI-VIII electrical transition of Bundy at 121,000 atm is equivalent to the Bi V-VI volumetric transition of Bridgman at 87,000 atm and that the Bridgman volumetric point is probably the correct value for the high bismuth transition inasmuch as the Bridgman volumetric transitions for low bismuth, thallium, cesium, and barium are more accurate

than the corresponding Bridgman electrical transitions for these elements. Recent measurements by Balchan and Drickamer[18] support this idea. They located the Bi V-VI transition at 90 kilobars (88,800 atm), presumably, as indicated in the discussion of the barium transition above, by means of electrical measurements in their optical apparatus[19] which was independently calibrated by means of Bridgman's volume transitions in halide salts. In the high-pressure work at Battelle, the Bi V-VI electrical transition is considered to be 87,000 atm.

To summarize, the following fixed pressure points located by electrical resistance discontinuities have been used to calibrate the Belt apparatus: the Bi I-II transition at 25,000 atm, the Tl II-III transition at 37,000 atm, the Ba II-III transition at 58,000 atm, and the Bi V-VI transition at 87,000 atm. These points constitute the "new" post-mid-1960 absolute pressure scale. The older pressure scale, based on Bridgman's electrical resistance transitions, needs to be adjusted downward at pressures greater than 25,000 atm, and the magnitude of the adjustment increases with increasingly higher pressure.

The characteristic form of the electrical resistance curves for several of these transitions is shown in Figure 24. A plot of the fixed pressure points against their respective ram-force requirements in the Belt apparatus as determined with both a 4-deg die and a 12-deg die using the internal geometry shown in Figure 23b and silver chloride as a pressure-transmitting medium shows that the Belt apparatus is essentially a linear pressure device to at least 90,000 atm (Figure 25).

A 4-deg die and a 12-deg die were monitored by means of the electrical resistance of a bismuth wire encased in silver chloride and loaded until disruption occurred. The 12-deg die used in this experiment had been used previously for two or three runs below 100 tons of ram force (60,000 atm) but showed one visible crack running from the interior sample chamber to the periphery. It withstood a ram force at 165 tons before disruption, which, by linear extrapolation from the calibration curve, represents about 95,000 atm on the sample. Correspondingly, the 4-deg die used in this experiment had been used previously for about 30 runs below 100 tons and at temperatures up to 1300 C, but it was free of visible cracks or gouges. It withstood a ram force of 180 tons before disruption which, by linear extrapolation from the calibration curve, represents about 105,000 atm on the sample. A sample pressure of about 100,000 atm is about the maximum pressure reported in the published literature thus far for any internally heated pressure device calibrated on the "new" (post-mid-1960) absolute pressure scale. Hall[23] reported that pressures up to 180,000 atm were obtained in the Belt apparatus, but it should be noted that his instrument was calibrated on the old electrical resistance scale. If a 40 per cent negative correction, which seems reasonable with respect to the 30 per cent correction for the Bi VI-VIII transition at 121,000 atm, is applied to 180,000 atmospheres, the resultant pressure is about 110,000 atm. The diamond-synthesis group at the General Electric Research Laboratory has recently adopted the revised pressure scale[24], and, as a consequence, the "diamond-growing region" in their Belt-type apparatus, which was formerly given as 60,000 to 120,000 atm[25], is now considered to be 45,000 to 85,000 atm.

The matter of die life in the Belt apparatus at or near 100,000 atm is of considerable importance. Die life is almost certainly shorter at higher pressures and particularly at higher pressures and high temperature, but experience at present is too limited to draw any quantitative conclusions. It will be necessary, at least in the immediate future, to be selective as to the samples which are subjected to these ultimate pressures.
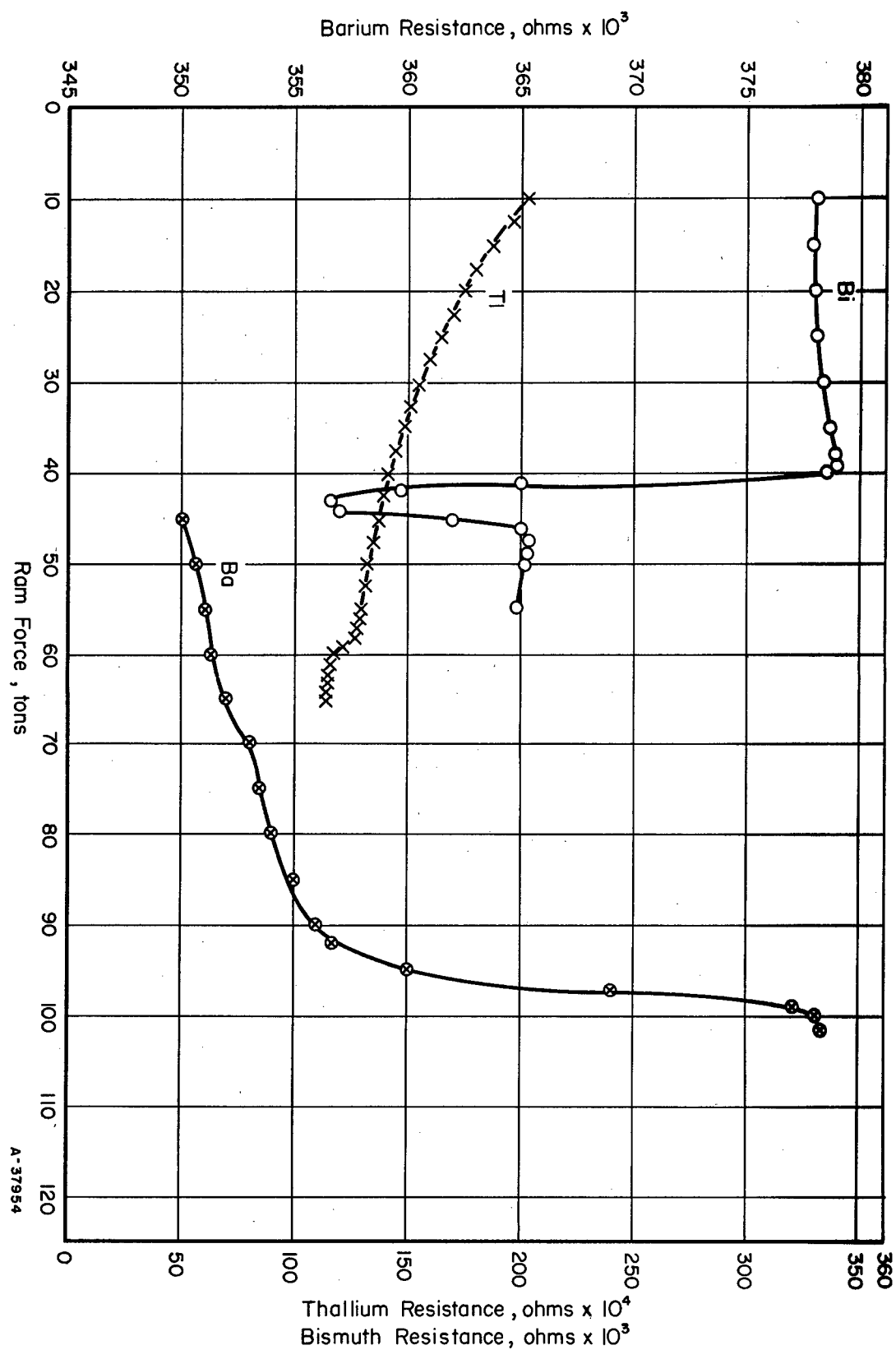
FIGURE 24. Bi I-II, Tl II-III, AND Ba II-III ELECTRICAL RESISTANCE DISCONTINUITIES USING A 12-DEGREE DIE WITH 0.415-INCH APERTURE IN BELT APPARATUS

57

A-39936
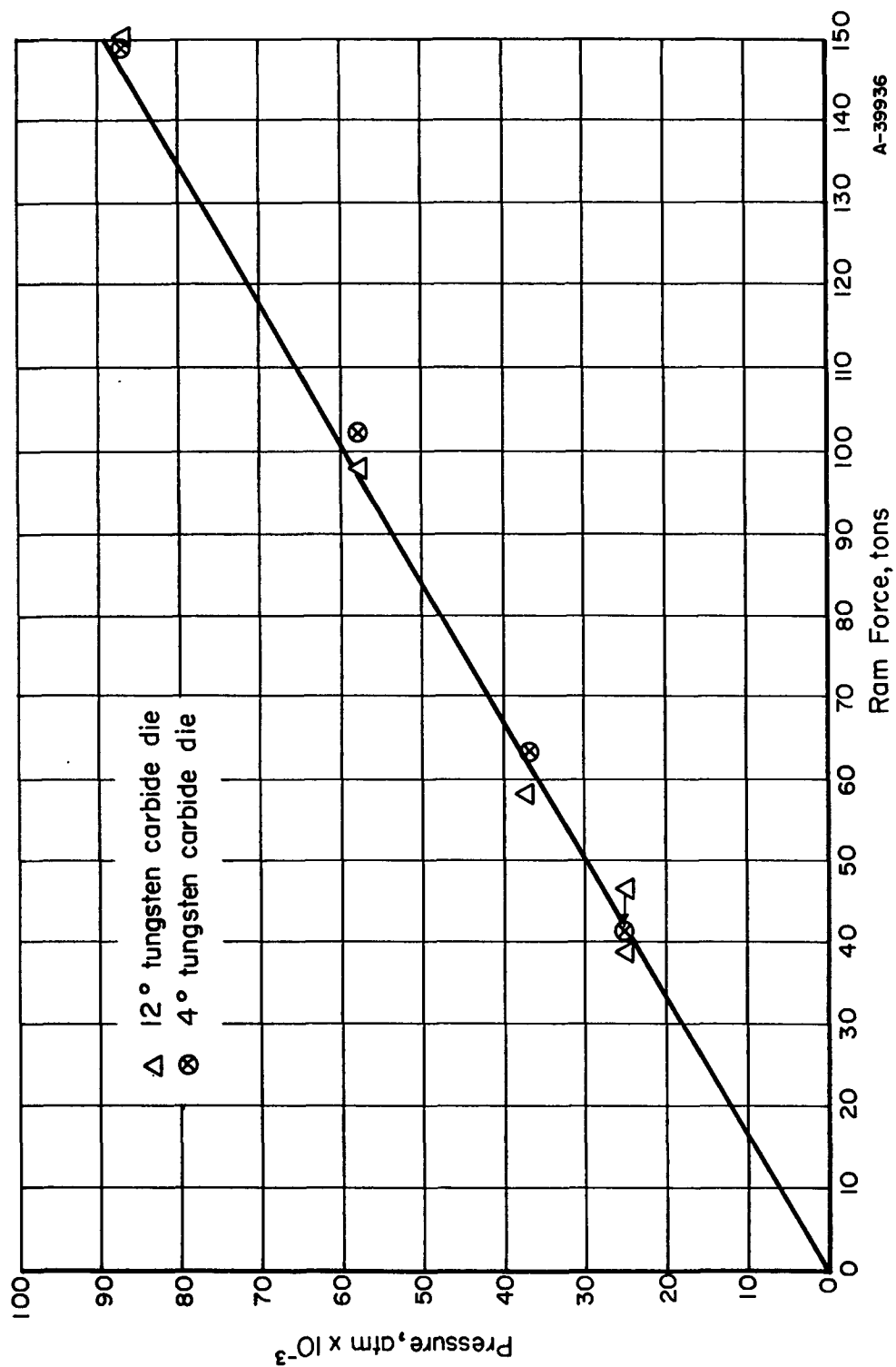
FIGURE 25. PRESSURE CALIBRATION OF THE BELT APPARATUS FOR THE INTERNAL GEOMETRY SHOWN IN FIGURE 23b

58

Actual Pressure on the Sample in the Belt Apparatus

Ram Force Required for the Bi I-II Transition. As discussed above, the Belt apparatus was calibrated by means of electrical resistance transition for bismuth, thallium, and barium which are run in a sleeve of silver chloride, a quasi-ideal hydrostatic medium. Bridgman[12] and subsequent workers have used silver chloride as the pressure-transmitting medium for studies on the effect of pressure on the resistance of metals and for electrical-resistance calibration purposes because of its low plastic yield point and because it is a good insulator whose electrical resistance increases with pressure. As a result of these properties, it is possible with the use of silver chloride to detect small changes in the electrical resistance of metals with increasing pressure which might otherwise go undetected or be only poorly resolved. It is evident, however, that the actual pressure on the sample at a given ram force may be less than that indicated by the calibration curve inasmuch as silver chloride is not used in pressure experimentation and the sample is enclosed in a platinum capsule which is jacketed directly in pyrophyllite. As a means of evaluating the magnitude of the departure from the pressure indicated by the calibration curve, several preliminary experiments were run using the Bi I-II transition. The experimental conditions were as follows:

(a) The normal cylindrical hole (0.073-in. diameter) in the cylindrical pyrophyllite jacket (sample holder) was filled with molten silver chloride. The hole is normally occupied by the platinum heater tube which contains the sample to be pressurized. A 15-mil hole was drilled axially through the silver-chloride cylinder and a bismuth-coated 3-mil Chromel wire with a total diameter of about 15 mils was forced through the hole. The setup was then pressurized.

(b) A cylindrical platinum heater tube (0.063 in. in ID) was packed with fine-grained GeO_2 powder through which a 15-mil hole was drilled axially and into which a bismuth-coated 3-mil Chromel wire with a total diameter of about 15 mils was inserted. The setup was then pressurized.

(c) A 15-mil hole was drilled in a solid cylindrical pyrophyllite sample holder through which a bismuth-coated 3-mil platinum wire with a total diameter of about 15 mils was drawn. The setup was then pressurized.

The results of these experiments are as follows:

Run	Type of Run	Midpoint of Bi I-II Slope on Plot of Electrical Resistance Versus Ram Force, tons	Minimum Point of Bi I-II Slope on Plot of Electrical Resistance Versus Ram Force, tons
1	AgCl	38	41
2	Pyrophyllite	39	47
3	Platinum	39	49

The data are shown graphically in Figure 26. Although the midpoints of the Bi I-II slopes are the same, the minima of Runs 2 and 3 are significantly higher than that for Run 1.
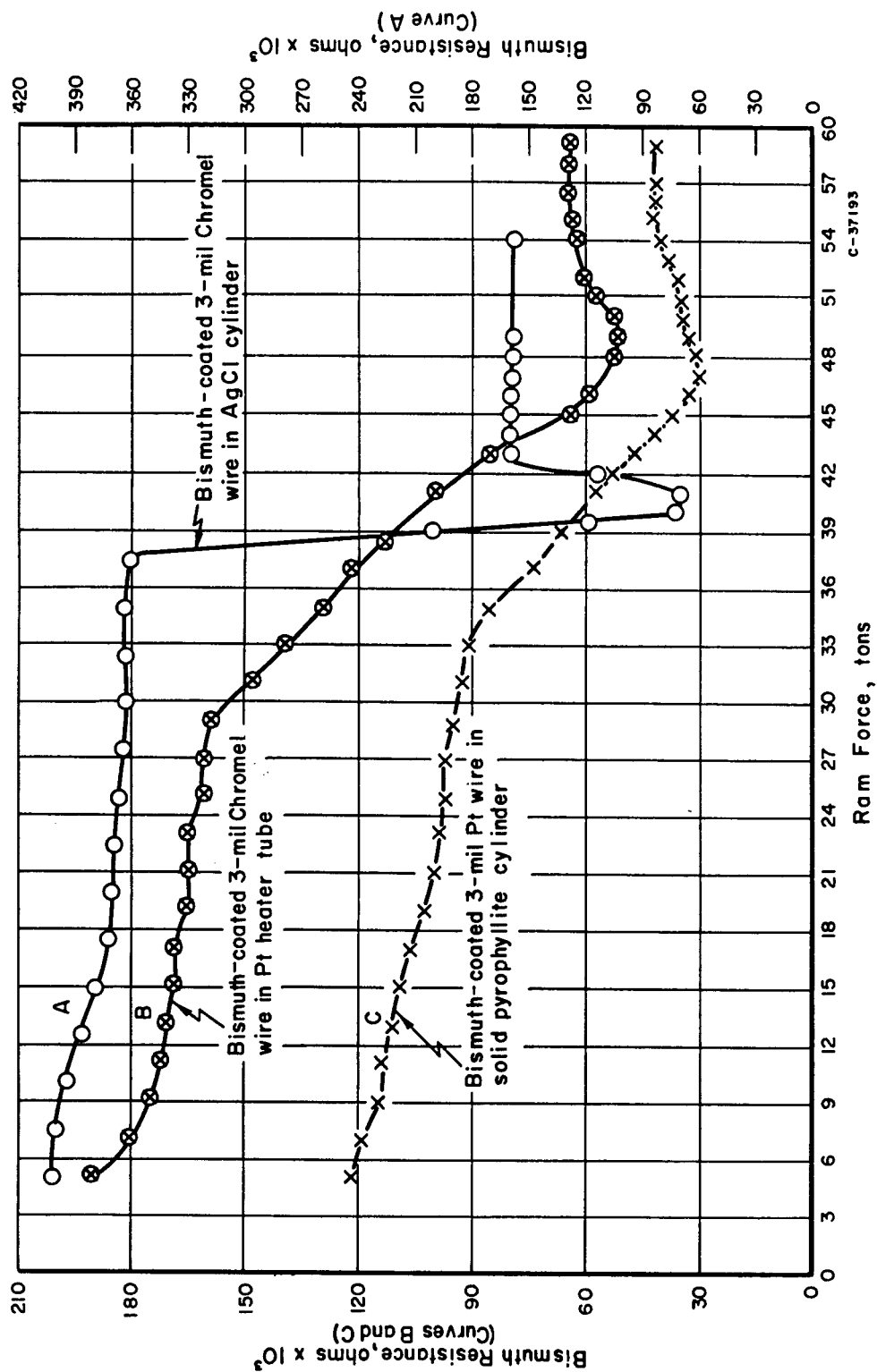
FIGURE 26. BISMUTH I-II ELECTRICAL RESISTANCE TRANSITION IN THE BELT APPARATUS USING A 4-DEGREE DIE

60

These results suggest that the use of pyrophyllite without the silver chloride requires an additional 6 tons of ram force to obtain a pressure of 25,000 atm on the sample in an actual experimental run. Correspondingly, the use of the platinum heater tube in a pyrophyllite jacket appears to require an additional two tons of ram force in order to reach 25,000 atm so that an actual run in a heater tube requires an additional 8 tons of ram force to reach the pressure indicated from the calibration curve.

As a means of quantitatively assessing the relative importance of the pyrophyllite jacket, the platinum heater tube, and the particulate sample itself with respect to the ram force required to achieve an internal pressure of 25,000 atm, a group of experiments was run using the Bi I-II electrical resistance transition. The experimental conditions are shown in Figure 27, and the results are as follows:

Experimental Setup	Minimum Point of Bi I-II on Plot of Electrical Resistance Versus Ram Force, tons
A	41
B	47
C	49 ($CaCO_3$)
D	43
E	45 ($CaCO_3$)
F	49
G	48 ($CaCO_3$); 49 (GeO_2)

The results may be evaluated as follows:

(A) Ideal AgCl run as used in calibrating the Belt apparatus.

(B) Influence of pyrophyllite = 47 - 41 = 6 tons.

(C) Influence of sample plus pyrophyllite = (49 - 41) = 8 tons; influence of sample = 8 - 6 = 2 tons.

(D) Influence of platinum heater tube = 43 - 41 = 2 tons.

(E) Influence of platinum heater tube plus sample = 45 - 41 = 4; influence of sample = 4 - 2 = 2 tons.

(F) Influence of platinum heater tube plus pyrophyllite = 49 - 41 ≐ 8 tons.

(G) Typical experimental setup for high-pressure run in Belt apparatus. Test of additivity of influence of pyrophyllite, platinum heater tube, and sample: 49(GeO_2) - 41 = 8 tons ≠ Σ (B + C + D) or (6 + 2 + 2); 48($CaCO_3$) - 41 = 7 tons ≠ Σ (B + C + D) or (6 + 2 + 2).

The conclusions that have been drawn from this analysis are:

(1) The pyrophyllite is about three times more important than either the platinum heater tube or the sample with respect to the ram force
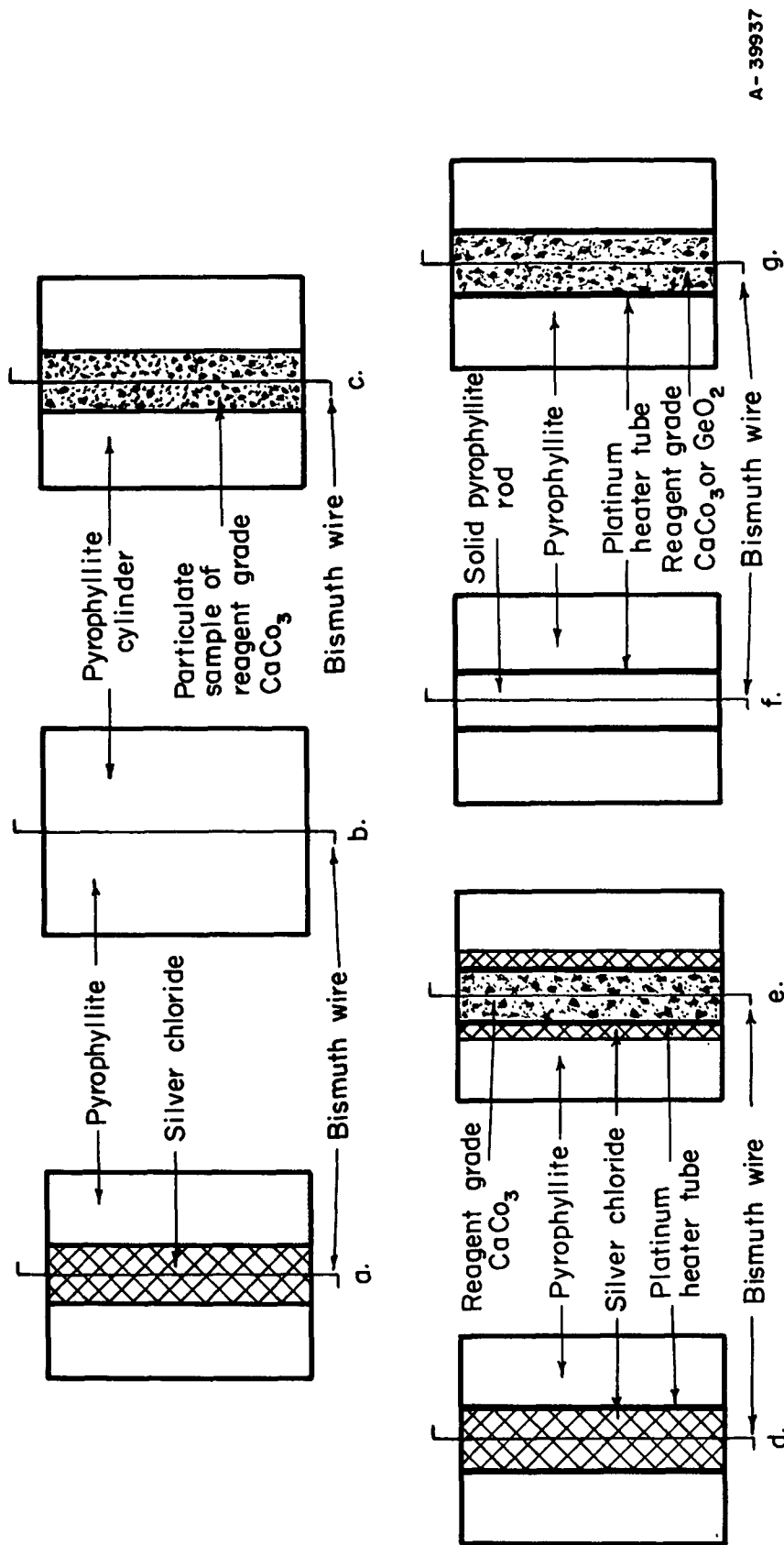
FIGURE 27. EXPERIMENTAL SETUPS IN BELT APPARATUS USING 4-DEGREE DIE TO INDICATE INFLUENCE OF PYROPHYLLITE, HEATER TUBE, AND SAMPLE ON RAM FORCE REQUIRED TO REACH 25,000 ATMOSPHERES

a. — Pyrophyllite, Silver chloride, Bismuth wire

b. — Pyrophyllite cylinder, Particulate sample of reagent grade CaCo₃, Bismuth wire

c.

d. — Reagent grade CaCo₃, Pyrophyllite, Silver chloride, Platinum heater tube, Bismuth wire

e.

f. — Solid pyrophyllite rod, Pyrophyllite, Platinum heater tube, Reagent grade CaCo₃or GeO₂, Bismuth wire

g.

A- 39937

62

required to obtain an internal pressure of 25,000 atm in the Belt apparatus.

(2) The individual influence of the platinum heater tube and of the sample is small.

(3) The combined effect of the platinum heater tube, the pyrophyllite, and the sample on the ram force required for the Bi I-II transition is not the sum of the three factors as ascertained separately. The magnitude of the combined effect is about 8 tons which is an increase of about 20 per cent as compared with the required load when AgCl is used.

(4) At about 25,000 atm in the Belt apparatus, the actual pressure on the sample is about 20 per cent less than that indicated on the AgCl-based calibration curve.

Although the difference between the pressure on the sample in an actual experimental run and the pressure deduced from the calibration curve in the 25,000 atm range is considered to be significant, it is probable that this difference decreases with increasing pressure and it might be negligible above 50,000 atm.

Calcite-Aragonite Transition. As a means of ascertaining some of the characteristics of the Belt apparatus, it was considered desirable in the early stages of the experimental program to study a well-known pressure-dependent first-order transformation. The calcite-aragonite transition was selected not only because the P-T equilibrium line to 600 C and 13,000 atm was known but because it had been determined experimentally in two different types of high-pressure high-temperature devices, and, at low pressures and temperatures, by electrical conductivity measurements. It was, therefore, of interest to determine the equilibrium line above 600 C and 13,000 atm in the Belt apparatus and to compare the slope and position of this line with the earlier results.

Calcium carbonate is known to occur in three polymorphic forms, viz., calcite (rhombohedral, density 2.71 g/cc), aragonite (orthorhombic, density 2.95 g/cc), and vaterite or μ-$CaCO_3$ (hexagonal, density 2.65 g/cc).

Calcite and aragonite are the common polymorphs of calcium carbonate and their atomic structures are well established. Although aragonite may be precipitated[26] from aqueous solution at 1 atm. its relatively high density coupled with thermochemical data for calcite and aragonite provided the basis for the long-standing argument that aragonite is the high-pressure form. Jamieson[27] determined the electrical conductivity of aqueous solutions in equilibrium with calcite and with aragonite as a function of temperature and pressure. Based on these experimental data he constructed the P-T equilibrium curve for calcite-aragonite between 25 and 80 C. Aragonite was shown to be the high-pressure phase. Subsequently, MacDonald[28] determined the equilibrium curve for calcite-aragonite between 250 and 600 C using the "simple squeezer" of Griggs and Kennedy[29], which is, in essence, a Bridgman anvil device equipped with an external heater. Aragonite is the high-pressure phase and it was shown to be the stable form at 30,000 atm and 490 C. The slope of the equilibrium curve, as determined by MacDonald, was in agreement with that of Jamieson, but was displaced about 1,500 atm toward the

temperature axis. To resolve this discrepancy, Clark[30] redetermined the calcite-aragonite equilibrium curve between 400 and 600 C using the more nearly hydrostatic nitrogen-gas pressure apparatus described by Robertson, et al.[31], in which the pressure is measured with a Manganin coil. Clark's data are in agreement with those of Jamieson and the curve is displaced from that of MacDonald by about 1,300 atm. Clark also reported that Kennedy has improved the accuracy of the pressure determinations in the apparatus used by MacDonald and that later results on $CaCO_3$ with this apparatus are in agreement with those of Jamieson and Clark.

Bridgman[32] investigated the effects of pressure on calcite to 50,000 atm and 200 C and found two reversible volume discontinuities which enabled him to delineate three areas on the P-T diagram designated I (normal calcite), II, and III. He concluded that these reversible transitions represented only minor structural changes. Jamieson[33] made an X-ray diffraction study of the effects of pressure on calcium carbonate to 24,000 atm at room temperature using a diamond pressure vessel which permits X-ray examination of the sample while it is subjected to pressure. Aragonite and vaterite showed no transition to 24,000 atm. Calcite underwent structural changes at 15,000 atm, the magnitude of which gradually increased to about 20,000 atm, at which point the diffraction pattern became very weak and diffuse. These effects are reversible and Jamieson ascribed them to anion disordering, a hypothesis which is consistent with the thermodynamic evidence. Jamieson also advanced a thermodynamic argument to show that calcite II and calcite III are metastable despite the reversible nature of the I-II and II-III transitions.

Vaterite is a relatively rare highly unstable form of calcium carbonate which is obtained by precipitation from aqueous solution under carefully controlled conditions. It dissolves in water at room temperature and pressure with concomitant precipitation of calcite and transforms rapidly to calcite at 400 C in air. Vaterite has recently been discovered in nature by McConnell[34] whose X-ray and electron-diffraction studies indicate that vaterite may be the hypothetical $CaCO_3$ end member of the bastnasite $(CeFCO_3)$-synchisite $(CeFCO_3 \cdot CaCO_3)$ atomic-substitution series.

The preceding discussion sets the background for the exploratory high-pressure high-temperature work carried out on Baker and Adamson calcium carbonate which is in the form of fine-grained calcite. A few runs were made with finely ground natural aragonite as the reactant. The experimental products were evaluated with the polarizing microscope and by X-ray powder diffraction. Some of the experimental data are tabulated in Table 5 and shown graphically in Figure 28. The results of this study have shown that:

(1) Aragonite is the high-pressure polymorph to at least 1,300 C and 60,000 atm; no other polymorphic form was detected.

(2) Below 200 C regardless of the pressure up to 60,000 atm, the final product is normal calcite (calcite I) when the reactant is calcite. Therefore, the apparently metastable anion-disordered field of calcite, as discussed by Bridgman and Jamieson, extends along the pressure axis below 200 C to at least 60,000 atm.

(3) The calcite-aragonite equilibrium line determined in the Belt apparatus has a slightly lower slope than that reported by earlier workers who used the "simple squeezer" and nitrogen-gas-pressure apparatus

64

TABLE 5.   EXPERIMENTAL RUNS ON $CaCO_3$

Temperature, C	Pressure, atm x 10^{-3}	Time, hr	Final Product
	Starting Material — Calcite		
950	60	15	Aragonite
700	59	15	Aragonite
400	32	50	Aragonite
500	22	12	Aragonite
120	32	13	Calcite
290	32	16	Aragonite
260	20	16	Aragonite
120	59	10	Calcite
240	58	2	Aragonite
860	21	2	Calcite
880	31	4	Aragonite
850	24	2	Calcite
1050	29	3	Calcite
1350	56	5	Aragonite
1200	42	3	Aragonite
680	18	11	Calcite
1250	35	2	Calcite
1180	31	4	Calcite
1190	37	4	1:1 calcite:aragonite
1430	46	2	Aragonite, trace calcite
1400	59	3	Aragonite
1320	45	2	Aragonite, trace calcite
720	25	3	Aragonite
1310	44	2	Aragonite
1300	38	2	Aragonite, trace calcite
1100	29	2	Calcite
700	20	17	Calcite
1330	36	5	Calcite, trace aragonite
1200	33	2	Calcite, trace aragonite
	Starting Material — Aragonite		
1000	26	2	Calcite
1200	29	11	Calcite
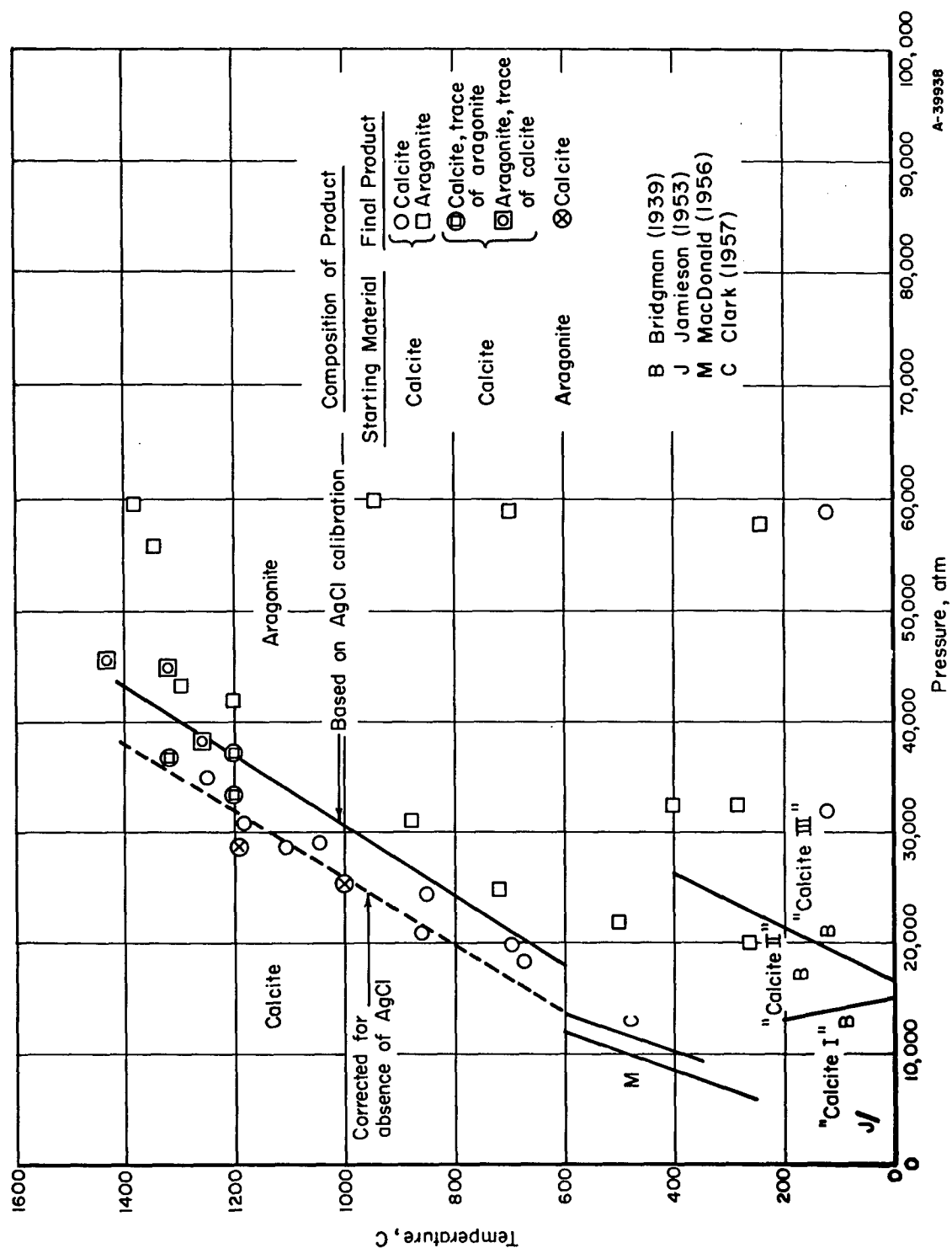
FIGURE 28. CALCITE-ARAGONITE EQUILIBRIUM LINE

and, in addition, is displaced along the pressure axis in the direction of higher pressures. The pressures related to the experimental points, however, were obtained from the calibration curve for the Belt apparatus which is based on electrical transitions run in silver chloride. For the pressure range related to the $CaCO_3$ experiments the Bi I-II transition at 25,000 atm is applicable. A ram force of 41 tons is required to obtain this transition in silver chloride, but the required ram force is 48 tons with the platinum heater tube and the $CaCO_3$ powder (without silver chloride). If the actual calibration point of 48 tons rather than the ideal point of 41 tons is used to calculate the pressure for each experimental point, the calcite-aragonite equilibrium line is displaced along the pressure axis in the direction of lower pressure so that it is in better agreement with the data of earlier workers. In these early runs in the Belt apparatus, it was found that the ram force from the 100-ton press would drop a few tons during the duration of a run and it was not restored to the desired magnitude in the belief that the pyrophyllite gaskets held the pressure seal. It was found, however, that if the experimental data were corrected for both the "actual pressure on sample" and the pressure drop, the equilibrium line determined in the Belt apparatus would be essentially the straight-line extrapolation of the Clark-Jamieson data (Figure 28).

Contamination Problem in the Belt Apparatus

Pyrophyllite Gasketing Material. The gasketing material used in the Belt apparatus is marketed under the trade name of Grade A Lava or Wonderstone by the American Lava Corporation of Chattanooga, Tennessee. This is the gasketing material originally selected by Hall[10] as having good thermal and electrical insulating properties and suitable frictional and flow characteristics for use in the Belt apparatus. It is a bluish-gray, soft, fine-grained, compact rock of uniform texture and with machinable properties which is quarried in the Transvaal, Union of South Africa, and it is composed predominantly of the sheet-structure micaceous mineral called pyrophyllite $(Al_2O_3 \cdot 4SiO_2 \cdot H_2O)$[35]. Published chemical analyses of different samples of this material are remarkably uniform for a natural material of this type and show consistently that its Al_2O_3/SiO_2 ratio is too high for it to be composed solely of pyrophyllite. Thus the material must contain other more aluminous minerals as well. Petrographic examination of thin sections reveals that the material is composed principally of 5- to 10-micron crystals of pyrophyllite which are tightly interlocked in random orientation. A combination of petrographic and X-ray diffraction methods revealed the presence of a suite of additional minerals and the quantitative mineral composition of the gasketing material as calculated from the chemical analyses is as follows:

	Calculated Weight, per cent
Pyrophyllite ($Al_2O_3 \cdot 4SiO_2 \cdot H_2O$)	75
Diaspore ($Al_2O_3 \cdot H_2O$)	8
Halloysite ($Al_2O_3 \cdot 2SiO_2 \cdot 2H_2O$)	6
Paragonite mica [$(Na,K)_3 \cdot Al_2O_3 \cdot 6SiO_2 \cdot 2H_2O$)]	4
Chloritoid ($FeO \cdot Al_2O_3 \cdot SiO_2 \cdot H_2O$)	4
Rutile (TiO_2)	2
Epidote ($4CaO \cdot 3Al_2O_3 \cdot 6SiO_2 \cdot 2H_2O$)	
Chlorite ($3MgO \cdot 2SiO_2 \cdot 2H_2O$)	
Hematite (Fe_2O_3)	1
Sphene ($CaTiSiO_5$)	
Carbonaceous matter	
	100

Thus, as originally indicated by the chemical analyses, the gasketing material is not pure pyrophyllite and contains significant amounts of alumina-rich minerals, the most important of which are diaspore and halloysite.

The behavior of the gasketing material under concomitant high temperature and high pressure is of interest inasmuch as any transformations it might undergo might result in changes in its pressure-transmitting characteristics which, in turn, could have a significant effect on the internal pressure obtained on the sample at a given press load. When the pyrophyllite is subjected to high pressures (>30,000 atm) at temperatures greater than 1,000 C, several white to light gray cylindrical zones coaxial with the platinum tube are formed. Examination of these zones by both X-ray diffraction and petrographic methods has revealed that they are composed of kyanite, the dense high-pressure polymorph of ($Al_2O_3 \cdot SiO_2$), and coesite, the dense high-pressure form of SiO_2. Kyanite is essentially the sole constituent of the first white zone in contact with a platinum heater tube from a run made at 60,000 atm at 1,300 C for 15 hr. This zone is about 0.2 mm thick and consists of a radially oriented stockadelike aggregate of bladed kyanite crystals up to 0.2 mm in length. Successive zones are composed of variable amounts of kyanite and coesite, and, in general, the kyanite/coesite ratio appears to decrease radially outward from the platinum heater tube. X-ray powder diffraction data for coesite given by Boyd and England[36] were used for determinative purposes. At high pressures and temperatures in the Belt apparatus, therefore, the pyrophyllite gasketing breaks down as follows:

$$Al_2O_3 \cdot 4SiO_2 \cdot H_2O \rightarrow Al_2O_3 \cdot SiO_2 + 3SiO_2 + H_2O$$
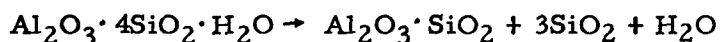
pyrophyllite $\rightarrow$ kyanite + 3 coesite + steam.

This reaction is not unanticipated, and indeed is predictable from the P-T stability fields for pyrophyllite, kyanite, and coesite given by Boyd and England[36], Kennedy[37], Clark, et al.[38], and Clark[39].

Giardini, et al.[40], in their work on diamond synthesis using a stepped-piston high-pressure device in which pyrophyllite is used as a gasketing material, also noted the formation of a "bleached zone" in the pyrophyllite when it was subjected to temperatures in excess of 1000 C and pressures greater than about 20,000 atm. In a recent paper[41] they report that the bleached zone is composed dominantly of kyanite and coesite which are accompanied frequently, but not always, by minor amounts of α-Al_2O_3 in high-pressure runs subjected to 1500 to 2000 C. No explanation is offered for the occurrence of α-Al_2O_3, but it is possible that this α-Al_2O_3 is the dehydration product of the original diaspore ($Al_2O_3 \cdot H_2O$) in the raw pyrophyllite which, at these elevated temperatures, becomes sufficiently coarse-grained to be detected by X-ray diffraction methods. No α-Al_2O_3 was detected in pressurized pyrophyllite subjected to temperatures up to 1300 C in the Belt apparatus, although a heavy-liquid sink product obtained from the raw pyrophyllite was shown to be enriched in diaspore which when heated to 600 C in air transformed to α-Al_2O_3 which was detected by X-ray methods.

Contamination of Pressurized Samples by Al, Si, and H_2O. During the experimental study of the calcite-aragonite equilibrium line, the petrographic microscope revealed the presence of an unusual minor component in several of the experimental products. This component was made up of abundant minute droplets (1 to 3 microns in size) of an anisotropic phase dispersed through an apparently isotropic matrix of relatively low refractive index (~1.47). This material was isolated by selectively leaching the calcite or aragonite, which constituted the bulk of each experimental product, with dilute HCl. The HCl-insoluble material was found in all the high-pressure products obtained at or near the calcite-aragonite equilibrium curve, that is, formed between 20,000 and 60,000 atm and at elevated temperatures between 500 and 1350 C. All but one of the HCl-leached residues give the same X-ray powder diffraction pattern, and both patterns are unique in that they are neither calcite nor aragonite (Table 6, Columns 1 and 2).

After the discovery of the HCl-insoluble phases in the calcium carbonate high-pressure, high-temperature products, there was considerable speculation as to its identity, and the question arose as to whether it might be either a new high-pressure high-temperature form of $CaCO_3$, a dissociation product such as CaO, or a dissociation-hydration product such as $Ca(OH)_2$, the water in the latter being derived from the pyrophyllite gasketing material. Although the powder diffraction pattern of the unknown phase is not equivalent to either ordinary cubic CaO or hexagonal $Ca(OH)_2$, the possibility of a hitherto unknown high-pressure form of either compound had to be considered. Accordingly, reagent grade cubic CaO and $Ca(OH)_2$ prepared from CaO by slaking were subjected to 53,000 atm at 1000 C. The $Ca(OH)_2$ remained unchanged but the CaO product, although very fine grained, was optically anisotropic and gave a unique X-ray powder diffraction pattern which was not equivalent to that of the HCl-insoluble material in the $CaCO_3$ products. The same cubic CaO reagent does not change, other than to become more coarsely crystalline, when heated in air at 800 C at 1 atm for 12 hr.

A limited amount of experimental work was done on CaO in the 30,000 to 60,000-atm range and between 1000 and 1350 C, mainly to establish the reproducibility of the final products. The results of the experiments showed that cubic CaO be converted to

TABLE 6. X-RAY POWDER DIFFRACTION DATA FOR CONTAMINATION PRODUCTS IN BELT APPARATUS

Fe Radiation, Mn Filter

1 (a)		2 (b)		3 (c)			4 (d)		5 (e)		6 (f)	
d, A	I	d, A	I	d, A	I	hkl	d, A	I	d, A	I	d, A	I
4.4	80	4.9	74	4.12	3	201	4.80	20	3.85	40	5.0	25
3.55	10	4.2	25	3.66	1	210	4.13	25	3.28	20	4.35	10
3.05	20	3.65	80	3.27	3	003	4.05	15	3.00	60	3.30	10
2.57	30	3.26	30	2.94	50	212	3.80	40	2.67	100	3.05	60
2.50	10	3.03	20	2.65	100	301	3.40	10	2.56	5	2.75	100
2.45	7	2.93	40	2.51	15	222	3.02	80	2.44	15	2.52	15
2.40	5	2.70B	30	2.41	30	302	2.90	5	2.34	10	2.42	10
2.24	15	2.63	100	2.31	30	312	2.73	100	2.26	10	2.24	40
2.11	100	2.43	45	2.16	30	223	2.62	5	2.19	20	1.98	55
1.87	40	2.27	25	2.09	10	303	2.55	10	1.94	40	1.70	25
1.68	5	2.13	70	1.91	40	331	2.47	10	1.83	5	1.64	40
1.64	10	1.97	20	1.72	25	215	2.32	10	1.73	15	1.53	50
1.48	5	1.27	20	1.64	50	431, 501	2.26	5	1.66	35	1.38	10
1.43	50	1.77	15	1.58	70	106	2.19	5	1.60	50	1.35	10
1.38	75	1.68	5	1.48	20	216	2.05	5	1.50	10	1.31	5
1.27	5	1.63B	35	1.46	10		1.91	50	1.34	15	1.14	10
1.157	10	1.55	65	1.325	25		1.88	10	1.31	20	1.12	10
1.125	5	1.465	50	1.292	35		1.80	30	1.28	15	1.081	3
1.057	5	1.39	20	1.262	20		1.75	20	1.21	10	1.025	3
0.998	30	1.36	5	1.248	5		1.68	40	1.113	50	1.013	3
		1.31	10	1.196	10		1.63	40	1.09	30	0.997	15
		1.28	15	1.161	10		1.53	10	1.06	30		
		1.19	5	1.130	3		1.50	10	1.035	30		
		1.15	5	1.100	70		1.47	5	1.000	15		
		1.09	15	1.083	65		1.27	25	0.985B	10		
		1.065	15	1.048	40		1.25	25	0.976B	15		
		1.025	10	0.9980	30		1.18	5				
		0.999	3	0.9753	35		1.16	20				
		0.985	3				1.14	20				
							1.11	5				
							1.095	5				
							1.08	5				
							1.037	5				
							1.015	20				
							1.002	20				
							0.9805	25				

(a) HCl leached residue from pressurized $CaCO_3$; pattern obtained from five products.
(b) HCl leached residue from pressurized $CaCO_3$; pattern obtained from one product (1320 C, 50Kb).
(c) Contamination Phase 1; tetragonal from CaO.
(d) Contamination Phase 2; orthorhombic from CaO.
(e) Contamination Phase 3 from CaO.
(f) Contamination Phase 4 from CaO.

three and possibly four discrete optically resolvable phases, all of which may occur in the same experimental product and two of which have been found as essentially single-phase segregations in zoned products. Although chemically pure reagents were used in the experimental work, direct chemical analytical data for the apparent "high-pressure forms" of both $CaCO_3$ and CaO were required. Accordingly, emission spectrochemical analyses were made of the high-temperature high-pressure products of both $CaCO_3$ and CaO. All of the products contained significant concentrations of aluminum and silicon. The source of these contaminants is evidently the pyrophyllite gasketing material. As discussed above, when pyrophyllite is subjected to high pressures at temperatures greater than 1000 C it decomposes to kyanite, coesite, and water. Supercritical steam under high pressure is an excellent carrier of silica and alumina in vapor solution, and it appears from the spatial distribution of the reaction products that the contaminants enter the cylindrical platinum sample capsule at the ends which are cold sealed mechanically with platinum foil. The significance of this discovery with respect to high-pressure experimentation at temperatures above 700 C is self-evident.

A description of the four calcium-aluminum-silicates formed by reaction of CaO with aqueously transported alumina and silica at high pressure and temperature follows:

(1) This phase occurs as a zone of transparent colorless material at either one or both ends of the platinum capsule (Figure 29). If it occurs at one end, it is the end which is sealed last, after the sample has been introduced, and this is evidently the end with the weaker seal. It has a vitreous luster, semiconchoidal fracture, and very weak optical anisotropy with an indication of complex polysynthetic twinning and a mean refractive index of 1.735 ± 0.002. It is insoluble in water and cold concentrated mineral acids (HCl, HNO_3, and H_2SO_4). It tends to break into thin plane-parallel tablets because of a closely spaced set of parallel fracture planes oriented normal to the axis of the platinum tube. The fractures do not appear to have a simple relationship to the internal structure of this phase, as shown by single-crystal X-ray methods, but instead appear to be tensional fractures that probably develop upon release of the pressure. Spectrochemical analysis indicates that the material contains about 30 per cent CaO, 20 per cent Al_2O_3, and 50 per cent SiO_2 from which an ideal formula of ($8CaO \cdot 3Al_2O_3 \cdot 12SiO_2 \cdot H_2O$) or $[HCa_4Al_3(Si_2O_7)_3]$ may be deduced. This is the ideal formula of a sorosilicate. X-ray powder diffraction data for this material have been indexed on a tetragonal basis with $c/a = 1.18$, $c = 9.8$ A and $a = 8.3$ A (Table 6, Column 3). Selected area electron-diffraction data support the contention that this material has a high symmetry and that it is probably tetragonal. The density of the material as measured by float-sink in Clerici's solution (aqueous solution of thallium formate-malonate) using diamond (d = 3.51), topaz (d = 3.58), and kyanite (d = 3.63) as density indicators is 3.57, and the calculated number of formula weights per cell is 2. The material was heated in air at 1100 C for 20 hr to determine whether it would transform to a more stable phase at ambient pressure. It changed from colorless to yellow and the mean index of refraction dropped slightly to about 1.726, but the X-ray diffraction pattern was unchanged. Spectroscopic analysis showed the presence of 0.05 to 0.5 per cent of iron in solid solution and the color change is probably related to the oxidation of this iron. The iron was certainly carried into the sample capsule with the alumina and silica and its source was the pyrophyllite.
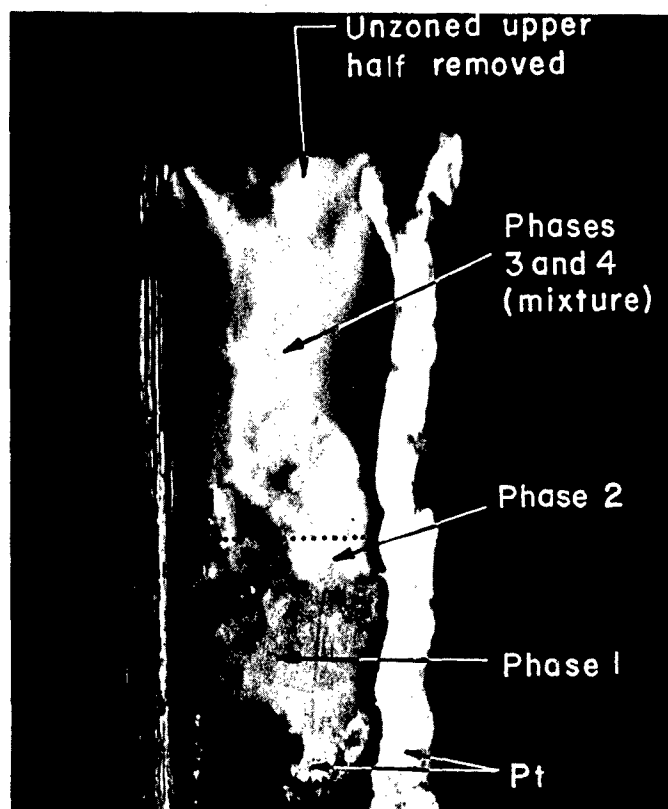
13X

FIGURE 29. LONGITUDINALLY SECTIONED PLATINUM
CAPSULE OF A HIGH-TEMPERATURE
HIGH-PRESSURE RUN ON CaO SHOWING
DEVELOPMENT OF CONTAMINATION
PRODUCTS

(2) This phase occurs as single-bladed to tabular colorless crystals as large as 0.23 mm in length and 0.1 mm in width which have rectilinear outlines. It characteristically occurs as a thin zone between Phase 1 and the bulk of the material in the platinum capsule which is a mixture of Phases 3 and 4 (Figure 29). It has an excellent cleavage (prismatic ?) parallel to the elongation and possibly parting normal to the elongation. Its optical properties are as follows: $\alpha = 1.640$, $\beta = 1.652$, $\gamma = 1.658$, all ± 0.002, (-)2V = 70 deg; optic plane transverse to the elongation; optical elongation ($\pm$); dispersion of optic axes $\rho > r$; parallel extinction. The symmetry is orthorhombic based on the optical properties and on cursory single-crystal X-ray diffraction work and selected area electron-diffraction data. Spectrochemical analysis shows that the phase contains 53 per cent CaO, 10 per cent Al_2O_3, and 37 per cent SiO_2, and trace amounts of iron and magnesium. The ideal formula ($10CaO \cdot Al_2O_3 \cdot 6SiO_2 \cdot H_2O$) or $[Ca_5Al(SiO_4)_3(OH)]$ has been deduced from the chemical analytical data. The phase dissolves in dilute HCl with evolution of gas. X-ray powder data for the phase are given in Table 6, Column 4. The structure of this phase is probably related to that of "Phase Z" of Roy, et al.[43], to $\gamma - Ca_2SiO_4$[44], and to calciochondrodite $[Ca_5(SiO_4)_2(OH)_2]$[43].

(3) This phase occurs as minute (1 to 10 micron) colorless grains dispersed in an intergranular matrix of Phase 4. This intimate mixture of Phases 3 and 4 typically constitutes the bulk of the experimental products from contaminated CaO runs. Phase 3 is weakly anisotropic with a mean index of refraction of about 1.69 ± 0.02. It is insoluble in water and cold concentrated mineral acids (HCl, HNO_3, H_2SO_4). X-ray powder diffraction data are given in Table 6, Column 5.

(4) This is the intergranular matrix for Phase 3 which together with Phase 3 constitutes most of the products from contaminated CaO runs. It is weakly anisotropic and has a relatively low index of refraction (about 1.63). It dissolves in HCl with evolution of gas and may be related to Phase 2. X-ray powder diffraction data are given in Table 6, Column 6.

Spectrochemical analysis of the mixtures of Phases 3 and 4 shows 25 per cent CaO, 25 per cent Al_2O_3, and 50 per cent SiO_2 with traces of magnesium and iron.

To summarize, alumina and silica derived from the pyrophyllite gasketing material are carried in vapor solution into the platinum sample capsule during high-pressure runs in the Belt apparatus when the temperature exceeds about 700 C. The degree of contamination of the sample appears to increase with increasing temperature and time. As shown by zonation of the contaminants in the sample capsule, the contaminants enter through the ends which are cold sealed mechanically with 0.5-mil platinum foil. Using CaO as an indicator of contamination, at least two and possibly four discrete unique phases in the system $CaO-Al_2O_3-SiO_2-H_2O$ have been synthesized by reaction of aqueously carried alumina and silica with CaO. These phases are possibly pressure-dependent compounds which are metastable at ambient pressure. Compositional differences coupled with spatial distribution of Phases 1 and 2 suggest that under the conditions

of synthesis there is some chemical partition between alumina and silica along the thermal gradient which parallels the axis of the sample tube, but the chemical composition of the mixture of Phases 3 and 4 shows that the chemical concentration gradients are complex. With the cold-sealing method employed, contamination does not necessarily occur in every high pressure run in the Belt apparatus, but the frequency of occurrence using CaO as an indicator at temperatures between 700 and 1300 C was about 3 out of 4.

Resolution of the Contamination Problem. Exploratory experiments using CaO as an indicator of contamination showed that (1) contamination of the sample with water, silica, and alumina may occur, (2) the source of the contaminants is the pyrophyllite gasketing material, and (3) the contaminants enter the sample at its mechanically sealed ends. Hydration of the sample may occur at temperatures as low as 750 C at a pressure as low as 20,000 atm. Alumina-silica contamination reactions with CaO are known only from high-pressure runs at temperatures greater than 950 C, but alumina-silica contamination reactions with $CaCO_3$ are known from runs at temperatures as low as 700 C and pressures as low as 20,000 atm.

Several approaches were taken with the objective of alleviating the contamination problem. These included (1) design and fabrication of several mechanical aids for cold sealing the platinum capsules, (2) increasing the thickness of the platinum end seals, (3) dehydrating the gasketing material prior to pressurization, and (4) consideration of anhydrous substitutes for pyrophyllite. Approaches 2 and 3 proved to be successful. The former consists of mechanically cold sealing each end of the capsule with a three-fold sandwich consisting in succession of 5-mil platinum disks, 0.5-mil platinum foil, and 5-mil platinum disks, whereas in earlier work the ends were sealed solely with 0.5-mil platinum foil. In the latter approach, the machined pyrophyllite cylinder which encloses the platinum sample capsule is prefired in air at 925 C. This is below the mullitization point (~1100 C) of pyrophyllite so that the fired product still has the structure of pyrophyllite, as shown by X-ray diffraction and microscopic examination. As a result, the fired pyrophyllite has mechanical and pressure-transmitting properties that are essentially the same as the raw material as shown by the ram force required to obtain the Bi I-II transition. The most significant factor related to the heat treatment, however, is the reduction in water content from 6.0 to 0.3 per cent by weight. The removal of water restricts the mobility of the aluminum and silicon so that experimental high pressure-high temperature products from CaO runs are free from contamination.

The contamination problem may thus be resolved by using the disk-foil sandwich to seal the tube ends or by prefiring the pyrophyllite jacket around the sample tube at 925 C. In practice, prefiring the pyrophyllite shows a linear expansion of about 2 per cent so that dimensional compensation should be applied when the raw pyrophyllite is machined.

Experimental Results

Effect of Pressure on Heteropolynuclear Acids
and Salts

Experimental high-pressure high-temperature work was done on two heteropolynuclear acids and two heteropolynuclear salts. The former pair are silicotungstic acid ($H_4SiW_{12}O_{40} \cdot nH_2O$) and phosphotungstic acid ($H_3PW_{12}O_{40} \cdot nH_2O$), and the latter pair are

hydrated ammonium phospho-vanado-tungstate $[(NH_4)_{3+x}PV_xW_{12-x}O_{40} \cdot nH_2O$ in which x approximates 1, crystallized from solution at high pH with initial solution weight ratios of P:V:W = 1:1:16] and hydrated ammonium arseno-vanado-tungstate $[(NH_4)_{3+x}AsV_xW_{12-x}O_{40} \cdot nH_2O$ in which x approximates 2, crystallized from solution at high pH with initial solution weight ratios of As:V:W = 1:3:16].* The experimental runs and the results obtained are summarized in a set of temperature-pressure diagrams (Figures 30, 31, 32, 33). The boundary lines on the diagrams which delineate the stability fields for the various structural modifications are solely schematic, and many more experimental data are required to determine their positions accurately. At this juncture, however, they are useful as guides for further experimental work. The products corresponding to the points on the diagrams have been evaluated by X-ray powder diffraction methods and, for some of the silicotungstic acid products, by optical crystallographic methods as well. X-ray powder diffraction data for the various structural modifications obtained in experimental products are given in Tables 7, 8, and 9. As a control on the validity of any conclusions regarding pressure-induced transformations, the effects of temperature at 1 atm on each of the materials under study has been determined.

Experimental High-Pressure Products From Silicotungstic Acid. Silicotungstic acid has been studied in greater detail than the other materials, and accordingly, descriptive notes on some of the products are recorded.

The starting material (Fisher Reagent A-289) is a colorless coarsely crystalline powder composed of single-crystal grains up to 2 mm in size. It is uniaxial negative with $\omega = 1.724$, $\epsilon = 1.692$, and a moderately high birefringence. It is probably a higher hydrate than the cubic material with $8H_2O$ listed in the ASTM index of X-ray powder diffraction patterns [data of Scroggie and Clark[45]]. When the Fisher compound is heated in air at 1 atm it transforms above about 125 C to a colorless isotropic material with an index of refraction of 1.915 ± 0.005 and a powder pattern corresponding to a body-centered cubic cell with $a_0 = 12.16$ A, which is equivalent to that given on the ASTM card. Two spacings (d = 8.6 A and d = 6.08 A for hkl of 110 and 200, respectively) were not obtained on a cylindrical film by Scroggie and Clark but were verified by them on a flat film. Because of these experimental differences the relative intensities of these two lines with respect to the rest of the pattern were not recorded, and, probably for this reason, these lines were not listed on the ASTM card. In the present study, both of these spacings were obtained with the entire pattern on a cylindrical film, using a 114.6-mm camera, and the 8.6 A spacing was found to be the strongest (100) line of the pattern; the 6.08 A spacing has a relative intensity of about 35.

When the Fisher reagent is heated to 500 C at 2600 atm, a black powder with a unique X-ray powder pattern (Table 7, Column 7) and optical properties is obtained.

The powder is composed of square to rectangular tablets with an average side length of about 10 microns; a few are as long as 35 microns. The tablets have an intense pleochroism with extraordinarily strong absorption when observed in transmitted light in the direction of the optic axis which is normal to the broad face of the tablets. The pleochroic formula is ω = deep green-blue to practically opaque even in strongly convergent light depending on thickness, and ϵ = pale yellow to colorless. Because of the strong absorption it is not possible to measure the index of refraction, but is probably greater than 2.00. The tablets show extinction between crossed Nicol prisms parallel to

*Synthesized by J. J. Bulloff and P. F. Kurz at Battelle Memorial Institute.
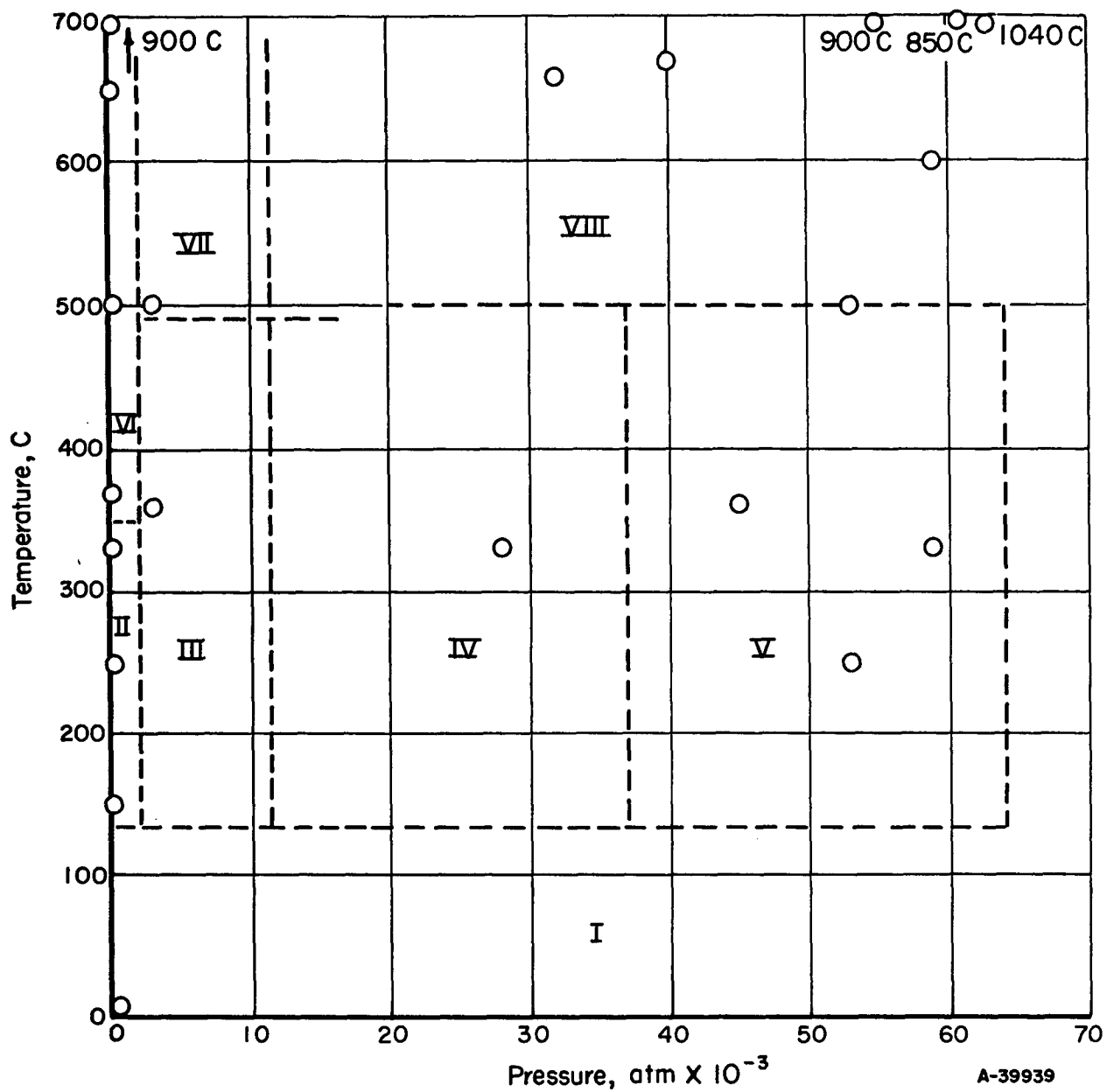
FIGURE 30. PLOT OF EXPERIMENTAL RUNS ON SILICOTUNGSTIC ACID

76
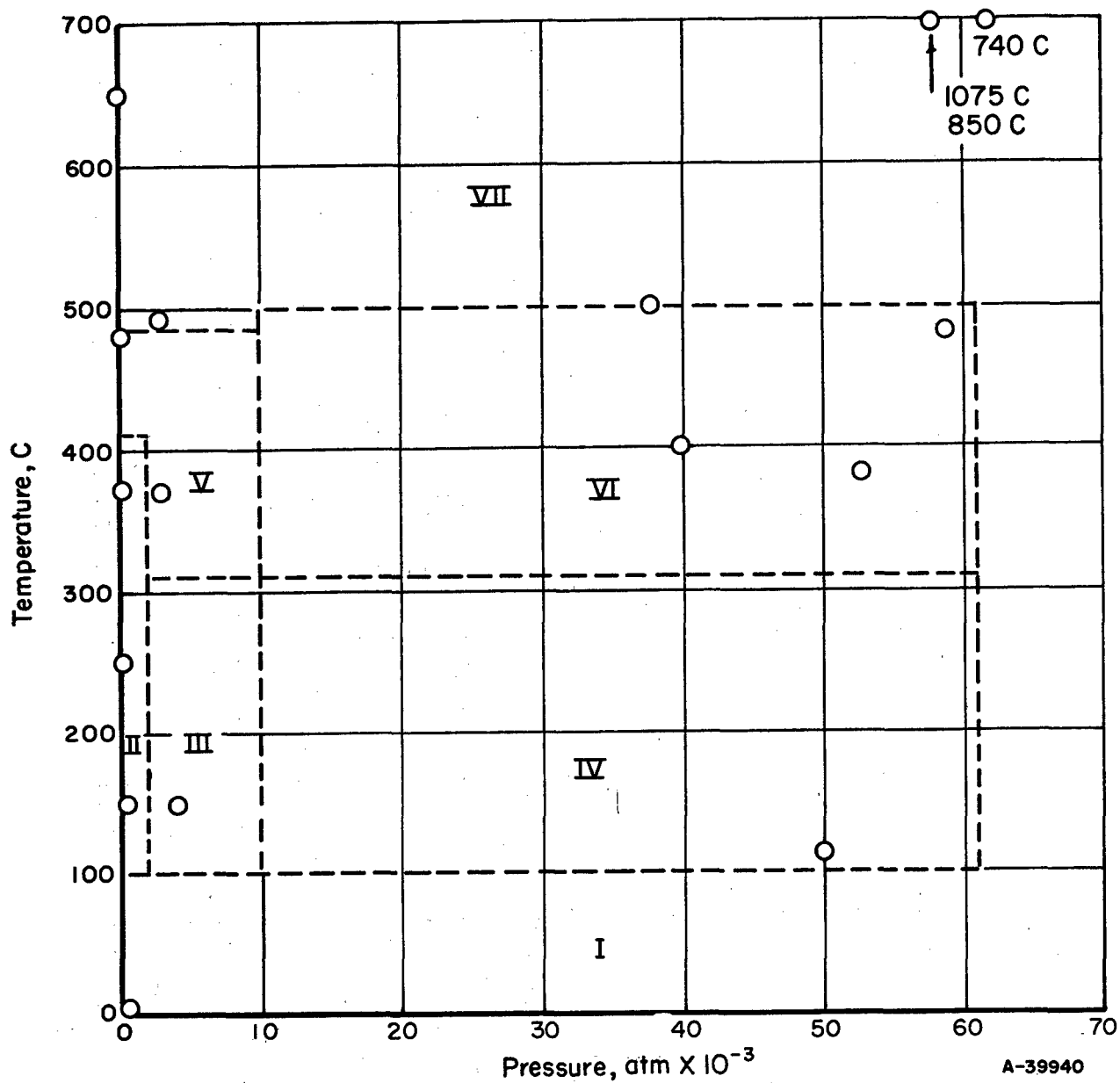
FIGURE 31. PLOT OF EXPERIMENTAL RUNS ON PHOSPHOTUNGSTIC ACID
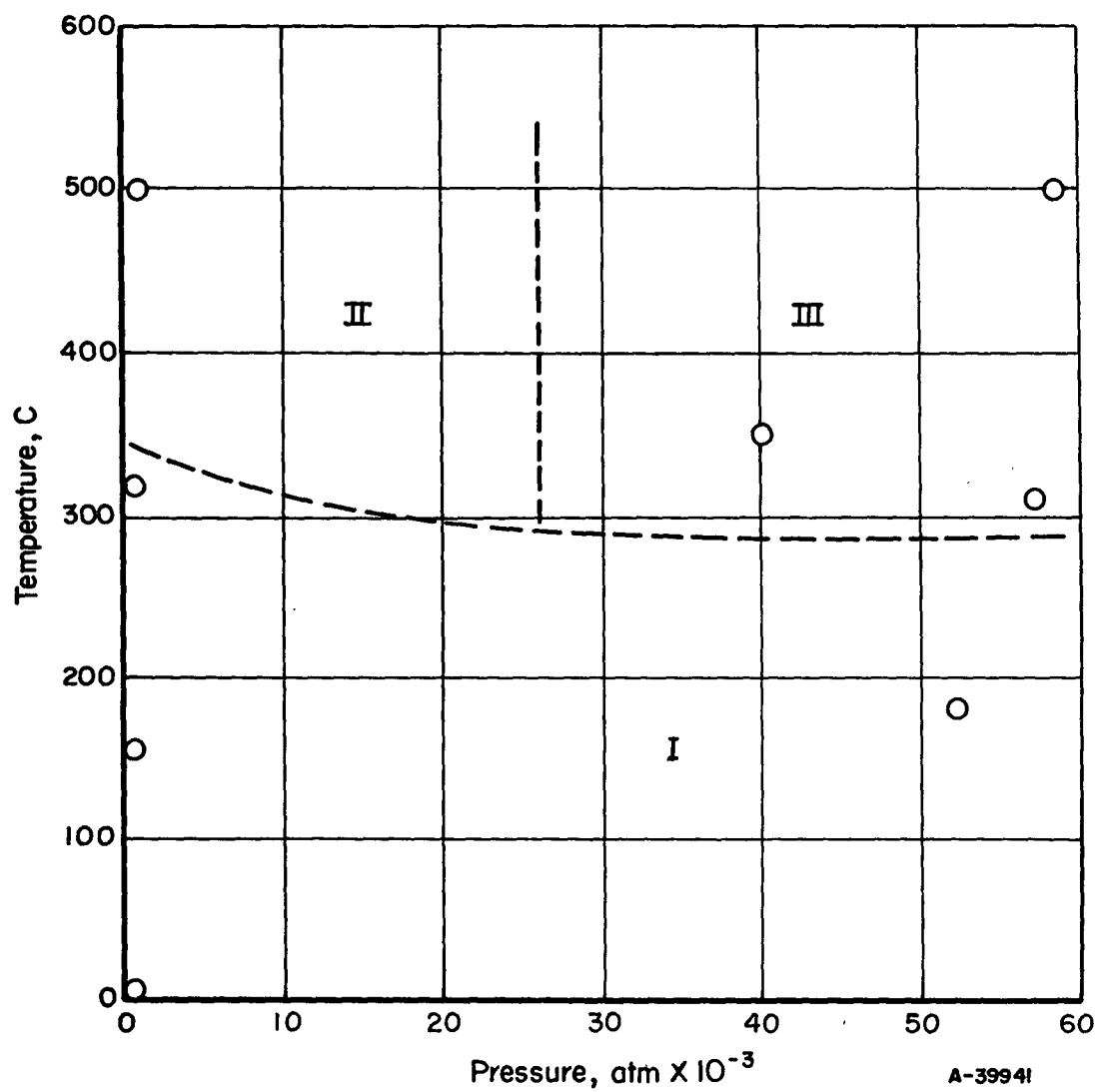
FIGURE 32. PLOT OF EXPERIMENTAL RUNS ON HYDRATED
AMMONIUM-ARSENO-VANADO-TUNGSTATE

FIGURE 33. PLOT OF EXPERIMENTAL RUNS ON HYDRATED
AMMONIUM-PHOSPHO-VANADO-TUNGSTATE

TABLE 7. X-RAY POWDER DIFFRACTION DATA FOR EXPERIMENTAL PRODUCTS FROM SILICOTUNGSTIC ACID

1 Cr Radiation, V Filter		2 Fe Radiation, Mn Filter		3 Fe Radiation, Mn Filter		4 Fe Radiation, Mn Filter		5 Fe Radiation, Mn Filter		6 Fe Radiation, Mn Filter		7 Fe Radiation, Mn Filter		8 Fe Radiation, Mn Filter	
d,A	I	d,A	I	d,A	I	d,A	I	d,A	I	d,A	I	d,A	I	d,A	I
19.7	40	9.5	20	5.7	10	6.2	50	12.2	10	7.20	10	5.3B	5	5.4B	10
14.6	10	8.6	100	5.0	10	5.3	25	11.2	20	3.80	50	3.82	70	3.83	100
12.1	60	6.1	30	3.80	100	4.8	70	10.2	10	3.65	100	3.74	50	3.75	75
10.95	100	5.0	30	3.70	30	4.2	40	5.93	70	3.07	20	3.62	100	3.68	20
10.06	5	4.3	70	3.60	50	3.83	70	5.38	90	2.64B	45	3.44	5	3.63	80
9.19	35	3.85	60	3.40	10	3.79	100	4.63	20	2.14	25	3.30	15	3.42	5
8.48	30	3.50	90	3.30	15	3.70	5	4.15	10	1.98	10	3.08	20	3.33	10
5.30B	5	3.04	40	3.16	30	3.60	30	3.83	70	1.91	10	2.94	10	3.09	20
4.75	15	2.86	30	3.05	20	3.44	30	3.75	30	1.84	35	2.87	10	2.95	10
4.57	20	2.72	20	2.70	50	3.25	60	3.47	100	1.80	10	2.66	50	2.88	10
4.41	25	2.58	80	2.60		3.13	70	3.14	10	1.71B	5	2.62	40	2.67	45
4.20B	10	2.38	50	2.50B	10	3.10	60	2.94	20	1.64B	40	2.52	5	2.63	40
3.80	10	2.22	10	2.40	10	2.67	10	2.88	50	1.54	10	2.38	5	2.53	5
3.35	70	1.97	20	2.30	30	2.64	10	2.69	60	1.52	15	2.16	20	2.38	5
3.20	40	1.88	10	2.14	40	2.42	40	2.63	60	1.47	7	2.00	30	2.16	20
3.12	50	1.72B	40	1.92	40	2.37	30	2.57	80	1.34	3	1.92	40	2.00	15
3.04B	15	1.55B	30	1.87	20	2.23	10	2.39	40	1.32	5	1.88	50	1.92	30
2.96	10	1.49B	20	1.82	50	2.15	5	2.36	40	1.24B	20	1.82	20	1.88	20
2.85	10			1.78	40	2.09	10	2.32	50	1.175	10	1.80	15	1.83	40
2.71B	10			1.70	30	2.02	20	2.12B	30	1.115B	15	1.72	20	1.80	15
2.63	5			1.65	40	1.96	5	2.03	20	1.075	5	1.70	15	1.72	20
2.46B	7			1.63	30	1.92	60	2.02	20	1.053	5	1.69	5	1.70	10
2.41	10			1.53	10	1.81	55	1.98	40	1.03B	5	1.64	20	1.69	10
2.37	7			1.50	30	1.78	10	1.96	40			1.56	5	1.64	20
2.33	7			1.46	10	1.74	10	1.92	20			1.54	10	1.56	5
2.24	5			1.40	5	1.69	10	1.91	20			1.51	20	1.54	5
2.04	10			1.38	5	1.65	10	1.85	50			1.48	30	1.52	10
2.02	10			1.33	10	1.64	60	1.84	60			1.47	10	1.49	20
1.98	15			1.31	20	1.60	10	1.80	20						
1.95	3			1.28	20	1.57	35	1.77	20						
1.92	5			1.24	60	1.55	10	1.75	20						
1.90	10			1.215	30	1.51	5	1.74	60						
1.85	10			1.195	10	1.45	40	1.70	30						
1.84	5					1.43	5	1.66	20						
						1.41	10	1.64	60						
						1.38	10	1.61	50						
						1.35	10								
						1.32	30								

TABLE 8. X-RAY POWDER DIFFRACTION DATA FOR EXPERIMENTAL
PRODUCTS FROM PHOSPHOTUNGSTIC ACID

1		2		3		4		5		6		7	
Cr Radiation, V Filter		Fe Radiation, Mn Filter		Fe Radiation, Mn Filter		Cr Radiation, V Filter		Fe Radiation, Mn Filter		Cr Radiation, V Filter		Fe Radiation, Mn Filter	
d, A	I	d, A	I	d, A	I	d, A	I	d, A	I	d, A	I	d, A	I
12.2B	20	8.5	70	10.5	100	10.7	20	11.2B	20	6.36	60	5.40B	10
11.1	100	7.3	5	9.5	50	9.84	10	9.8B	20	3.76	50	3.83	100
10.1	70	6.0	20	8.7	5	9.58	100	4.44	3	3.68	10	3.74	75
9.5	50	4.9	20	8.0	5	9.06	40	4.3	3	3.62	5	3.68	20
7.8	5	4.22	40	5.5	40	7.83	10	4.05	5	3.50	30	3.63	80
5.55	10	3.79	30	4.7	25	5.86	10	3.82	60	3.31	20	3.42	5
5.06	40	3.45	100	4.5	25	5.37 } 5.17	15	3.68	100	3.24	5	3.33	10
4.78	30	3.30	5	4.2	20			3.46	5	3.19	100	3.09	20
4.57	5	3.20	5	3.8	10	4.86	15	3.13	20	3.07	2	2.95	10
4.45	30	3.00	35	3.45	15	4.68	40	3.07	30	2.89	3	2.88	10
4.33	7	2.83	20	3.35	40	4.59	3	2.67	60	2.64	30	2.67	45
4.21	20	2.68	10	3.15B	70	4.39	1	2.61	50	2.44	60	2.63	40
3.97	5	2.56	50	2.95	10	4.03	5	2.50	10	2.30	10	2.53	5
3.83	3	2.35	35	2.71	40	3.55B	3	2.32	3	2.14	7	2.38	5
3.45	50	2.19	10	2.50	30	3.39	45	2.17	30	2.08	5	2.16	20
3.24	20	2.12	10	2.37B	10	3.26	45	1.99	10	1.91	10	2.00	15
3.14	50	2.00	10	1.91	30	3.08	60	1.91	20	1.85	50	1.92	30
2.98	10	1.95	30	1.85	15	3.01	5	1.84	30	1.77	5	1.88	20
2.90	20	1.90	3	1.74	20	2.95	40	1.79	30	1.73	20	1.83	40
2.75	10	1.87	3	1.65	20	2.85	40	1.70	30	1.68	2	1.80	15
2.72	20	1.85	10	1.62	10	2.68	20	1.65B	35	1.66	40	1.72	20
2.64	20	1.81	3	1.56	7	2.61B	15	1.58	3	1.63	40	1.70	10
2.57	10	1.70	40	1.53	5	2.51	15	1.54	10	1.60	30	1.69	10
2.51	25	1.635	10	1.47	20	2.45	5	1.50	5	1.48	40	1.64	20
2.45	10	1.59	7	1.45	10	2.34	3	1.48	5	1.455	15	1.56	5
2.42	15	1.53	45	1.42	20	2.00	10	1.33B	3	1.44	3	1.54	5
2.39	5	1.49	20			1.96	5			1.415	3	1.52	10
2.33	30	1.42	10			1.93	5			1.40	3	1.49	20
2.00	10					1.87	20			1.37	15		
1.94B	15									1.345	5		
1.88B	10									1.33	3		
1.72	10									1.32	30		
1.70	10									1.31	5		
1.67	30									1.295	5		

81

TABLE 9. X-RAY POWDER DIFFRACTION DATA FOR EXPERIMENTAL PRODUCTS FROM AMMONIUM ARSENO-VANADO-TUNGSTATE HYDRATE AND AMMONIUM PHOSPHO-VANADO-TUNGSTATE HYDRATE

Ammonium Arseno-Vanado-Tungstate Hydrate						Ammonium Phospho-Vanado-Tungstate Hydrate							
1		2		3		1		2		3		4	
Cr Radiation, V Filter		Fe Radiation, Mn Filter		Fe Radiation, Mn Filter		Cr Radiation, V Filter		Fe Radiation, Mn Filter		Cr Radiation, V Filter		Fe Radiation, Mn Filter	
d, A	I	d, A	I	d, A	I	d, A	I	d, A	I	d, A	I	d, A	I
11.0	100	5.5B	40	11.04	10	9.30	100	8.2	50	6.28	60	5.5B	40
7.7	30	4.3B	10	6.93	10	8.30	10	5.80	30	3.82	60	4.3B	10
5.41	20	3.75B	100	6.15	50	7.30	10	4.75	10	3.61	30	3.75B	100
4.88	50	3.40B	10	4.23	15	5.40	40	4.55	3	3.45	30	3.40	10
4.24	5	3.10	10	3.85	40	4.90	5	4.10	40	3.27	30	3.10	10
4.00	5	2.65	50	3.62	20	4.60	10	3.69	10	3.14	100	2.65	50
3.87	15	2.16	20	3.45	20	4.45	5	3.45	100	2.88	3	2.16	20
3.64	30	2.00	10	3.28	20	4.10	5	3.20	3	2.63	10	2.00	10
3.46	15	1.91	5	3.14	100	3.80	5	3.0	3	2.42	50	1.91	5
3.15	80	1.85	10	2.67	5	3.73	10	2.91	40	2.09	5	1.85	10
3.02	5	1.79	10	2.63	5	3.50	20	2.74	20	2.02	5	1.79	10
2.91	10	1.67B	30	2.43	30	3.38	20	2.60	10	1.96	5	1.67B	30
2.73	40	1.52B	20	2.08	3	3.30	30	2.48	40	1.92	10	1.52B	20
2.65	60			2.02	3	3.17	30	2.28	30	1.84	10		
2.57	5			1.93	5	3.10	5	2.13	10	1.81	20		
2.44	.5			1.84	5	3.05	15	2.06	20	1.74	10		
2.33	10			1.81	20	2.97	5	1.94	10	1.69	5		
2.23	5			1.64	30	2.80	5	1.89	20	1.64	70		
2.14	5			1.57	10	2.68	10	1.85	5	1.59	5		
2.02	10			1.45	10	2.64	20	1.80	15	1.57	10		
1.93	30			1.317	15	2.56	20	1.75	15	1.45	30		
1.90	5			1.290	3	2.42	10	1.68	5	1.41	5		
1.87	3			1.255	3			1.65	30	1.37	5		
1.70	30			1.215B	10			1.59	15	1.35	7		
1.68	5			1.185B	10			1.56	3	1.32	30		
1.65	30							1.53	3	1.29	20		
1.56B	20							1.48	35	1.24	5		
1.48	3							1.435	20	1.22	30		
1.45	40							1.375	5	1.187	30		
1.39	20							1.355	5				
								1.320	3				
								1.280	3				

their sides; this suggests tetragonal symmetry. The product might be anhydrous ($SiO_2 \cdot 12WO_3$), possibly a defect structure, and it may have useful properties as a pigmenting and opacifying agent in refractory paint. It should impart a jet-black appearance to paints because the tablets tend to lie on their broad faces whose poles are the direction of greatest light absorption.

The product obtained at 28,000 atm and 350 C (Figure 30, Field IV) is a white fine-grained material which is barely resolvable with the light microscope. It has a high birefringence and indices of refraction greater than 2.00. By contrast, Field V is occupied by a fine-grained canary-yellow material with an average crystallite size of 1 to 2 microns and individual crystals as large as 5 microns. The crystals are yellow square to rectangular tablets, probably tetragonal in symmetry, and with the optic axis apparently normal to the broad face of the tablets. The extinction positions are parallel to the diagonals of the tablets, and the indices of refraction are $\omega > 2.10$ and $\epsilon \approx 2.00$ with high birefringence.

The product obtained at 53,000 atm and 500 C was zoned, with a yellow core and a pale, greenish peripheral zone. The yellow core material was shown to be equivalent to Field V by both optical measurements and by X-ray powder diffraction. It is, however, more coarsely crystalline, and many tablets have side lengths up 10 microns. The greenish peripheral zone gives the diffraction pattern of Field VIII. The peripheral zone is composed of relatively large square and rectangular tablets commonly with side lengths as great as 30 microns and, rarely, as great as 90 microns. The tablets are pale yellow to colorless in transmitted light and have extinction positions parallel to the sides, which suggests tetragonal symmetry. Most of the crystals have a very high birefringence when viewed normal to their broad faces; this suggests that the optic axis is probably in the plane of the tablets. Many crystals of this green peripheral zone are internally zoned with a central, irregularly shaped, deep-blue core (Field VII material) which is in apparent optical continuity with the pale yellow to colorless peripheral zone.

The product obtained at 59,000 atm and 600 C is a pale yellowish-green well-crystallized powder composed of crystals with rectilinear outlines, many of which approach the equidimensionality of cubes. Eighty-five to 90 per cent of the crystals are homogeneous and pale yellow to colorless in transmitted light. Their mean index of refraction is greater than 2.10. The remaining 10 to 15 per cent are zoned with deep blue to almost opaque irregular cores (Field VII material) and pale yellow to colorless peripheral zones. The cores of the zoned crystals are typically volumetrically dominant and are in optical continuity with peripheral zones, and the direction with the deep-blue color appears to coincide with the direction of an optic axis. The crystals are probably tetragonal and uniaxial negative. They appear to be equivalent to those which constitute the greenish peripheral zone of the zoned product, described in the preceding paragraph.

General Conclusions. The experimental results to date may be summarized as follows:

(1) Silicotungstic acid transforms above 475 C to a phase which is stable at pressures between 20,000 and 60,000 atm and at temperatures to at least 1100 C. This phase may be obtained by pressurizing either reagent-grade hydrated silicotungstic acid as received or silicotungstic acid which was preheated in air at 1 atm at 650 C. The phases obtained by preheating reagent-grade silicotungstic acid in air at 1 atm between 300 and 700 C

are not equivalent to the stable phase obtained by pressurization above 450 C and 20,000 atm.

(2) Phosphotungstic acid transforms above 500 C to a phase which is stable at pressures between 1 and 60,000 atm to at least 1075 C. This phase is obtained by pressurizing either reagent-grade hydrated phosphotungstic acid as received or phosphotungstic acid which was preheated in air at 1 atm and 650 C. It may also be obtained by heating reagent-grade phosphotungstic acid to 650 C in air at 1 atm. This phase is not equivalent to other phases obtained from both preheated and hydrated phosphotungstic acid at temperatures below 500 C and at pressures up to 60,000 atm.

(3) Both silicotungstic acid and phosphotungstic acid appear to have at least three pressure-dependent hydrated (?) forms which occupy regions on a P-T diagram between 200 and 500 C and between 5,000 and 75,000 atm.

(4) It is interesting to note that although silicotungstic acid preheated at 650 C will transform at 60,000 atm and between 850 and 1000 C to the same phase as is obtained by application of the same P-T conditions to reagent grade silicotungstic acid, both silicotungstic and phosphotungstic acid preheated to 370 C at 1 atm and then subjected to 75,000 atm at 370 C remain unchanged. The reason for this anomalous condition is unknown.

(5) The heteropolynuclear salts also appear to have pressure-dependent (ammonia-deficient ?) modifications (Figures 32 and 33).

Effect of Pressure on Polynuclear Sulfides

In preliminary experimentation prior to intensive study of polynuclear sulfides, a group of sulfides of diverse structure including As_2S_3, Bi_2S_3, Ag_3SbS_3, $PbCuSbS_3$, FeS, and HgS were subjected to pressures between 60,000 and 75,000 atm at temperatures between 250 and 1000 C under anhydrous conditions. Finely ground natural crystalline compounds were used as reactants. Experimental details are assembled in Table 10. No pressure-dependent changes were found in any of these materials, but one problem has arisen, namely, that Sb_2S_3 reacted with and largely digested the platinum tube at high pressures and at temperatures above 550 C. The reaction products are a crystalline multiphase mixture, the components of which may be resolved microscopically in incident light in polished section. The phases have thus far defied identification by either optical or X-ray powder methods. Reactions between sulfides and metallic platinum at relatively low pressures (<3000 atm) and temperatures between 300 and 800 C have long been known and have been ascribed to the formation of stable sulfides of platinum. Recent hydrothermal investigations[46] on sulfide systems between 200 and 800 C and up to 6000 atm have shown that gold may be employed successfully as an inert sample container. Accordingly, experiments are now under way in which gold is being used as both sample container and heater tube in the Belt apparatus. In addition, high-pressure experiments on sulfides in which mineralizers will be employed are being planned.

TABLE 10. HIGH-PRESSURE EXPERIMENTS ON SULFIDES

Starting Material	Temperature, C	Pressure, atm x 10^{-3}	Time, hr
Stibnite (Sb_2S_3)	200	75	42
	300	60	45
	490	75	25
	550	60	25
Troilite (FeS)	200	50	24
	500	65	24
	1000	60	24
Pyrrhotite ($Fe_{1-x}S$)	700	50	20
Pyrargyrite (Ag_3SbS_3)	400	60	14
Bournonite ($PbCuSbS_3$)	200	75	15
	400	75	20
Bismuthinite (Bi_2S_3)	400	60	16
Orpiment (As_2S_3)	240	60	20
Cinnabar (HgS)	400	60	15

Effects of Pressure on Phosphates

An exploratory study of the effects of combined pressure and temperature on phosphates of diverse atomic structure has been started. In preliminary experimentation finely ground natural crystalline apatite [$Ca_5(PO_4)_3(OH,F)$] was subjected anhydrously to 60,000 atm at 1100 C for 15 hr. No change was detected. Other experiments are under way with this and other phosphates using hydrothermal as well as anhydrous conditions and finely divided chemical components to prepare the reactant.

Effects of Pressure on Germanium Dioxide and Zirconium Orthosilicate

In the early stages of this experimental program a number of exploratory high-pressure high-temperature runs were made on stable substances of simple chemistry, fixed stoichiometry, and known structures. Although this work was only of a cursory nature, some of the results and observations are considered to be worthy of record.

The dimorphism of GeO_2 has long been known[47]. The low-temperature high-density "insoluble" modification is tetragonal and has the rutile structure whereas the high-temperature low-density "soluble" form is hexagonal and has the low-quartz structure. The enantiotropic inversion point is 1033 C ± 10 C. The soluble form is obtained

by hydrolysis of germanium tetrahalides and the insoluble form may be prepared from the "soluble" form by hydrothermal methods at a few hundred degrees C. In view of the structural equivalence of the soluble form with low quartz, the possibility of producing a coesite[48] analogue from this form of GeO_2 was considered, and several exploratory runs were made at 1000 C and between 40,000 and 50,000 atm. The resultant products were composed of well-developed tetragonal prisms of the "insoluble" form of GeO_2 as large as 80 microns in length and 30 microns in width. The measured indices of refraction are: $\epsilon \doteq 2.04 \pm 0.01$ and $\omega = 1.96 \pm 0.005$. These data are believed to be more accurate than those given by Mason who "estimated" the indices as $\epsilon = 2.05 - 2.10$, $\omega = 1.99$ at time when calibrated sets of stable high-refractive index liquids were not readily available[47]. The X-ray powder diffraction pattern of these products is equivalent to that given for insoluble GeO_2 prepared hydrothermally at the National Bureau of Standards[49]. Shortly after this experimental work was started, it was found that a paper by Dachille, Shafer, and Roy entitled "High Pressure Studies in the System GeO_2-SiO_2" was in press.[50] As a result, further work on GeO_2 was stopped pending the publication of this paper.

Zircon ($ZrSiO_4$) is a refractory substance with a melting point of 2550 C and a density of 4.7 g/cc which is commonly used as a molding sand in foundries. It is a tetragonal nesosilicate built of isolated SiO_4 tetrahedral and zirconium in eightfold coordination with oxygen. The effect of pressure on such a material is of interest. Two runs were made with natural zircon molding sand* composed of closely sized single-crystal prismatic grains with c-axes between 150 and 250 microns in length. The first run was made using ammonium chloride as a mineralizer at 900 C and 60,000 atm for 14 hr. The product was fine-grained zircon which was evidently the comminuted and recrystallized equivalent of the original zircon in view of the small but measurable changes in indices of refraction from $\epsilon \doteq 1.988$ and $\omega = 1.927$ to $\epsilon = 1.972$ and $\omega = 1.920$ (Na light; all indices ± 0.002). The second run was made with ammonium fluoride as a catalyzer at 1300 C and 60,000 atm for 15 hr. The fine-grained product was equivalent to the first run. Both products give the X-ray diffraction pattern of zircon. Two additional runs were made using a charge of zirconium nitrate and silicic acid which were mixed in the proportions required for zircon and a small amount of excess silica. These charges were pressurized at 60,000 atm at 600 and 800 C for 19 and 16 hr, respectively. The products were composed of very fine-grain zircon as shown by X-ray diffraction powder patterns.

VI. THEORETICAL CONSIDERATIONS – THE THERMODYNAMICS AND KINETICS OF HIGH-PRESSURE REACTIONS

General Consideration

Since little is known about reactions that take place at very high pressures, the work directed toward the synthesis of polymers under pressure must necessarily be largely empirical. The results of early experiments will serve as a guide for the work to follow. In this way experience may lead to conclusions of general validity. Nevertheless, one should be guided by the experience of the past in high-pressure work. This experience is probably best summarized in thermodynamic and kinetic terms. Thermodynamics may give us some ideas concerning what reactions may be expected to take place. Kinetics treats of the rate at which the thermodynamic equilibrium is approached.

---

*Zircon Sand, Titanium Alloy Division, National Lead Corporation.

This discussion is presented largely in terms of the free-energy change (ΔF) accompanying a process, whether it be a phase change or a chemical reaction. In general, the criterion for equilibrium in a process is that the accompanying free energy change be equal to zero. However the quantity most easily obtained is the standard free-energy change ($\Delta F°$), that is, the change in free energy when all reactants and products are in their standard states. For our purposes the standard state may be defined as the pure material at the existing temperature and pressure. The system will then differ from standard-state conditions only inasmuch as solutions are found rather than pure materials.

Data upon which to base thermodynamic calculations are very incomplete. Such thermodynamic data as are available apply usually only at atmospheric pressure, and compressibilities are mostly known only at ordinary temperatures. Because of the uncertainties involved in extrapolating the data the fact will be ignored that it is not quite precise to treat the equilibrium as though it will occur under just those conditions that correspond to $\Delta F = 0$. The difference between ΔF and $\Delta F°$ will be neglected, and it will be supposed that equilibrium between products and reactants exists under conditions of pressure and temperature corresponding approximately to $\Delta F = 0$. It is emphasized that approximations and trends will be dealt with, not precise results.

The basic relationships showing the effect of temperature and pressure on the free energy of a material are

$$\left(\frac{\partial F}{\partial T}\right)_P = -S \; , \tag{1}$$

and

$$\left(\frac{\partial F}{\partial P}\right)_T = V \; . \tag{2}$$

The symbol S is the molar entropy and V the molar volume; S and V are always positive. Therefore, the free energy always decreases with a rise in temperature and increases with a rise in pressure. This is the basis for the generalization that temperature and pressure have opposite effects. It should be noted, however, that in a process involving reactants and products one is dealing with a change in free energy, a ΔF, and therefore with a ΔS and a ΔV. While V and S are always positive, ΔV and ΔS may be positive or negative. Usually ΔS and ΔV have the same sign, so that increases in pressure and temperature have opposite effects on ΔF. However, this is not necessarily so. The common example is the melting of ice, which is accompanied by an increase in entropy and a decrease in volume.

If the free energy change is a function only of temperature and pressure, we can write

$$d\Delta F = \left(\frac{\partial \Delta F}{\partial T}\right)_P dT + \left(\frac{\partial \Delta F}{\partial P}\right)_T dP \; . \tag{3}$$

For an equilibrium process ΔF is always equal to zero. Therefore, using Equations (1) and (2),

$$\left(\frac{\partial T}{\partial P}\right)_{\Delta F = 0} = \frac{\Delta V}{\Delta S} \; . \tag{4}$$

This is the well-known Clapeyron equation, which shows the relationship between temperature and pressure for a phase change, or for any equilibrium process.

Internal Pressure

For a system at temperature T and pressure P the first law of thermodynamics gives

$$dE = TdS - PdV , \tag{5}$$

where E is the energy of the system, usually called the internal energy. Equation (5) may be rewritten:

$$P_i \equiv \left(\frac{\partial E}{\partial V}\right)_T = T\left(\frac{\partial S}{\partial V}\right)_T - P . \tag{6}$$

The so-called "internal pressure", P_i, is defined by Equation (6). An equivalent form is

$$P_i = \left(\frac{\partial E}{\partial V}\right)_T = T\left(\frac{\partial P}{\partial T}\right)_V - P . \tag{7}$$

Wentorf[51] treats the internal pressure as a measure of the attractive forces tending to hold a solid or liquid together. Thus when a liquid boils the internal pressure becomes less than the disruptive pressures of thermal agitation. For a perfect gas $P_i = 0$, and the gas is contained only by the external pressure. If the repulsive pressures exceed the attractive pressures, the internal pressure may be negative, but the sum of the internal and external pressures must be greater than zero. Wentorf says that P_i decreases as P is increased and that it approaches -P asymptotically. This would require, however, that $(\partial S/\partial V)_T$ or $(\partial P/\partial T)_V$ approach zero at high pressures. There seems to be no good justification for this assumption. Wentorf goes on to postulate that a pressure-induced transition is the more likely to be reversed on lowering the pressure the closer $P_i + P$ is to zero. Thus, diamond, with a high internal pressure, does not revert to graphite, while the transitions in bismuth, with low internal pressure, are easily reversed. In general, this correlation seems reasonable. The theoretical justification does not seem to be well established, however, and it would probably be unwise to put great reliance on predictions based on a consideration of the internal pressure.

Kinetics

The rate at which substances react may probably best be described by a consideration of the "activated complex" theory. According to this description, the first step in a reaction is the formation of an activated complex. This is an association of reactant molecules which is to be treated very much as an ordinary molecule. It has only a momentary existence, however, and immediately decomposes either to form the reaction products or to reform the reactants. The reaction will be thought of as taking place a long way from equilibrium, so that the activated complex almost always yields the reaction products. The reaction proceeds in only one direction through the activated

complex. The reaction rate will be proportional to the concentration of the activated complex ($C^{\ddagger}$), and statistical thermodynamics yields the result,

$$\text{rate of reaction} = C^{\ddagger}\left(\frac{kT}{h}\right) , \tag{8}$$

where k is the Boltzmann constant and h is the Planck constant. The ordinary reaction-rate constant is defined by

$$\text{rate of reaction} = k_r C_A C_B \ldots \tag{9}$$

where C_A, $C_B \ldots$ are the concentrations of the reactants. Combining these equations gives

$$k_r = \frac{kT}{h}\frac{C^{\ddagger}}{C_A C_B \cdot \cdot} = \frac{kT}{h} K^{\ddagger} , \tag{10}$$

where $K^{\ddagger}$ is the equilibrium constant for the formation of the activated complex. Since, from thermodynamics,

$$\Delta F^{\circ} = -RT\ln K , \tag{11}$$

we can write Equation (10) in the form

$$k_r = \frac{kT}{h} e^{-\frac{\Delta F^{\ddagger}}{RT}} . \tag{12}$$

Here, $\Delta F^{\ddagger}$ is the standard free energy of formation of the activated complex. Although thermodynamics has been used in developing the equation, it is plain that $\Delta F^{\ddagger}$ can be determined experimentally only by kinetic measurements.

Equations (1) and (2) can now be applied to show the way in which the rate constant varies with temperature and pressure. The results are

$$\left(\frac{\partial \ln k_r/T}{\partial T}\right)_P = \frac{\Delta H^{\ddagger}}{RT^2} \tag{13}$$

and

$$\left(\frac{\partial \ln k_r}{\partial P}\right)_T = -\frac{\Delta V^{\ddagger}}{RT} , \tag{14}$$

where $\Delta H^{\ddagger}$ and $\Delta V^{\ddagger}$ are the standard heat and volume change of formation of the activated complex from the reactants. $\Delta H^{\ddagger}$ may be identified with the energy of activation. In its usual form the Arrhenius equation is expressed in terms of $(\partial \ln k_r/\partial T)_P$. The change in k with T is so great, however, that this expression is not greatly different from $(\partial \ln(k_r/T)/\partial T)_P$.

Reaction rates are usually thought of in terms of the energy of activation. Thus it is necessary for reactants to pass over an energy barrier to form the products. The greater the energy barrier the more the rate will be accelerated by raising the temperature. The energy of activation is always positive and bears no necessary relationship to the heat of reaction. In most cases the energy of activation is found to be relatively constant with temperature changes. The application of pressure may change the energy of

activation in either direction. For the dimerization of cyclopentadiene it is increased by about 1 kcal for a 2000-atm increase in pressure.

In analogy with the preceding discussion it may be considered that the volume of activation represents a volume barrier in the reaction. At atmospheric pressure this would contribute to the free energy of activation only a fraction of a calorie. At high pressures, however, the volume of activation may be significant. There are several differences in behavior of the quantities $\Delta H^{\ddagger}$ and $\Delta V^{\ddagger}$. Whereas $\Delta H^{\ddagger}$ is usually constant with changes in temperature, $\Delta V^{\ddagger}$ may change rapidly with the application of pressure To extrapolate kinetic results to higher pressures by the use of an integrated form of Equation (14) will therefore be dangerous. On the other hand, it may be possible to make some general predictions without any kinetic data. If a reaction has a highly negative free energy change, this does not assure that the reaction will be fast or that the energy of activation will be low or high. A negative volume change in a reaction does indicate, however, that the volume of activation is probably also negative. Thus, if at high pressures certain products are favored thermodynamically because of their high density, the rate of formation of these products will probably also be favored. The reverse is also true if the products of a reaction are less dense than the reactants, the application of pressure will probably retard the rate of reaction. Thus, whereas the energy of activation is always positive, the volume of activation may be either positive or negative. This comes about because the activated complex will always have an energy higher than that of either the reactants or the products, whereas its volume will probably, but not necessarily, be intermediate between the volume of the reactants and products. A consideration of the density changes will therefore probably give a good indication of the effect of pressure on the reaction rate.

A special case is involved with the formation of electrical charges in a reaction taking place in solution. The development of a charge on a molecule causes the surrounding solvent to contract. This volume change contributes to the volume of activation. The effect may be considerably larger than the volume change in the reactants themselves. Thus, a reaction mechanism involving the formation of ions can be expected to be accelerated by the application of pressure. Conversely, the neutralization of charges indicates that the rate will be retarded by increasing the pressure.

Specific Applications

It is the purpose of this section to apply the foregoing, especially the initial comments, to a few specific reactions, in order to get some numerical ideas about the effect of pressure. The sets of conditions of pressure and temperature corresponding to the condition $\Delta F = 0$ will be estimated. This will separate the temperature-pressure diagram roughly into regions favoring the forward and reverse reactions. As shown in the preceding section, the reactions favored thermodynamically by high pressures will probably also be accelerated kinetically by high pressures. Some rather tenuous assumptions will have to be made, so no great reliance should be placed in any particular result.

Equation (3) can readily be integrated over the range 298 to T deg K and to P atm if it is assumed that ΔS and ΔV are constant. Both V and S are positive, increase with rising temperature, and decrease with rising pressure. The changes in these functions for a reaction may be either positive or negative, and may increase or decrease with rising

temperature and pressure. For some reactions it would be possible to obtain at least a little indication of the changes of ΔS and ΔV with temperature and pressure, but for our present purposes the effort would not be justified. The integrated form of Equation (3), obtained under the above named assumptions, will be less reliable the higher the temperature and pressure. The integration yields

$$\Delta F_{T,P} = \Delta F_{298;1\ atm} - \Delta S(T-298) + \Delta V(P-1) \ . \tag{15}$$

This can be changed slightly, neglecting 1 in comparison with P, and multiplying the last term by a factor to convert cc-atm into cal;

$$\Delta F_{T,P} = \Delta F_{298;1\ atm} + 298\ \Delta S - T\Delta S + 0.024\ P\Delta V \ . \tag{16}$$

The term $\Delta F_{298;1\ atm}$ gives an indication of the thermodynamic driving force at ordinary pressure and temperature, being negative if the forward reaction is favored. ΔS is a measure of the effect of temperature, the equilibrium being displaced in the direction of the forward reaction as temperature is increased if ΔS is positive. The forward reaction is favored by increasing the pressure if ΔV is negative, the reverse reaction if ΔV is positive.

As an example, the conversion of graphite to diamond may be considered. From the room-temperature densities it is found that $\Delta V = 1.92$ cc/g-atom. The free energy of formation of diamond from graphite is 685 cal. The entropy change is -0.778 cal/(deg)(g-atom). Thus, graphite is the stable phase under ordinary conditions. The conversion to diamond is favored by pressure, but graphite is favored by higher temperatures. Substitution of these values in Equation (16) gives

$$\Delta F = 453 + 0.778\ T - 0.0465\ P \ . \tag{17}$$

In the tabulation below, values of T_e, the temperature at which $\Delta F = 0$, are given for various pressures as calculated from Equation (17). Corresponding values from a diagram presented by Wentorf[51] are presented for comparison.

P, atm	T_e K	T_e(Wentorf)
0	ΔF is always positive	
1,000	ΔF is always positive	
10,000	15	0
20,000	600	500
50,000	2400	1000-1500
100,000	5400	2000-2700

Qualitatively, Equation (17) gives a true picture. Since ΔV and ΔS are doubtlessly both pressure and temperature dependent to some extent, one would not expect better agreement for extreme conditions. Some years ago Rossini and Jessup[52] carried out a similar calculation, but more carefully, arriving at a similar result.

As a second example we may take the reaction

$$Ca + 2C\,(graphite) \ \rightarrow \ CaC_2 \ .$$
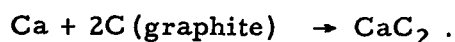
For this process $\Delta F_{298} = -16.2$ kcal, $\Delta V = 0.6$ cc, and $\Delta S = 4.1$ eu. Substituting in Equation (16) gives

$$\Delta F = -15,000 - 4.1\,T + 0.015\,P \quad . \tag{18}$$

According to this equation ΔF is negative for all pressures below 10^6 atm, which is completely outside its limits of applicability. The carbide is always stable with respect to the elements. Since ΔV is positive one might expect the rate of formation of the carbide to be retarded by increasing the pressure. Since its value is so very small, however (2%), one can conclude only that no appreciable pressure effect can be predicted from these data.

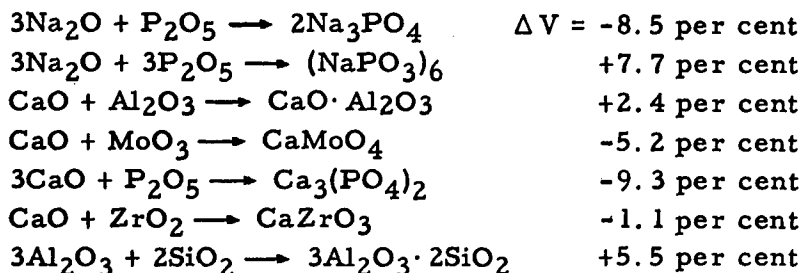As a further example we may consider the formation of a silicate:

$$MgO + SiO_2 \longrightarrow MgSiO_3 \quad .$$

Here $\Delta F_{298} = -9.0$ kcal, $\Delta V = -6.2$ cc, and $\Delta S = -0.4$ eu, so that Equation (16) becomes

$$\Delta F = -9100 + 0.4\,T - 0.15\,P \quad . \tag{19}$$

From this equation one estimates that ΔF is negative at all reasonable temperatures, and the silicate is therefore thermodynamically stable with respect to the oxides. This has been obvious. However, in this case the decrease in volume amounts to 17 per cent at ordinary pressures and temperatures. One might predict, therefore, that the formation of the silicate would be accelerated by the application of pressure.

Further examples of volume changes accompanying similar reactions are given below. In each case the product is no doubt stable with respect to the reactants under all ordinary conditions. Some idea of the effect of the pressure on the tendency to form the products can be obtained from these indications of volume change.

$3Na_2O + P_2O_5 \longrightarrow 2Na_3PO_4$	$\Delta V = -8.5$ per cent
$3Na_2O + 3P_2O_5 \longrightarrow (NaPO_3)_6$	$+7.7$ per cent
$CaO + Al_2O_3 \longrightarrow CaO \cdot Al_2O_3$	$+2.4$ per cent
$CaO + MoO_3 \longrightarrow CaMoO_4$	-5.2 per cent
$3CaO + P_2O_5 \longrightarrow Ca_3(PO_4)_2$	-9.3 per cent
$CaO + ZrO_2 \longrightarrow CaZrO_3$	-1.1 per cent
$3Al_2O_3 + 2SiO_2 \longrightarrow 3Al_2O_3 \cdot 2SiO_2$	$+5.5$ per cent

There seems to be no general trend here, unless it would be in terms of a comparison of the ionic character of the products and reactants.

An examination of some inorganic hydrates may be of interest. The data for a number of hydration reactions are shown below. Water is treated as a liquid in all cases.

ΔF_{298}, kcal	ΔV, cc	ΔS, cal/deg	T (K) at Which $\Delta F = 0$			dT/dP, deg/atm
			1 Atm	10^3 Atm	10^4 Atm	

$$NH_4Al(SO_4)_2 + 12H_2O \longrightarrow NH_4Al(SO_4)_2 \cdot 12H_2O$$

ΔF_{298}, kcal	ΔV, cc	ΔS, cal/deg	1 Atm	10^3 Atm	10^4 Atm	dT/dP, deg/atm
-12.8	-56	-85.7	447	460	600	0.016

$$Na_2SO_4 + 10H_2O \longrightarrow Na_2SO_4 \cdot 10H_2O$$

-1.2	-12.9	-61.2	318	320	370	0.005

$$Ca(NO_3)_2 + 4H_2O \longrightarrow Ca(NO_3)_2 \cdot 4H_2O$$

-2.4	-11.6	-32	370	380	460	0.009

$$BaCl_2 + 2H_2O \longrightarrow BaCl_2 \cdot 2H_2O$$

-2.5	-11.1	-14.9	466	480	650	0.018

$$Al_2O_3 + H_2O \longrightarrow Al_2O_3 \cdot H_2O$$

-1.5	-8.2	-5.8	565	600	900	0.034

$$Al_2O_3 \cdot H_2O + 2H_2O \longrightarrow Al_2O_3 \cdot 3H_2O$$

+0.5	-6.9	-23.1	275	280	350	0.007

The results are distorted more than in most of the other examples because of the fact that the equilibrium actually involves a solution rather than the pure reactants. The figures in the last column are too high, especially for the more soluble salts. The sign is probably correct, however, so that in all cases an increase in pressure makes the hydrate stable at higher temperatures. One may expect to find new hydrates, therefore, in the high-pressure region, but it would be surprising if any of these retained meta-stability upon reducing the pressure.

A general correlation may be mentioned at this point. In the equilibria examined, ΔV and ΔS have been of the same sign almost without exception. This relationship means that the equilibrium temperature of a reaction will almost always be raised when the pressure is increased [Equation (4)]. This is another way of saying that temperature and pressure are expected to have opposite effects on an equilibrium.

Hydrocarbons

In order to write the equation for ΔF of even the simplified form used here, it is necessary to know the heat of formation, the entropy, and the density of each of the reactants and products. This information is not generally available for polymerization reactions. A good idea of the kind of relationship to be expected can be obtained, however, by an examination of the data for some simple hydrocarbons. These results can be applied in a fairly direct manner to organic polymers, especially of the polyolefin type, but they probably have some general validity also for metal-organic and even inorganic polymers.

The reactions used here for illustration may not be realistic from the standpoint of experimental realization, but they show the relative stability of reactants and products and so are applicable for the present purpose.

Chain Lengthening

For the reaction 2 n-pentene $\rightarrow$ n-decene; ΔF_{298} = -12. 34 kcal, ΔV = -29. 65 cc, and ΔS = -23. 4 eu. For Equation (16) we have

$$\Delta F = - 19,300 + 23. 4 T - 0. 72 P. \qquad (20)$$

At ordinary pressures, the equilibrium temperature is about 820 K. At 1000 atm it would be 850 K; at 10,000 atm, 1100 K. Reactions involving similar olefins give similar results. The conclusions, not very surprising, are these:

(1) At ordinary temperature the larger molecules are more stable than the smaller.

(2) Heating to 500 or 600 C brings about the reverse reaction, cracking or pyrolysis into smaller molecules.

(3) At higher pressures the temperature limits of stability are raised, so that it should be possible to heat to higher temperatures without pyrolysis.

It should be noted, however, that all of these molecules are metastable with respect to carbon and hydrogen at ordinary pressures, so that thermodynamically there is a tendency to form the elements. The stability with respect to carbon and hydrogen is enhanced at higher pressures, assuming that hydrogen is contained. In general, polymerization results in an increase in density, since van der Waals distances are replaced by bond distances. Thus, higher pressures tend to enhance formation of larger molecules. This will usually result in an increase in the rate of polymerization as well, as has been found experimentally in certain polymerization reactions.

Ring Closure

As an indication of the tendency toward cross-linking we may consider the reaction n-hexene $\rightarrow$ cyclohexane. This is hardly the same as cross-linking, but is close to it in terms of simple hydrocarbons. For this reaction we find ΔF_{298} = -13. 7 kcal, ΔV = -16. 92 cc, and ΔS = -20. 86 eu, which lead to

$$\Delta F = - 19,900 + 20. 86 T - 0. 41 P . \qquad (21)$$

At P = 0, ΔF = 0 at T = 950 K. For P = 1000, the temperature is 970 K, for P = 10,000, we calculate 1150 K. Thus, the strong tendency toward ring closure is enhanced by increasing the pressure. This tendency may be considered favorable in terms of the formation of cross linkages in linear polymers. It may also be considered unfavorable for polymerization in the sense that the formation of closed-ring dimers or trimers may be favored at the expense of more extensive polymerization.

Ring Opening With Dimer Formation

A tendency has been noticed for an olefin to form a closed ring and also to dimerize to form a longer molecule. It will be of interest to compare these. In other words, having formed a cyclic molecule, will the thermodynamics favor the breaking of this ring to form a larger molecule, especially under pressure? To answer this question we may examine the reaction 2 cyclohexane $\rightarrow$ n-dodecene. Here we find ΔF_{298} = 15. 20 kcal, ΔV = 5. 76 cc, and ΔS = 15. 3 eu. The resulting equation for ΔF is

$$\Delta F = 19,800 - 15.3\,T + 0.14\,P \quad . \tag{22}$$

The entropy used for dodecene is uncertain, so the solution for equilibrium temperatures is ignored. It can be seen that the free energy is unfavorable for the reaction as written and becomes more so at high pressures. On this basis it would not be expected to be possible to break up ring structures by applying pressure. It would be unwise to generalize this particular conclusion, however, since the volume change here is small; similar reactions may well involve a volume change of the opposite sense, though it would probably still be small. The relationships for cyclopentane are similar to those shown for cyclohexane.

Of course the equilibrium temperatures which have been calculated are not realistic, since they involve extrapolation of data for liquids under ordinary conditions to temperatures above the critical.

Conclusion

The use of data obtained at ordinary temperature and atmospheric pressure to predict results under extreme conditions is obviously not altogether satisfactory. The effect of temperature is shown by ΔS, which in turn can be corrected for temperature change by the use of heat capacities. Now heat capacities are well known, and where there are no data good estimates can be made; but temperature effects are not a primary concern. The effect of pressure on the free-energy change is shown by ΔV. The effect of pressure on the volume change is given by compressibilities. Although a considerable effort has gone into determination of compressibilities, the data are far less abundant than those for heat capacities. It is therefore difficult to make predictions and generalizations in the direction of increasing pressure. Even if corrections could be made for the effect of temperature on ΔS and of pressure on ΔV, to correct for both (that is, for the effect of pressure on ΔS and or temperature on ΔV) would require a knowledge of thermal-expansion coefficients. The information in this area is also limited. Both entropy and volume will be increased by higher temperatures and decreased by higher pressures, and it may be expected that ΔS and ΔV will show the same effects. This tells us nothing about the ratio of ΔV to ΔS, however, so that we cannot generalize about the slope of the equilibrium line on a T-P diagram [Equation (4)]. Many melting-point curves, to cite one example, show a slight concavity toward the pressure axis, but there are exceptions.

In general, then, it is supposed that the most common situation to be faced will correspond roughly to the following diagram.
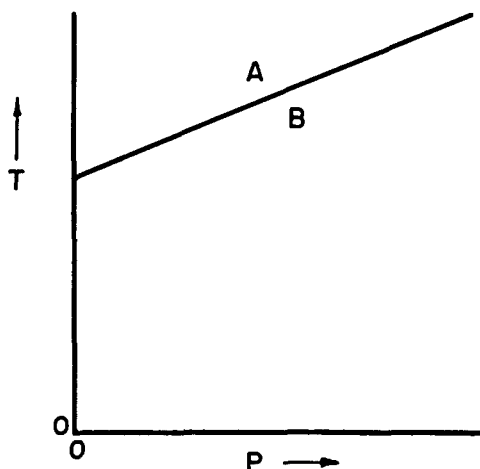
A represents the region of stability of the reactants, B for the polymeric products. The diagram will actually be complicated by other equilibrium lines showing the regions of stability of unwanted products. The formation of B will be favored thermodynamically throughout the region below the equilibrium line.

Kinetics are being given primary consideration. Raising the temperature will accelerate the reaction except near the equilibrium line, where the reverse reaction may become significant. In general, raising the pressure will also accelerate the reaction. The greater the decrease in volume accompanying the reaction, the greater will be the expected effect of pressure in increasing the rate. The foregoing must not be taken as a hard and fast rule, however. Suppose that a liquid monomer forms a solid polymer. An increase in pressure may result in solidifying the monomer, which will greatly retard the reaction. A similar effect may be encountered if the viscosity is increased too much by high pressure. In general, then, it can be said that the temperature should be as high as possible without encountering the reverse reaction or the formation of undesired products. However, the optimum pressure cannot be predicted with confidence on the basis of data now available.

VII. FUTURE WORK

Organic Polymers

Polymer Compressions

It is planned to continue polymer compressions such as are needed to complete data under comparable conditions to verify the effect of generic materials and polymer types. Limited work is contemplated on the effect of prolonged holding times to determine whether compressed polymer equilibrium density values are primarily time dependent or also compression dependent such that higher compressions will give greater density increases at equilibrium. It is hoped to complete this study concurrently with the orientation studies on polymer-monomer and monomer systems.

Activated Polymer Systems

Several methods for activating polymer systems are under consideration. These include incorporation of an unsaturated reactive site by copolymerization with a diene, irradiation and chemical modification of polymers by treatment, such as ozonization.

Since materials contemplated for study in this category are polymeric, compression techniques developed in the homopolymer studies will be suitable. However, sample fabrication will be required and possibly development of techniques for dispersing different polymeric materials. Presently, broad screening of irradiated and copolymer systems does not appear advisable, rather a selective study of irradiated materials and copolymers to determine whether either method appears to promote compression activation.

Polymerization Under Superpressure Conditions

Tentative steps are under way on this phase of the program at the present time. The use of the polystyrene-styrene system to check encapsulation compression and characterization techniques also may well initiate work in the polymerization area due to residual catalyst in the polymer. If compression techniques alone and/or in the presence of polymer do not show catalytic activity, work will progress into the study of catalyzed systems.

Graft Reactions

It is known that graft and block polymerizations can be promoted in polymer-monomer mixtures by ozonization or irradiation prior to grafting. Encapsulation techniques should be readily adaptable to studies in this area to determine the effect of super-pressures on graft and block activity and on the properties of copolymers formed in this fashion.

Semiorganic Polymers

Additional experiments at pressures up to 100,000 atm will be performed with the most promising materials developed in this program, and other semiorganic materials will be added to the study.

The reaction conditions under which dimethyldicyanosilane can be polymerized will be established more precisely. Emphasis will be placed on higher pressures at low temperature.

Experiments at pressures up to 100,000 atm will be performed on the polyalumino-siloxanes to discover whether or not the effects observed at 60,000 atm will be the same at higher pressures.

A few experiments at higher pressure will be carried out with ethyldicyanophosphine to see if polymerization rather than decomposition can be induced.

The cyclic arsenosiloxane will be examined at higher pressure to see if the trend toward decreased thermal stability continues.

The residue from the phosphinoborine trimer preparation will be subjected to higher pressure and examined for increased thermal stability.

No further work is planned on the phosphonitrilic chlorides, the linear arsenosiloxane, or the phosphinoborine trimer.

Additional semiorganic materials of the following types are to be prepared:

(1) Polyaluminoxanes

(2) Polystannoxanes

(3) Coordination compounds of copper, nickel, or zinc.

These materials, along with selected ferrocene derivatives, will be subjected to the extreme pressures and examined for structural changes.

Inorganic Polymers

In the projected experimental program for 1962, the effects of ultrahigh pressure and concomitant high temperature on the following classes of inorganic materials will be investigated.

Polynuclear Sulfides

As indicated by the high electronegativity of oxygen (3.5) relative to that of sulfur (2.5), the bond M-S is more covalent in nature than the bond M-O. The sulfides as a group, therefore, have dominantly covalent and subordinately metallic bonding, and, as a result, they represent a group of inorganic compounds that, in the sense of bond type, are more closely related to organic compounds than the inorganic ionic compounds.

The polynuclear sulfides, such as Bi_2S_3, Sb_2S_3, SiS_2, and, possibly, As_2S_3 have chain structures containing complexes which are infinite in one direction with only relatively weak forces between chains. These structures look attractive for polymerization studies under pressure.

Although oxides and fluorides show a close structural similarity, the sulfides tend to form structures equivalent to those of chlorides, bromides, and iodides of equivalent formula type. This is a result of the high electronegativity of both oxygen and fluorine relative to that of chlorine, bromine, iodine, and sulfur. A number of well-defined structure types occur in sulfides and related halides which have no counterpart among oxide structures such as two-dimension sheet-type (layer) structures (CdI_2), pyrite and marcasite (FeS_2) structures which contain discrete S_2 groups for which the bonding is homopolar, and the NiAs structure. Further, there are, in addition to sulfides with three-dimensional network structures, ferromagnetic sulfides such as cubanite ($CuFe_2S_3$) and pyrrotite ($Fe_{1-x}S$), and the remarkable noncentrosymmetric structure of

HgS (cinnabar) which has the symmetry of quartz and shows strong optical rotatory activity due to enantiomorphism. Finally, it should be possible to prepare for high-pressure experiments selenium- and tellurium-doped sulfides or completely substituted selenides and tellurides which are structurally equivalent to sulfides of corresponding formula.

The effect of pressure on representative examples of these sulfide structures with respect to polymerization-type reactions should be a very interesting and fruitful study.

Phosphates

The oxygen chemistry of pentavalent phosphorus is based on PO_4 tetrahedra which, like SiO_4 tetrahedra, may be linked together in various ways to form P_2O_7 ions, ring and chain ions of composition $(PO_3)_n$, layers, and infinite three-dimensional complexes. As a result, the phosphates, and analogous vanadates and arsenates, represent a wide range of structures and compositional variants on which to study the effects of ultrahigh pressure with respect to polymerization.

In the experimental work on all of these materials the effect of water at supercritical temperatures on the reactions will be studied. The presence of supercritical water should have a mineralizing effect which would tend to promote polymerization.

VIII. REFERENCES

(1) Larsen, H. A., and Drickamer, H. G., "Mechanical Degradation and Crosslinking of Polymers by Plastic Deformation at High Pressure", J. Phys. Chem., 61, 1643 (1957).

(2) Roy, R., Professor, University of Pennsylvania. Private communication to E. J. Bradbury.

(3) Bridgman, P. W., "Effects of Pressure on Binary Alloys", Proc. Am. Acad. Arts Sci., 84 (3), 23.

(4) McBride, J. J., and Beachell, H. C., "Methylisocyanosilanes", J. Am. Chem. Soc., 74, 5247 (1952).

(5) Gibbs, C. F., Tucker, H., Shkapenko, G., and Park, J. C., "Development of Inorganic Polymer Systems", WADC Technical Report 55-453 (May, 1956).

(6) Schuyten, H. A., Weaver, J. W., and Reid, J. D., "Preparation of Substituted Acetoxy Silanes", J. Am. Chem. Soc., 69, 2110 (1947).

(7) Gibbs, C. F., Tucker, H., Shkapenko, G., and Park, J. C., "Development of Inorganic Polymer Systems", WADC TR-55-453, Part II (September, 1957).

(8) Sacco, A., "Halophosphines by Alkylation of the Phosphorus Halides", Lincei-Rend. Sc. Fis. mat. e nat., 11, 101 (1951).

(9) Chamberland, B. L. , and MacDiarmid, A. G. , "Monomers and Polymers Containing Si-O-As Linkages", J. Am. Chem. Soc., 82, 4542-46 (1960).

(10) Hall, H. T. , "Ultra-High-Pressure High-Temperature Apparatus: The 'Belt'", Rev. Sci. Instr., 31, 125-131 (1960).

(11) Hall, H. T. , "High-Pressure Apparatus", Proc. Conf. Very High Pressure, Lake George, New York (June, 1960).

(12) Bridgman, P. W. , "The Resistance of 72 Elements, Alloys, and Compounds to 100,000 Kg/Cm^2", Proc. Am. Acad. Arts Sci. , 81, 165-251 (1952).

(13) Bridgman, P. W. , "The Measurement of Hydrostatic Pressure to 30,000 Kg/Cm^2", Proc. Am. Acad. Arts. Sci. , 74, 1-10 (1940).

(14) Kennedy, G. C. , and La Mori, P. N. , "Fixed Pressure Points for Calibration of High Pressures", (abstract) Bull. Geol. Soc. Amer. , 71, 1903 (1960); also personal communication with La Mori at Annual Meeting, Geol. Soc. Am. , Denver (November, 1960).

(15) Boyd, F. R. , and England, J. L. , "Apparatus for Phase Equilibrium Measurements at Pressures Up to 50 Kilobars and Temperatures Up to 1750°C", J. Geophys. Research, 65, 741-748 (1960).

(16) Bridgman, P. W. , "Polymorphism, Principally of the Elements, Up to 50,000 Kg/Cm^2", Phys. Rev. , 48, 893-906 (1935).

(17) Bridgman, P. W. , "Pressure-Volume Relations for 17 Elements to 100,000 Kg/Cm^2", Proc. Am. Acad. Arts Sci. , 74, 425-440 (1942).

(18) Balchan, A. S. , and Drickamer, H. G. , "High Pressure Electrical Resistance Cell, and Calibration Points Above 100 Kilobars", Rev. Sci. Instr., 32, 308-313 (1961).

(19) Fitch, R. A. , Slyhouse, T. E. , and Drickamer, H. G. , "Apparatus for Optical Studies to Very High Pressures", J. Opt. Soc. Am. , 47, 1015-1017; Drickamer, H. G. , "Optical Studies at High Pressure", Proc. Conf. Very High Pressure, Lake George, New York (June, 1960).

(20) Bridgman, P. W. , "The Compression of 39 Substances to 100,000 Kg/Cm^2", Proc. Amer. Acad. Arts Sci. , 76, 55-70 (1948).

(21) Bridgman, P. W. , "The Physics of High Pressure", G. Bell and Sons, Ltd. , London (1952), Figure 93.

(22) Bundy, F. P. , "Phase Diagram of Bismuth to 130,000 Kg/Cm^2, 500 C", Phys. Rev. , 110, 314-318 (1958).

(23) Hall, H. T. , "The Melting Point of Germanium as a Function of Pressure to 180,000 Atmospheres", J. Phys. Chem. , 59, 1144-1146 (1955).

(24) Bundy, F. P. , Bovenkirk, H. P. , Strong, H. M. , and Wentorf, R. H. , "Diamond-Graphite Equilibrium Line From Growth and Graphitization of Diamond", J. Chem. Phys. , 35, 383-391 (1961).

(25) Bovenkirk, H. P. , Bundy, F. P. , Hall, H. T. , Strong, H. M. , and Wentorf, R. H. , "Preparation of Diamond", Nature, 184, 1094-1098 (1959).

(26) De Keyser, W. L. , and Dequeldre, L. , "Contribution a l'Étude de la Formation de la Calcite, Aragonite et Vaterite", Chem. Soc. Belg. Bull. , 59, 40-71 (1950).

(27) Jamieson, J. C. , "Phase Equilibrium in the System Calcite-Aragonite", J. Chem. Phys. , 21, 1385-1390 (1953).

(28) MacDonald, G. J. F. , "Experimental Determination of Calcite-Aragonite Equilibrium Relations at Elevated Temperatures and Pressures", Am. Mineral. , 41, 744-756 (1956).

(29) Griggs, D. T. , and Kennedy, G. C. , "A Simple Apparatus for High Pressures and Temperatures", Am. J. Sci. , 254, 722-735 (1956).

(30) Clark, S. P. , "A Note on Calcite-Aragonite Equilibrium", Am. Mineral. , 42, 564-566 (1957).

(31) Robertson, E. C. , Birch, F. , and MacDonald, G. J. F. , "Experimental Determination of Jadeite Stability Relations to 25,000 Bars", Am. J. Sci. , 255, 115-137 (1957).

(32) Bridgman, P. W. , "The High-Pressure Behavior of Miscellaneous Minerals", Am. J. Sci. , 237, 7-18 (1939).

(33) Jamieson, J. C. , "Introductory Studies of High-Pressure Polymorphism to 24,000 Bars by X-Ray Diffraction With Some Comments on Calcite II", J. Geol. , 65, 334-343 (1957).

(34) McConnell, J. D. C. , "Vaterite From Ballycraigy, Larne, Northern Ireland", Mineral. Mag. , 32, 535-544 (1960).

(35) Nel, L. T. , Jacobs, H. , Allan, J. T. , and Bozzoli, G. R. , "Wonderstone", S. African Dept. Mines, Geol. Ser. , Bull. 8 (1937); Bosazza, V. L. , "Wonderstone – A Unique Refractory Material", Trans. Brit. Ceram. Soc. , 39, 369-476 (1940); Carte, A. E. , "Thermal Constants of Pyrophyllite and Their Change on Heating", Brit. J. Appl. Phys. , 6, 326-328 (1955).

(36) Boyd, F. R. , and England, J. W. , "The Quartz-Coesite Transition", J. Geophys. Res. , 65, 749-756 (1960).

(37) Kennedy, G. C. , "Pyrophyllite-Sillimanite-Mullite Equilibrium Relations to 20,000 Bars and 800°C" (Abstract), Bull. Geol. Soc. Am. , 66, 1584 (1955).

(38) Clark, S. P. , Robertson, E. C. , and Birch, F. , "Experimental Determination of Kyanite-Sillimanite Equilibrium Relations at High Temperatures and Pressures", Am. J. Sci. , 255, 628-640 (1957).

(39) Clark, S. P., "Kyanite Revisited", (Abstract) J. Geophys. Research, 65, 2482 (1960).

(40) Giardini, A. A., Tydings, J. E., and Levin, S. B., "A Very High-Pressure High-Temperature Research Apparatus and the Synthesis of Diamond", Am. Mineral., 45, 217-221 (1960).

(41) Giardini, A. A., Kohn, J. A., Eckart, D. W., and Tydings, J. E., "The Formation of Coesite and Kyanite From Pyrophyllite at Very High Pressure and High Temperatures", Am. Mineral., 46, 976-982 (1961).

(42) Gillingham, T. E., "The Solubility and Transfer of Silica and Other Non-Volatiles in Steam", Econ. Geol., 43, 242-271 (1948); Kennedy, G. C., "A Portion of the System Silica-Water", Econ. Geol., 45, 629-653 (1950); Morey, G. W., and Hesselgesser, J. M., "The Solubility of Some Minerals in Superheated Steam at High Pressure", Econ. Geol., 46, 821-835 (1951).

(43) Roy, D. M., Gard, J. A., Nicol, A. W., and Taylor, H. F. W., "New Data for the Calcium Silicate, 'Phase Z'", Nature, 188, 1187-1188 (1960).

(44) Heller, L., and Taylor, H. F. W., "Crystallographic Data for the Calcium Silicates", Bldg. Res. Sta., Dept. Sci. Ind. Res., London, H. M. S. O. (1956), 17-18.

(45) Scroggie, A. G., and Clark, G. L., "The Crystal Structure of Anhydrous Silicotungstic Acid and Related Compounds and Their Probable Molecular Formulas", Proc. Natl. Acad. Sci., 15, 1-8 (1929).

(46) Kullerud, G., and Yoder, H. S., "Pyrite Stability Relations in the Fe-S System", Econ. Geol., 54, 533-572 (1959); Clark, L. A., "The Fe-As-S System: Phase Relations and Applications", Econ. Geol., 55, 1345-1381, 1631-1652 (1960).

(47) Laubengayer, A. W., and Morton, D. S., "Germanium XXXIX. The Polymorphism of Germanium Dioxide", J. Am. Chem. Soc., 54, 2302-2320 (1932).

(48) Zoltai, T., and Buerger, M. J., "The Crystal Structure of Coesite, The Dense, High-Pressure Form of Silica", Z. Krist., 111, 129-141 (1959).

(49) Swanson, H. E., et al., "Standard X-Ray Diffraction Patterns", Natl. Bur. Standards Circular 539, 28-29 (1959).

(50) Dachille, F., and Roy, R., "High-Pressure Studies of the System Mg_2GeO_4-Mg_2SiO_4 with Special Reference to the Olivine-Spinel Transition", Am. J. Sci., 258, 225-246 (1960); Dachille, F., and Roy, R., "The High-Pressure Region of the Silica Isotypes", Z. Krist., 111, 451-461 (1959).

(51) Wentorf, R. H., Jr., "Condensed Systems at High Pressures and Temperatures", J. Phys. Chem., 63, 1934-1940 (1959).

(52) Rossini, F. D., and Jessup, R. S., "Heat and Free Energy of Formation of Carbon Dioxide, and of the Transition Between Graphite and Diamond", J. Research Natl. Bur. Standards, 21, 491-513 (1938).

AC Spark Plug
General Motors Corporation
Attn. Mr. Robert R. Kupfer
Milwaukee, Wisconsin

Advanced Systems Dev Div.
Cleveland Pneumatic Industries
1301 E. El Segundo Avenue
El Segundo, California

Aeronca Aircraft Corporation
Attn. Mr. Leon C. Wolfe, Chief Eng.
Germantown Road
Middletown, Ohio

AFSC (RDSFIL)
Andrews AFB
Washington 25, D. C.

AiResearch Manufacturing Division
Garrett Corporation
Attn. Mr. W. R. Ramsaur, Vice President
9851 Sepulveda Blvd.
Los Angeles 45, California

Aerospace Industries Association
Attn. Mr. J. P. Reese
610 Shoreham Building
Washington 5, D. C.

Beech Aircraft Corporation
Attn. Mr. Dean E. Burleigh
Chief Adm. Eng.
9709 E. Central Avenue
Wichita 1, Kansas

Bell Aircraft Corporation
Attn. Mr. Neil MacKenzie
Chief Tech Eng.
Fort Worth 1, Texas

Bell Aerosystems Company
Attn. Mr. G. Kappelt, Director
Eng. Laboratory
Buffalo 5, New York

Bendix Aviation Corporation
Attn. Dr. G. H. Messerly
Bendix Products Division
South Bend 20, Indiana

Bendix Aviation Corporation
Bendix Prod Division
Attn. Technical Library
401 N. Bendix Drive
South Bend 20, Indiana

Bendix Aviation Corporation
Pioneer Central Division
Attn. Mr. Kingsland Hobein
Davenport, Iowa

Bendix Aviation Corporation
Pacific Division
Attn. Mr. E. I. Nolan
11600 Sherman Way
North Hollywood, California

Bendix Products Division
Attn. Mr. Frank C. Albright,
  Staff Engineer
Systems Dev Section
3300 South Sample Street
South Bend, Indiana

The Boeing Company
Pilotless Aircraft Division
Attn. Mr. R. R. Barber,
  Library Supervisor
P. O. Box 3925
Seattle 24, Washington

The Boeing Company
Attn. Mr. H. A. Welch, Mgr.
Eng. Laboratory
P. O. Box 707
Renton, Washington

The Boeing Company
Attn. Mr. C. B. Barlow,
  Assistant to Chief
Tech. Staff
Wichita, Kansas

The Boeing Company
Attn. Mr. E. C. Bovee,
  Staff Engineer
Materials and Processes
Seattle 14, Washington

Cessna Aircraft Company
Attn. Mr. John Dussault
Chief of Structures
Wichita, Kansas

Cessna Aircraft Company
Attn. Mr. Obed T. Wells
Chief Structure Engineer
Wichita, Kansas

Chance Vought Aircraft, Inc.
Attn. Mr. M. J. Rudick,
  Supervisor Test Laboratory
P. O. Box 5907
Dallas, Texas

Chief, Bureau of Ships
Attn. Code 343
Dept. of Navy
Washington 25, D. C.

Cleveland Pneumatic Industries
Attn. Librarian
3781 E. 77th St.
Cleveland 3, Ohio

AFSC
RDTAPR
Attn. Lt. Col. R. W. Conners
Andrews AFB
Washington 25, D. C.

Commanding General
HDQS Ordnance Weapons Command
Attn. ORDOW-TX
Rock Island, Illinois

Continental Aviation 7, Eng Corporation
Attn. Mr. J. W. Kinnucan, Vice President
1500 Algonquin Avenue
Detroit 14, Michigan

Convair
Attn. Mr. H. A. Swift, Chief
Structures and Materials
Pomona, California

Convair
Attn. Mr. J. F. Robinson, Chief
Eng Test Laboratory
Fort Worth, Texas

Convair Astronautics Division
Attn. Mr. J. F. Watson
Senior Research Engineer
San Diego 12, California

Convair-Div. Gen Dynamics Corporation
Attn. Mr. N. H. Simpson, Chief
Eng Test Laboratory
K. C. Brown Eng Library
Fort Worth, Texas

Curtiss-Wright Corporation
Propeller Division
Attn. Mr. George W. Brady, Dir Eng.
Attn. Mr. Wm. C. Schulte, Chief Met.
Caldwell, New Jersey

Curtiss-Wright Corporation
Wright Aeronautical Division
Attn. Mr. J. D. Charshafian, Chief Eng
Wood-Ridge, New Jersey

Director
Air University Library
Attn. 7575
Maxwell AFB, Alabama

Douglas Aircraft Company, Inc.
Attn. Mr. L. J. Devlin, Chief Engr.
El Segundo, California

Douglas Aircraft Company, Inc.
Attn. Mr. E. P. Troeger, Chief
Materials Research and Process Engr.
Santa Monica, California

Douglas Aircraft Company, Inc.
Attn. Mr. D. E. Dunlap, Chief Engineer
2000 North Memorial Drive
Tulsa, Oklahoma

Electrol, Inc.
Attn. Mr. Hugh E. Burke
85 Grand Street
Kingston, New York

Fairchild Aircraft Division
Fairchild Engine and Airplane Corporation
Attn. Mr. E. Williams
Chief of Process and Materials
Hagerstown 10, Maryland

Federal Aviation Agency
Bureau of Research and Dev.
Attn. Records Officer
Washington 25, D. C.

General Dynamics
Attn. Mr. P. R. De Tonnancour
Division Research Library
Fort Worth, Texas

General Electric Company
Attn. Mr. R. F. Koenig, Mgr.
Materials and Process Laboratory
3198 Chestnut Street
Philadelphia 4, Pennsylvania

General Electric Company
Malta Test Station
Attn. Librarian
Ballston Spa, New York

General Electric Company
Attn. Mr. W. C. Elcan
118 West First Street
Dayton 2, Ohio

General Motors Corporation
Allison Division
Attn. Mr. C. E. Mines, Chief Eng. Services
Indianapolis, Indiana

Martin-Marietta Corporation
Attn. Mr. F. D. Jewett,
  Structural Staff Engr.
Baltimore, Maryland

Goodyear Aircraft Corporation
Attn. Mr. R. S. Ross, Mgr.
Aeromechanics R and D
1210 Massillon Road
Akron 15, Ohio

Goodyear Aircraft Corporation
Attn. Mr. J. P. McKee
1210 Massillon Road
Akron 15, Ohio

California Institute of Technology
Jet Propulsion Laboratory
Attn. Mr. I. E. Newlan
Technical Reports Section
Pasadena, California

California Research Corporation
Attn. Dr. Robert O. Bolt
P. O. Box 1627
Richmond 1, California

Carbide and Carbon Chemicals Co.
Attn. Dr. W. J. Toussaint
Research and Development Dept.
South Charleston, West Virginia

Case Institute of Technology
Attn. Director, Armed Services
Plastic Project
Cleveland 8, Ohio

Celanese Polymer Company
Attn. Dr. R. N. Clarke
744 Broad Street
Newark, New Jersey

Chemstrand Research Center, Inc.
Research Triangle Park
Attn. Mr. C. J. Stemman
P. O. Box 731
Durham, North Carolina

Chicago Rawhide Mfg. Company
Technical Information Center
Attn. Mr. Kenneth D. Carroll, Librarian
1301 Elston Avenue
Chicago 22, Illinois

Coast Pro-Seal and Mfg. Company
Attn. Mr. L. C. Boller
P. O. Box 57428
Flint Station
Los Angeles 57, California

Convair
Attn. Dr. Rip G. Rice
3462 Hancock Street
San Diego 10, California

Convair Division
General Dynamics Corporation
Attn. Mr. R. I. Lemmon
Project Office 125
Ft. Worth, Texas

Cornell University
Dept. of Chemistry
Attn. Dr. W. T. Miller
Ithaca, New York

Deecy Products Company
Attn. Mr. C. H. Taft
120 Potter Street
Cambridge, Massachusetts

Denver Research Institute
Attn. Dr. J. J. Schmidt
University of Denver
Denver 10, Colorado

Dow Chemical Company
Polymer Research Laboratory
Attn. Dr. R. W. Lenz
Midland, Michigan

Dow Corning Corporation
Attn. Dr. Ogden Pierce
Midland, Michigan

Dow Corning Corporation
Silastic Research Group
Attn. Miss Anna L. Coleman
Midland, Michigan

Drexel University
Department of Chemistry
Attn. Dr. Robert S. Hanson
Philadelphia, Pennsylvania

Duke University
Department of Chemistry
Attn. Dr. J. H. Saylor
Durham, North Carolina

E. I. DuPont de Nemours and Company
Pioneering Research Division
Attn. Dr. A. H. Frazer
Wilmington 98, Delaware

E. I. DuPont de Nemours and Company
Chemical Department
Attn. Dr. H. S. Rothrock
Experimental Station
Wilmington, Delaware

E. I. DuPont de Nemours and Company
Explosives Department
Attn. Mr. Wiley Brannon
Gibbstown, New Jersey

E. I. DuPont de Nemours and Company
Polychemicals Division
Attn. Dr. F. C. McGrew
P. O. Box 98
Wilmington, Delaware

ESD (Capt. W. Schlotterbeck)
L. G. Hanscom Field
Bedford, Massachusetts

Esso Research and Engineering Company
Products Research Division
Attn. Mr. A. B. Crampton
P. O. Box 51
Linden, New Jersey

Ethyl Corporation
Attn. Dr. Walter Foster
Baton Rouge, Louisiana

Ethyl Corporation
Attn. Mr. Philip Savage
1000 West Eight Mile Road
Ferndale, Detroit, Michigan

Frankford Arsenal
Pitman-Dunn Laboratory
Attn. Dr. Jack Radell
Philadelphia 37, Pennsylvania

Federal Telecommunication Labs.
Attn. Dr. F. A. Muller
500 Washington Avenue
Nutley 10, New Jersey

Firestone Tire + Rubber Company
Attn. Dr. L. J. Kitchen
1200 Firestone Parkway
Akron 17, Ohio

Food Machinery and Chemical Corporation
Central Research Department
Attn. Dr. B. F. Landrum
161 E. 42nd Street
New York 17, New York

Ford Motor Company
Scientific Laboratory
Attn. Technical Information Section
Dearborn, Michigan

Ford Motor Company
Aeronutronics Division
Attn. Dr. Norman Byrd
Newport Beach, California

Frankford Arsenal
Attn. Dr. H. Gisser
Pitman-Dunn Laboratories
Philadelphia 37, Pennsylvania

Franklin Institute
Benjamin Franklin Pkwy at 20th Street
Philadelphia 3, Pennsylvania

George Washington University
Department of Chemistry
Attn. Dr. D. C. White
Washington 6, D. C.

General Aniline and Film Corporation
Attn. Dr. J. W. Wilkinson, Jr.
Central Research Laboratory
Easton, Pennsylvania

General Chemical Research Laboratory
Attn. Dr. Hans Neumark
P. O. Box 405
Morristown, New Jersey

General Electric Company
General Engineering Laboratory
Attn. Dr. S. Aftergut
Attn. Dr. J. R. McLoughlin
Schenectady, New York

General Electric Company
General Engineering Laboratory
Attn. Dr. G. P. Brown
Attn. Dr. Charles Doyle
Schenectady, New York

General Electric Company
Silicone Products Department
Attn. Dr. F. M. Lewis
Waterford, New York

General Tire and Rubber Company
Attn. Lois Brock, Librarian
1708 Englewood Avenue
Akron 9, Ohio

General Motors Corporation
Research Laboratories
Attn. Mr. E. P. Jackson
12 Mile Round Roads
Warren, Michigan

General Precision Corporation
Attn. Dr. Dan Grafstein
Kearfott Division
Little Falls, New Jersey

Glidden Company
Attn. Mr. R. E. Demarco
Research Department
3901 Hawkins Point Road
Baltimore 26, Maryland

Harvard University
Mallinckrodt Laboratory
Attn. Dr. E. C. Rochow
Cambridge 38, Massachusetts

Hercules Powder Company
Research Center Library
Attn. Ella Mae Baer
Wilmington 99, Delaware

Hooker Chemical Corporation
Attn. Mr. W. F. Zimmer
Attn. Dr. C. F. Baranauches
Attn. Dr. C. T. Bean
Niagara Falls, New York

Indiana University
Department of Chemistry
Attn. Mr. Riley Schaeffer
Bloomington, Indiana

Industrial Research Institute
University of Chattanooga
Attn. Dr. J. H. Cowlliette
Chattanooga, Tennessee

Iowa State College
Chemistry Department
Attn. Dr. H. Gilman
Ames, Iowa

Grumann Aircraft Engineering
Attn. Mr. A. R. Mead,
  Metallurgical Engineer
Bethpage, Long Island, New York

Hamilton Standard Division
United Aircraft Corporation
Attn. Mr. T. B. Rhines,
  Assistant Chief Engineer
Windsor Locks, Connecticut

Hayes Aircraft Corporation
Attn. Mr. C. D. Reymann,
  Sup Mat Lab
P. O. Box 2287
Birmingham, Alabama

HDQS
AF Office of Scientific Research
ARDC
Attn. SREC
Washington 25, D. C.

USAS (AFDRT)
Attn. Col. J. V. Hearn, Jr.
Washington 25, D. C.

Hiller Aircraft Corporation
Attn. Mr. Glenn Lattin
Chief Process Engineer
Palo Alto, California

Hiller Helicopters, Inc.
Attn. Mr. Stanley Hiller, Jr., President
1350 Willow Road
Palo Alto, California

Hughes Aircraft Company
Attn. Mr. G. L. Robinson
Building 6, Room Z-1054
Member of Technical Staff
Culver City, California

Hughes Tool Company
Aircraft Division
Attn. Mr. H. C. Smith,
  Chief Stress Engineer
Florence and Teale Street
Culver City, California

Kaman Aircraft Corporation
Attn. Mr. R. H. Daniels, Chief
Test and Development
Bloomfield, Connecticut

Lear, Inc.
Astonics Division
Attn. Mr. Andrew F. Haiduck,
  VP and Gen. Mgr.
3171 South Bundy Drive
Santa Monica, California

Lear, Inc.
Lear Romec Division
Attn. Mr. R. N. MacLead, Chief Engineer
241 S. Abbe Road
Elyria, Ohio

Lockheed Aircraft Corporation
Attn. Mr. H. P. Gilpin
Production Engineer
Marietta, Georgia

Lockheed Aircraft Corporation
Attn. Mr. E. A. Green, Mgr.
Production Engineer
Burbank, California

Lockheed Aircraft Corporation
Dept. 72-25 Building 66
Attn. Mr. George W. Papen
Prod. Eng. Dept. Eng.
Burbank, California

Marquardt Corporation
Attn. Mr. J. W. Chambers, Supervisor
Materials and Process Section
Van Nuys, California

Marquardt Aircraft Company
Attn. Mr. J. S. Winter
Chief Eng. Powerplants
16555 Saticoy Street
Van Nuys, California

Martin-Marietta Corporation
Attn. Mr. G. C. Pfaff
Chief Structures Engineer
Orlando, Florida

Martin-Marietta Corporation
Attn. Mr. P. M. Knox, Chief
Adv. Missile and Booster Design Section
Mail Station No. M-275
Denver 1, Colorado

McDonnel Aircraft Corporation
Municipal Airport
Attn. Mr. E. C. Szabo,
  Chief Prod. Eng.
P. O. Box 516
St. Louis 3, Missouri

Menasco Manufacturing Company
Engineering Division
Attn. Mr. G. F. Vescelus, Director
805 South San Fernando Blvd.
Burbank, California

National Waterlift Division
Cleveland Pneumatic Industries
Kalamazoo, Michigan

Norair
Division of Northrop Corporation
Attn. Library 3145-31
1001 East Broadway
Hawthorne, California

North American Aviation, Inc.
Attn. Mr. L. P. Spalding
Chief Research Engineer
Los Angeles International Airport
Los Angeles 45, California

North American Aviation, Inc.
Attn. Mr. F. A. Wedberg
Engrg. Tech. Representative
Columbus 16, Ohio

North American Aviation, Inc.
Attn. Mr. M. C. Sanz, Consultant
Dept. 3028-56 Building 602
915 E. Imperials Highway
Downey, California

Northrop Corporation, Radioplane Division
Attn. Mr. A. G. Fitak, Supervisor
Materials and Process Section, Area 6
Van Nuys, California

Northrop Corporation, Norair Division
Attn. Mr. R. B. Jackman, Chief
Engrg. Laboratory
Hawthorne, California

OSR (SRYS, L/Col. R. W. Conners)
Building T-D
4th and Independance, S. W.
Washington 25, D. C.

Pacific Airmotive Corporation
2940 North Hollywood Way
Burbank, California

Pidletless Aircraft Division
Boeing Airplane Company
Attn. Mr. R. R. Barber, Lib. Supvr.
P. O. Box 3925
Seattle 24, Washington

Pneumo Dynamics Corporation
Systems Engineering Division
Attn. Tech Library
4936 Fairmont Avenue
Bethesda 14, Maryland

Pratt and Whitney Aircraft Division
United Aircraft Corporation
Attn. Mr. A. F. Smith, Assistant Eng. Mgr.
362 South Main Street
East Hartford 8, Connecticut

Radioplane Company
Attn. Mr. John J. Jacobson,
  Chief Engrg.
8000 Woodley Avenue
Van Nuys, California

Reaction Motors, Inc.
Attn. Margaret Becker, Librarian
Eng. and Research Division
Denville, New Jersey

Republic Aviation Corporation
Attn. Mr. P. L. Waters, Building 55
Farmingdale, Long Island, New York

Republic Aviation Corporation
Attn. Mr. Robert Wichser
Farmingdale, Long Island, New York

Rohr Aircraft Corporation
Attn. Mr. Hugh M. Rush, Lab. Mgr.
Chula Vista, California

Ryan Aeronautical Company
Attn. Mr. L. J. Hull, Chief Metallurgist
Materials and Process Laboratory
San Diego 12, California

Ryan Aeronautical Company
Attn. Mr. W. S. Cockrell,
  Chief Dev. Laboratory
Lindberg Drive
San Diego 12, California

Sikorsky Aircraft
Attn. Mr. H. T. Jensen
Chief of Test Branch
Stratford, Connecticut

Sikorsky Aircraft Corporation
United Aircraft Division
Attn. Mr. M. E. Gluhareff, Eng. Mgr.
Bridgeport 1, Connecticut

Simmonds Aerocessories, Inc.
Attn. Mr. William Enyart
105 White Plainsroad
Tarrytown, New York

Society of Automotive Engineers, Inc.
Attn. Mr. M. I. Stoner, Mgr.
Aeronautical Dept.
485 Lexington Avenue
New York 17, New York

Solar Aircraft Company
Attn. Mr. R. E. Day, Mgr.
Components Engr.
San Diego 12, California

Solar Aircraft Company
Main Plant and Offices
Attn. Librarian
2200 Pacific Highway
San Diego 12, California

J. T. Baker Chemical Company
Attn. Mr. Frederic W. Hammesfhar
Director of Commercial Development
Phillipsburg, New Jersey

Koppers Company, Incorporated
Research Department
Attn. Dr. C. E. Donath
Pittsburgh 19, Pennsylvania

Laurence Radiation Laboratory
Process and Materials Development
Attn. Dr. B. Rubin
P. O. Box 808
Livermore, California

Lockheed Aircraft Corporation
Missiles and Space Division
Attn. Technical Information Center
3251 Hanolver Street
Palo Alto, California

Lubrizol Corporation
Attn. Dr. L. E. Coleman
P. O. Box 3057
Cleveland 17, Ohio

Massachusetts Institute of Technology
Department of Chemistry
Attn. Dr. W. C. Schumb
Cambridge, Massachusetts

Massachusetts Institute of Technology
Attn. Dr. Dietmar Seyferth
Cambridge, Massachusetts

Mellon Institute
Department of Chemistry
Attn. Dr. Thomas Fox
Pittsburgh, Pennsylvania

Melpar, Inc.
Attn. Dr. Paul E. Ritt
3000 Arlington Boulevard
Falls Church, Virginia

Metal and Thermit Corporation
Attn. Miss M. K. Moran
Box 471
Rahway, New Jersey

Merck-Sharpe and Dohme Research Labs.
Attn. Dr. Carl Pfister
Rahway, New Jersey

Metcut Research Associates, Inc.
Attn. Mr. John F. Kahles
3980 Rosslyn Drive
Cincinnati 9, Ohio

Michigan State University
Department of Chemistry
Attn. Dr. Kinsinger
Attn. Dr. Hammer
East Lansing, Michigan

Midwest Research Institute
Attn. Librarian-3675
425 Volker Boulevard
Kansas City, Missouri

Minnesota Mining and Mfg. Company
Attn. Dr. John Copenhaver
900 Bush Avenue
St. Paul, Minnesota

Minnesota Mining and Mfg. Company
Central Research Department
Attn. Dr. George Crawford
2301 Hudson Road
St. Paul 19, Minnesota

Monsanto Chemical Company
Inorganic Division
800 N. Lindberg Blvd.
St. Louis 66, Missouri

Monsanto Chemical Company
Attn. Dr. E. S. Blake
Central Research Laboratories
Dayton 7, Ohio

Monsanto Chemical Company
Special Projects Department
Attn. Mr. K. W. Easley
Everett, Massachusetts

Monsanto Chemical Company
Attn. Miss H. A. Diekman
Director of Research
Springfield 2, Massachusetts

NAMC (Mr. J. Bowen)
Air Materials Laboratory
Philadelphia 12, Pennsylvania

National Academy of Sciences
National Research Council
Attn. Dr. Clem O. Miller
2101 Constitution Avenue
Washington 25, D. C.

National Lead Company
Attn. Mr. W. H. Hoback
111 Broadway
New York, New York

National Lead Company
Attn. Dr. F. L. Cuthbert
P. O. Box 39158
Cincinnati, Ohio

National Science Foundation
Rubber Research Group
Attn. Mr. P. S. Greer
Washington 25, D. C.

Naugatuck Chemical Division
U. S. Rubber Company
Attn. Dr. R. C. Nelb
Naugatuck, Connecticut

New York State University
Department of Chemistry
Attn. Dr. M. Szwarc
Syracuse, New York

New York University
Department of Chemical Engineering
Attn. Prof. Charles J. Marsel
New York 53, New York

North American Aviation Corporation
Attn. Mr. J. W. Mahoney
Inglewood, California

NRL (Dr. W. A. Zisman)
Washington 25, D. C.

NOL (Dr. A. Lightbody)
Silver Spring 19, Maryland

NOL (Dr. C. P. Haber)
Corona, California

NOTS (Code 4526)
China Lake, California

Ohio State University
Department of Chemistry
Attn. Dr. Albert Henne
Columbus 10, Ohio

Office of Chief of Ordnance
Department of the Army
Attn. ORDTB
Washington 25, D. C.

Olin-Mathieson Chemical Corporation
Attn. Technical Library
New Haven, Connecticut

Olin-Matheson Chemical Corporation
Attn. Dr. T. L. Heying
275 Winchester Avenue
New Haven, Connecticut

ONR Branch Office (Dr. S. H. Herzfeld)
The John Crerar Library Building
10th Floor, 86 East Randolph Street
Chicago 1, Illinois

ONR (Code 425)
Washington 25, D. C.

Peninsular Chemical Research Inc.
Attn. Dr. Paul Tarrant
1103-5 W. Fifth Avenue
Gainesville, Florida

Pennsalt Mfg. Company
Attn. Dr. John Gall
P. O. Box 4388
Philadelphia 18, Pennsylvania

Pennsylvania State University
Department of Chemistry
Attn. Prof. L. H. Sommer
Attn. Prof. W. C. Fernelius
University Park, Pennsylvania

Pennsylvania State University
Petroleum Refining Laboratory
Attn. Mr. E. R. Klaus
University Park, Pennsylvania

Phillips Petroleum Company
Attn. Dr. W. Reynolds
Bartlesville, Oklahoma

Plastics Technical Evaluation Center
Attn. ORDBB-VP3
Picatinny Arsenal
Dover, New Jersey

Polytechnic Institute of Brooklyn
Attn. Dr. C. G. Overberger
333 Jay Street
Brooklyn 1, New York

Princeton University
Plastics Laboratory
Attn. Prof. Rahm
Princeton, New Jersey

Purdue University
Department of Chemistry
Attn. Mr. A. F. Clifford
Lafayette, Indiana

RADC (RCS, Mr. O. Tallman)
Griffiss AFB, New York

Reaction Motors Division
Thiokol Chemical Corporation
Attn. Dr. David Mann
Denville, New Jersey

Research Triangle Institute
Attn. Howard G. Clark III
P. O. Box 490
Durham, North Carolina

Rohm and Haas Company
Special Products Department
Attn. Dr. B. P. Dahlstrom
Washington Square
Philadelphia 5, Pennsylvania

Rohm and Haas Company
Attn. Dr. Ellington M. Beavers
Box 219
Bristol, Pennsylvania

Royal Lubricants Company
Attn. Mr. W. Craessle
River Road, P. O. Box 95
Hanover, New Jersey

SCEL (SIGEL-SMB)
Fort Monmouth, New Jersey

Shell Chemical Company
Attn. Librarian
1120 Commerce Avenue
Union, New Jersey

University of Akron
Department of Chemistry
Attn. Dr. M. Morton
Akron, Ohio

Shell Development Company
Attn. Mr. C. Wagner
4560 Horton Street
Emeryville, California

University of Arizona
Department of Chemistry
Attn. Dr. C. S. Marvel
Tucson, Arizona

Southern Research Institute
Attn. Mr. W. C. Sheehan
2000 Ninth Avenue South
Birmingham, Alabama

University of Buffalo
Department of Chemistry
Attn. Dr. H. Post
Buffalo, New York

Southern Research Institute
Applied Chemistry Division
Attn. Dr. P. E. Feazel
Birmingham, Alabama

University of California
Department of Chemistry
Attn. Mr. W. C. Drinkard, Jr.
Los Angeles, California

Southwest Research Institute
Attn. Chemistry and Chemical Engr.
8500 Culebra Road
San Antonio, Texas

University of Cincinnati
Department of Chemistry
Attn. Dr. H. H. Jaffe
Cincinnati 21, Ohio

Standard Oil Co. of Indiana
Whiting Research Laboratories
Attn. Dr. C. E. Johnson
P. O. Box 431
Whiting, Indiana

University of Colorado
Department of Chemistry
Attn. Dr. J. I. Park
Boulder, Colorado

University of Florida
College of Engineering
Stanford Research Institute
Attn. Mr. C. L. Himel
Menlo Park, California

Attn. Dr. H. C. Brown
Gainesville, Florida

SSD (SSRTH, Lt. Col. J. F. Clyde)
AF Unit Post Office
Los Angeles 45, California

University of Florida
Department of Chemistry
Attn. Dr. George Butler
Gainesville, Florida

Thiokol Corporation
Attn. Mr. A. D. Yazujian
780 N. Clinton Street
Trenton 7, New Jersey

University of Illinois
Department of Chemistry
Attn. Dr. J. C. Bailar, Jr.
Attn. Dr. T. Moeller
Urbana, Illinois

Union Carbide and Carbon Corporation
Bakelite Division
Attn. Mr. J. K. Honish
30 E. 42nd Street
New York 17, New York

University of North Carolina
Department of Chemistry
Attn. Mr. S. Young Tyree, Jr.
Chapel Hill, North Carolina

Union Carbide Corporation
Silicones Division
Attn. Mr. T. H. Welch
E. Park Dr. and Woodward Avenue
Tonawanda, New York

University of Pennsylvania
Department of Chemistry
Attn. Mr. E. Charles Evers
Philadelphia, Pennsylvania

United States Air Force Academy
Department of Chemistry
Attn. Capt. C. H. Schmid
Denver, Colorado

University of Southern California
Department of Chemistry
Attn. Dr. A. B. Burg
University Park
Los Angeles 7, California

University of Texas
Department of Chemistry
Attn. Dr. G. W. Watt
Austin, Texas

University of Wisconsin
Department of Chemistry
Attn. Professor John D. Ferry
Madison 6, Wisconsin

University of Western Ontario
Attn. Dr. D. C. Bradley
London, Ontario, Canada

U. S. Atomic Energy Commission
Reference Branch
Technical Information Center
Attn. Document Control Section
P. O., Box 62
Oak Ridge, Tennessee

U. S. Borax Research Corporation
Attn. Dr. C. L. Randolph
412 Crescent Way
Anaheim, California

U. S. Department of Agriculture
Forest Service
Forest Products Laboratory
Attn. Dr. Don Brouse
Madison 5, Wisconsin

U. S. Department of Agriculture
Agriculture Research Laboratory
Attn. Mr. W. A. Reeves
New Orleans 19, Louisiana

U. S. Department of Commerce
National Bureau of Standards
Attn. Dr. B. M. Kline
Attn. Dr. Maxhellman
Attn. Dr. Dibeler
Washington 25, D. C.

U. S. Industrial Chemicals Company
Attn. Mr. Charles E. Frank
1275 Section Road
Cincinnati 37, Ohio

USAFA
Quarters 64551 (Capt. W. Massengale)
USAF Academy, Colorado

Westinghouse Electric Corporation
Materials Engineering Department
Attn. Dr. C. C. Gainer
E. Pittsburgh, Pennsylvania

Westinghouse Research Laboratory
Attn. Mr. J. M. Ferteg
Attn. Mr. Robert E. Lacroix
Beulah Road, Churchill Borough
Pittsburgh 35, Pennsylvania

Wyandotte Chemical Corporation
Attn. Dr. Carl Lenk
Research and Engineering Division
Wyandotte, Michigan

ASD (ASAPT) (2 copies)
Wright-Patterson AFB,
Ohio

Allied Chemical Corporation
Central Research Laboratory
Attn. Dr. Herbert Reimschuessel
Morristown, New Jersey

ASRCE
Applications Laboratory
Wright-Patterson Air Force Base
Ohio

ASRCEM-1A
Materials Information Branch
Wright-Patterson Air Force Base
Ohio

ASRCM
Metals + Ceramics Laboratory
Wright-Patterson Air Force Base
Ohio

ASRCN
Nonmetallic Materials Laboratory
Wright-Patterson Air Force Base
Ohio

ASRCNC
Plastics + Composites Branch
Wright-Patterson Air Force Base
Ohio

ASRCNE
Elastomers + Coatings Branch
Wright-Patterson Air Force Base
Ohio

ASRCNF
Fibrous Materials Branch
Wright-Patterson Air Force Base
Ohio

ASRCNL
Fuels + Lubricants Branch
Wright-Patterson Air Force Base
Ohio

ASRCP
Physics Laboratory
Wright-Patterson Air Force Base
Ohio

ASRE
Evaluation Office Deputy for Tech.
Wright-Patterson Air Force Base
Ohio

ASRM
Directorate of Aeromechanics
Wright-Patterson Air Force Base
Ohio

ASRMP
Propulsion Laboratory
Wright-Patterson Air Force Base
Ohio

ASRNE
Electronics Tech. Lab.
Wright-Patterson Air Force Base
Ohio

ASROO
Technical Operations Division
Wright-Patterson Air Force Base
Ohio

B. F. Goodrich Company
Research Center
Attn. Dr. C. F. Gibbs
Brecksville, Ohio

Ballistic Research Laboratories
Aberdeen Proving Ground
Maryland

Battelle Memorial Institute
Attn. Dr. P. B. Stickney
505 King Avenue
Columbus, Ohio

Bell Telephone Laboratories
Attn. Dr. F. H. Winslow 1A-231
Murray Hill, New Jersey

Bendix System Division
Attn. Mr. J. McNabb
327 S. Fourth Street
Ann Arbor, Michigan

Bloomingdale Rubber Company
Attn. Dr. H. C. Engel
Box 191
Aberdeen, Maryland

The Boeing Company
Wichita Division
Attn. Mr. H. I. Paxhia
Chief, Process Staff
Wichita, Kansas

The Boeing Company
Wichita Division
Attn. Mr. Joseph R. Galli
Dept. 7100-Engineering, Plant 1
Wichita, Kansas

Borden Company
Chemical Division
Attn. Dr. B. D. Halpern
P. O. Box 9524
Philadelphia, Pennsylvania

BUSHIPS (Mr. L. E. Sieffert,
  Code 346)
Washington 25, D. C.

BUSHIPS (Mr. Edward Wagman,
  Code 634A)
Washington 25, D. C.

BUWEPS (Code -AE44)
Washington 25, D. C.

Sundstrand Corporation
Aviation Division
Attn. Mr. E. Erikson, Chief Engr.
Rockford, Illinois

Systems Engineering Division
Pneumo-Dynamics Corporation
4936 Fairmont Avenue
Bethesda 14, Maryland

Temco Electronics and Missiles Company
Attn. Mr. C. L. Caudill
Sr. Grp. Eng. Producibility
Dallas, Texas

Thermodynamics Dept. 53-15
Lockheed Missile and Space Division
Attn. Dr. Roger Gaumer
P. O. Box 504
Sunnyvale, California

Transco Products, Inc.
Attn. Mr. Walter F. McGinty
12210 Nebraska Avenue
Los Angeles 25, California

USAFE (DCS/INT/ATILO)
APO 633
New York, New York

Vicker Inc. , Div. Sperry Rand Corp.
Attn. Mr. Frank Moncher, Dir. Eng.
Adm. and Eng. Center
Detroit 32, Michigan

6593 Test Gp.
Attn. Lt. R. A. Suehrstedt
Edwards AFB, California

A. O. Smith Corporation
Government Research and Development Div.
Attn. Mr. Lowell R. Newton
Milwaukee 1, Wisconsin

Adhesives Engineering Company
Division of Heller Helicopter Corporation
Attn. Dr. D. W. Elam
1411 Industrial Road
San Carlos, California

AEDC (Dr. H. K. Doetsch)
Arnold AFB, Tennessee

Aerospace Corporation Library
Attn. Technical Rep rtr. Section
2400 East El Segundo Blvd.
El Segundo, California

Aerospace Industries Association
Attn. Mr. J. P. Reese
610 Shoreham Building
Washington 4, D. C.

AFCCDD (CCR)
L. G. Hanscom Field
Bedford, Massachusetts

AFCIN
Foreign Technology Division
Wright-Patterson AFB, Ohio

SSD (SSBSD, Lt. Col. E. Finke)
AF Unit Post Office
Los Angeles 45, California

AFSWC (SWOI 4874)
Kirtland AFB, New Mexico

Allied Chemical and Dye Company
General Chemical Division
Attn. Mr. Paul Jones
P. O. Box 405
Morristown, New Jersey

American Cyanamid Company
Attn. Dr. L. A. Peikeral
1937 W. Main Street
Stamford, Connecticut

American Potash and Chemical Corporation
Attn. Dr. K. Eilar
201 W. Washington Street
Whittier, California

APGC (PGAPI)
Eglin AFB, Florida

AFSC (SCR-2, Mr. Kniffin)
Andrews AFB
Washington 25, D. C.

ASD (ASAPRL)
Wright-Patterson AFB, Ohio

ASRCNP (25 copies+ 1 reproducible)
Wright-Patterson AFB, Ohio

ASTIA (TIPOR)
Arlington Hall Station (30 copies)
Arlington 12, Virginia

Armour Research Foundation
Dept. of Chemistry
Technology Center
35 W. 33rd Street
Chicago 16, Illinois

ASAPTT
Advanced Technology + Test
 Publication
Wright-Patterson Air Force Base
Ohio

ASEH
Historical Division
Wright-Patterson Air Force Base
Ohio

ASRC
Directorate of Materials + Processes
Wright-Patterson Air Force Base
Ohio

Aeronautical Systems Division, Wright-Patterson
Air Force Base, Ohio. Rept. No. ASD-TDR
62-73. EFFECTS OF ULTRAHIGH PRESSURES
ON THE FORMATION AND PROPERTIES OF
ORGANIC, SEMIORGANIC, AND INORGANIC
MATERIALS. Final rept. Jan. 1962, 102 p.
incl. illus and tables.   Unclassified report.

The effect of ultrahigh pressures (up to
90,000 atm) was studied on organic polymers and
a variety of semiorganic and inorganic materials.

Results on organic polymers indicate that the
effect of compression is influenced by the com-
pression attained, the compression rate, the
(over)

1. Pressures
2. Organic Compounds
3. Metalorganic Compounds
4. Inorganic Substances
I. ASD Project 7340,
   Task 73404
II. Contract AF 33(616)-7471
III. Battelle Mem. Inst.
    Columbus, Ohio
IV. E. J. Bradbury
    H. H. Krause
    C. B. Sclar and others
V. In ASTIA collection
IV. Not available from OTS

holding period, and the polymer used. The
most influential parameters within the target
range of compression appear to be the polymer
and the holding period. No generalized pattern
of behavior for polymers was noted.

Ultrahigh-pressure high-temperature studies of
heteropolynuclear acids (2) and salts (2) appear
to have pressure dependent modifications over a
broad pressure-temperature range to 75,000 atm
and 1300 C.